2013

Global and regional scale constraints to bioenergy potential and the human appropriation of net primary production

William Kolby Smith

GLOBAL AND REGIONAL SCALE CONSTRAINTS TO BIOENERGY POTENTIAL AND THE HUMAN APPROPRIATION OF NET PRIMARY PRODUCTION

By

WILLIAM KOLBY SMITH

M.S., Ecology, Colorado State University, Fort Collins, Colorado, 2008
B.S., Mathematics, Western Carolina University, Silva, North Carolina, 2005

Dissertation

presented in partial fulfillment of the requirements
for the degree of

Doctor of Philosophy
in Forestry, Ecosystem Science

The University of Montana
Missoula, MT

May 2013

Approved by:

Sandy Ross, Dean of The Graduate School
Graduate School

Dr. Steven W. Running, Chair
Department of Ecosystem and Conservation Sciences

Dr. Cory C. Cleveland
Department of Ecosystem and Conservation Sciences

Dr. Solomon Z. Dobrowski
Department of Ecosystem and Conservation Sciences

Dr. Sasha C. Reed
Department of Ecosystem and Conservation Sciences

Dr. Dane Scott
Department of Ecosystem and Conservation Sciences

Dr. Derek Kellenberg
Department of Economics

ProQuest LLC.
789 East Eisenhower Parkway
P.O. Box 1346
Ann Arbor, MI 48106 - 1346

ABSTRACT

Smith, William, Ph.D., May 2013 Forestry, Ecosystem Science

Global and Regional Scale Constraints to Bioenergy Potential and the Human Appropriation of Net Primary Production

Chairperson: Dr. Steven W. Running

Expansion of the human appropriation of net primary production (HANPP) is a future certainty, given a growing global food demand – driven by near-exponential population growth coupled with increasing global meat consumption – and an increasing global investment in bioenergy – promoted by nearly all global energy policy. Yet, our current understanding of the impacts associated with increased HANPP is limited and the subject of intense debate in the scientific community. The focus of my dissertation is to improve our understanding of the impacts of, and future potential for, HANPP through the use of satellite data and landuse modeling.

In chapter 1, I develop a framework to evaluate global bioenergy potential using Moderate Resolution Spectroradiometer (MODIS) net primary productivity (NPP) data in an effort to put fundamental quantitative sideboards on the overall potential for global bioenergy production. In chapter 2, I apply the framework developed in the first chapter to quantify the gross bioenergy potential of the conterminous United States (U.S.) and evaluate the feasibility of current U.S. bioenergy policy, namely the Energy Independence and Security Act of 2007 (EISA). In chapter 3, I evaluate the potential for intensifying productivity on existing agricultural land by controlling for management intensity and comparing current rates of agricultural and natural productivity across long-term, global-scale climate zones.

The results of this work show that global-scale bioenergy potential has been generally overestimated by previous analyses, due to the under-representation of biophysical constraints on yield potential. Further, using EISA as a case-study, I show over-optimistic bioenergy estimates have resulted in unrealistic future bioenergy targets. Finally, I present strong evidence that agricultural productivity does not exceed natural rates of productivity, except in limited cases of intense management inputs, suggesting that humanity may be reaching a HANPP planetary boundary within the next few decades.

ACKNOWLEDGMENTS

Many people contributed to the research presented in this dissertation. First, I would like to thank Steve Running, my advisor, whose contributions to this work are immeasurable. As a student of Steve's I benefitted immensely from a near-limitless creative freedom, Steve's always-open office door, and Steve's seemingly endless stream of sage advice. I owe a special thanks to Cory Cleveland and Sasha Reed for their invaluable guidance and advice, their openness and genuine regard for my best interests, and their continued efforts to involve me both inside and outside of work. I would also like to sincerely thank my remaining Ph.D. committee members – Solomon Dobrowski, Dane Scott, and Derek Kellenburg – who helped to make every committee meeting positive and extremely productive, such that I always left feeling full of new ideas. Finally, I would like to acknowledge the support provided by the NTSG team, especially Youngee Cho, whose good humor, support, and knowledge seems to be the glue holding everything together. I will always look back on my time as a Ph.D. student at the University of Montana with fond memories.

I would not be where I am today if it were not for my family. My dad is the scientist I have always aspired to be. He has freely followed his own ideas and interests, produced novel and exciting research, worked with friends, fostered many highly successful students, and he continues to live a full and storied life inside and outside of academia. I cannot thank my dad enough for setting such a great example, and for always being there to provide guidance for all my big life decisions. I am also forever in debt to my mom, who selflessly made certain that my siblings and I grew up happy, kind, open-minded, and curious. My mom always pushed me to follow my dreams no matter how far from home they took me, and I will always be grateful. I would also like to thank my sisters – Liana, Kaylyn, and Chelsey – and brother – Matthew – who have been my life-long supporters and best friends. Finally, I share all my success with my fiancée, Lisa Mason. Lisa makes me the best possible version of myself, understands my sometimes single-minded focus on research, and is always there to provide invaluable insight and feedback. Without her, I would not have the same appreciation for outreach, activism and using knowledge to make the world a better place; and thus my life would not be nearly as fulfilling.

.

TABLE OF CONTENTS

LIST OF TABLES

LIST OF FIGURES

DISSERTATION OVERVIEW

I present herein, an analysis of humanity's current and future domination of the terrestrial biosphere. I divide this analysis into three separate chapters that separately explore the global-scale potential for bioenergy, current national-level bioenergy policy, and the current impact of human-driven landcover conversion on terrestrial vegetation growth. While I incorporate a variety of data, the common data source throughout is satellite-derived – Moderate Resolution Imaging Spectroradiometer (MODIS) – annual terrestrial plant growth (NPP) data. A brief description of each chapter follows.

Chapter 1. Global bioenergy capacity as constrained by observed biospheric productivity rates

Virtually all global energy forecasts include an expectation that bioenergy will be a substantial future energy source. Yet, the scale of the potential resource remains poorly understood due to large uncertainty regarding land availability and yield expectations. Here, we utilized climate-constrained, satellite-derived net primary productivity data computed for 110 million km^2 of terrestrial plant production, as an upper-envelope constraint on primary bioenergy potential (PBP). We estimate maximum PBP to realistically range from 12 to 35% of 2009 global primary energy consumption, with yield potential ranging from 6.6 to 18.8 MJ m^{-2} yr^{-1}, a range roughly four times lower than previous evaluations. Our results highlight many recent bioenergy evaluations as over-optimistic, which we attribute to a lack of biophysical constraints on yield potential. We do not advocate bioenergy production at the levels reported in this analysis; instead,

we simply report the ceiling for primary bioenergy production based on current planetary productivity.

Chapter 2. Bioenergy capacity of the conterminous United States as constrained by biospheric productivity rates

Currently, the United States (U.S.) supplies roughly half the world's biofuel (secondary bioenergy), with the Energy Independence and Security Act of 2007 (EISA) stipulating an additional three-fold increase in annual production by 2022. Implicit in such energy targets is an associated increase in annual biomass demand (primary bioenergy) from roughly 2.9 to 7.4 EJ. Yet, many of the factors used to estimate future bioenergy potential are relatively unresolved, bringing into question the practicality of the EISA's ambitious bioenergy targets. Here, our objective was to constrain estimates of primary bioenergy potential (PBP) for the conterminous U.S. using satellite-derived net primary productivity (NPP) data (measured for every 1 km^2 of the 7.2 million km^2 of vegetated land in the conterminous U.S) as the most geographically explicit measure of terrestrial growth capacity. We show that the annual primary bioenergy potential (PBP) of the conterminous U.S. realistically ranges from approximately 5.9 (± 1.4) to 22.2 (± 4.4) EJ, depending on land use. The low end of this range represents current harvest residuals, an attractive potential energy source since no additional harvest land is required. In contrast, the high end represents an annual harvest over an additional 5.4 million km^2 or 75% of vegetated land in the conterminous U.S. While we identify EISA energy targets as achievable, our results indicate that meeting such targets using current technology would require either an 80% displacement of current croplands or the

conversion of 60% of total rangelands. Our results differ from previous evaluations in that we use high resolution, satellite-derived NPP as an upper-envelope constraint on bioenergy potential, which removes the need for extrapolation of plot-level observed yields over large spatial areas. Establishing realistically constrained estimates of bioenergy potential seems a critical next step for effectively incorporating bioenergy into future U.S. energy portfolios.

Chapter 3. A global scale quantification of the impact of agricultural conversion and management intensity on terrestrial vegetation productivity.

Current forecasts indicate that increases in global population and consumption coupled with expansion of bioenergy will likely drive an unprecedented doubling of global biomass demand from 2005 to 2050. Yet, at current levels of intensity and extent, agricultural systems are already severely degrading soil, water, and biodiversity, while accounting for roughly 20% of global greenhouse gas emissions. Thus, finding ways to increase agricultural output, while simultaneously minimizing impacts on the biosphere, has become an unparalleled challenge for humanity, and an area of intense scientific focus and debate. In this analysis, we set out to quantify the net impact of current agricultural landcover conversion on a key foundation of the biospheric carbon cycle, total terrestrial vegetation growth (i.e., net primary productivity or NPP). We find that current agricultural landcover conversion has reduced biospheric primary production by 6-9% annually, a range equivalent to roughly 30% of annual fossil-fuel emissions. Further, we show that achieving agricultural output comparable to that of natural system replaced, and thus avoiding the degradation of global vegetation growth, depends heavily

on intensive management (i.e., irrigated or high input management) within highly biophysically constrained climate zones (i.e., cold and arid climates). These results indicate that increased resource use efficiency on existing agricultural land plus agricultural expansion into cold and arid climate could increase agricultural output while minimizing the impact of agriculture on global vegetation growth. In contrast, further expansion into temperate and tropical climates will likely drive disproportionately large decreases in global vegetation growth. Overcoming the numerous socioeconomic factors driving agricultural expansion in temperate and tropical climate must be prioritized in future global policy portfolios.

CHAPTER 1

Global bioenergy capacity as constrained by observed biospheric productivity rates

Introduction

Climate change policy and concerns regarding future energy security continue to stimulate an unprecedented rise in the production of bioenergy - a renewable energy source with the potential to reduce greenhouse gas (GHG) emissions (Haberl *et al.* 2010; Edenhofer *et al.* 2011). Yet, determining the scale at which bioenergy can be sustained globally requires knowledge of two complex factors: (1) future land availability for bioenergy production; and (2) future yield expectations (Haberl *et al.* 2010). These factors are not independent, as yield potential greatly varies depending on land quality, which in turn is largely determined by biophysical (e.g., solar radiation, temperature, and precipitation) as well as human management (e.g., irrigation and fertilization) factors.

Numerous studies have attempted to resolve bioenergy potential at the global scale using a wide range of methodologies. Most commonly, crop-specific average yield values recorded at the plot level have been applied across land areas considered suitable for bioenergy production (Hoogwijk *et al.* 2005; Smeets *et al.* 2007; van Vuuren *et al.* 2009; Pacca & Moreira 2011). However, this type of approach can greatly over-estimate biofuel potential since average yield values do not reflect variability in yield driven by biophysical factors and human management (Johnston *et al.* 2009). Others have applied process models that combine plot-level yield potential estimates, spatially-explicit climatic data, and human management to more realistically estimate spatial variability in yield (Erb *et al.* 2009; Beringer *et al.* 2011). Yet, results of these analyses are highly sensitive to crop type, extrapolation technique, and calibration data (Field *et al.* 2008; Campbell *et al.* 2008). Moreover, validation of model performance is limited since crop-specific field data remains sparely available at the global scale (Field *et al.* 2008;

Campbell *et al.* 2008). Currently, average yield potential estimates reported in the literature vary by nearly an order of magnitude, from 6.9 to 60 MJ m^{-2} yr^{-1} (Haberl *et al.* 2010), which significantly contributes to variability in global bioenergy potential estimates, documented to range from roughly 5% to as high as 300% of 2009 Global Primary Energy Consumption (GPEC09; USEIA 2011).

Reducing the range of variability associated with current estimates of bioenergy potential represents a significant first step towards a more quantitative understanding of the scale of bioenergy as a future energy source. Here, we estimate primary bioenergy potential (PBP) – or bioenergy potential before energy conversion losses (e.g., during liquefaction) – from satellite-derived net primary productivity (NPP) data [Earth Observing System (EOS), Moderate Resolution Imaging Spectroradiometer net primary production (MODIS NPP)] (see, e.g., Running *et al.* 2004; Zhao *et al.* 2005; Zhao & Running 2010). NPP varies as a function of multiple factors including vegetation type, soil type, climate, and human management (Vitousek *et al.* 1986; DeFries 2002; Haberl *et al.* 2007). At the global scale however, conversion of natural ecosystems to agricultural lands has been shown to result in significant reductions in NPP (Vitousek *et al.* 1986; DeFries 2002; Haberl *et al.* 2007). In fact, Haberl *et al.* (2007) estimated that large-scale cropland productivity is consistently lower than that of the natural vegetation replaced, independent of landcover type or region. Only under intensive human management (i.e., irrigation and/or fertilization) – which is often limited to relatively small scales due to resource availability – has cropland productivity been shown to exceed that of the natural potential (DeFries 2002; Haberl *et al.* 2007). Yet, even in these relatively localized cases, DeFries *et al.* (2002) showed cropland productivity does not exceed decadal-scale

variability in natural productivity, highlighting the limited potential for increasing productivity beyond that of the natural vegetation. Since current bioenergy systems are subject to similar agriculturally-based human management practices, we argue that constraining yield potential by natural observed rates of NPP represents a realistic upper-envelope evaluation of PBP.

MODIS NPP quantifies current terrestrial biomass growth capacity for every 1-km^2 of the entire 110 million km^2 (Mkm^2) vegetated Earth by integrating remotely-sensed vegetation dynamics [e.g., Fraction of Photosynthetically Active Radiation (FPAR) and Leaf Area Index (LAI) data] and global climatic data (e.g., temperature and moisture) (Zhao *et al.* 2005). Using MODIS NPP as a top-down evaluation of PBP removes the need for extrapolation of plot-level observed yields, an approach identified above to generally overestimate PBP. Satellite data has been previous used to assess the bioenergy potential of abandoned agricultural land, as described in Campbell *et al.* (2008) and Field *et al.* (2008). Our analysis builds upon these previous studies in that we consider all vegetation, and then systematically remove landcover types according to current availability. Thus, we provide a continuous quantification of PBP across broad land use scenarios, which elucidates the relationship between land availability and yield potential, and allows for comparison across all current bioenergy analyses independent of land use assumptions. Ultimately, our objective with this study is to estimate the upper-envelope for global bioenergy production across future land use options, utilizing MODIS NPP as the most geographically explicit measure of the current growth capacity of the terrestrial biosphere (Running *et al.* 2004; Zhao *et al.* 2005; Zhao & Running 2010).

Methods

Global vegetation productivity. We start with Moderate Resolution Imaging Spectroradiometer (MODIS) net primary production (NPP) data as a fundamental constraint on global bioenergy potential (Running *et al.* 2004; Zhao *et al.* 2005; Zhao & Running 2010; Smith *et al.* 2012a). The MODIS GPP/NPP algorithm was used to calculate 1-km^2 MODIS NPP from 2000 through 2010 (Running *et al.* 2004). Collection 5 (C5) 8-day composite 1-km^2 Fraction of Photosynthetically Active Radiation (FPAR) and Leaf Area Index (LAI) data collected from the MODIS sensor were used as remotely sensed vegetation property dynamic inputs (Running *et al.* 2004). For daily meteorological variables required to drive the algorithm, we used data obtained from the Data Assimilation Office (DAO) datasets (Schubert *et al.* 1993). 1-km^2 MODIS NPP from 2000-2010 was averaged and aggregated to a 10-km^2 (10 km x 10 km) spatial resolution (Fig. 1.1). For more detail as well as a validation of the MODIS GPP/NPP algorithm see Running *et al.* (2004), Zhao *et al.* (2005), and Zhao & Running 2010, 2011.

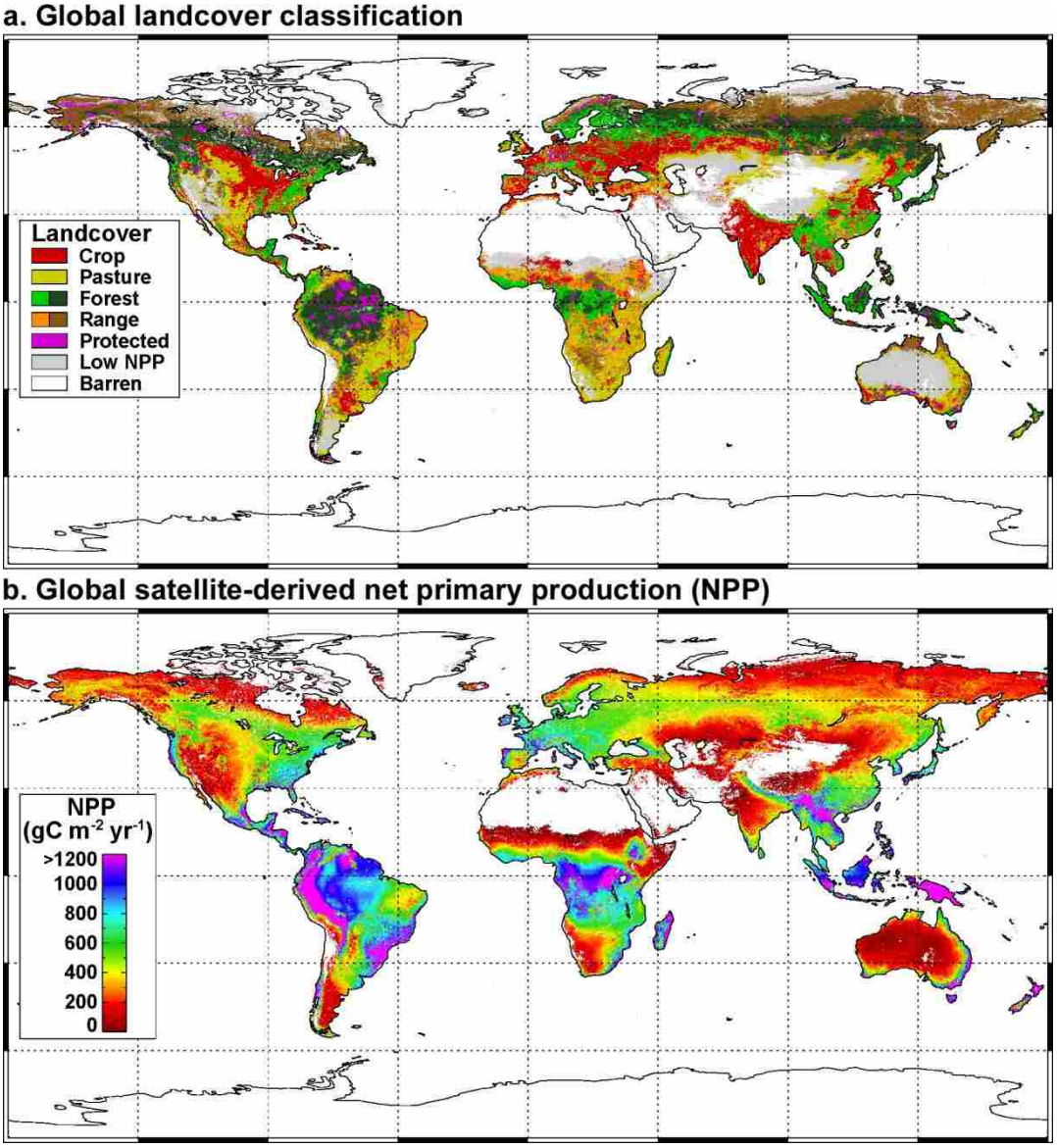

Figure 1.1. Global landcover and net primary productivity. **a**, Global landcover divided into crop, pasture, forest, range, protected, low NPP (i.e., "low productivity" land), and barren landcover classes. Forests and rangelands are partitioned into "accessible" and "remote" land, designated by light and dark shades, respectively. **b**, Global net primary productivity averaged from 2000-2010, estimated from the MODIS GPP/NPP algorithm at a 10-km^2 (10 km x 10 km) spatial resolution (Running et al. 2004, Zhao et al. 2005, Zhao and Running 2010, Zhao and Running 2011).

Global land use. We utilized a 10-km^2 composite land use classification consisting of socioeconomically relevant land use types including crop, pasture, forest, rangeland, and protected (Fig 1.1). We did not consider urban-dominated or barren landcover classes - defined according to University of Maryland (UM) MODIS landcover data (Friedl *et al.* 2010) - since they contribute negligibly to global vegetation productivity(Zhao *et al.* 2005). Croplands were defined to include permanent and temporarily fallow (less than 5 years) croplands only, while pasturelands were defined to include permanent (five years or more) pasturelands specifically managed for livestock grazing, according to Ramankutty *et al.* (2008). For both crop and pasture areas, we converted percentage coverage data to discrete data utilizing a 40% occupancy threshold, meaning that a given pixel was reclassified as occupied if the landcover type of interest had a percent coverage greater than or equal to the threshold. In the case where both crop and pasture coverage was greater than or equal to the threshold, the pixel was characterized according to the landcover type with greater percent coverage. Forests were defined from UM MODIS landcover data (Friedl *et al.* 2010) as the combination of evergreen needleleaf, evergreen broadleaf, deciduous needleleaf, deciduous broadleaf, and mixed forest landcover types. Rangelands were classified as all remaining vegetated (non-barren) land as defined by UM MODIS landcover data (Friedl *et al.* 2010).

Additionally, we partitioned natural landcover types (i.e., forests and rangelands) into either "accessible" or "remote" (Fig 1.1), utilizing the human footprint index dataset (*http://sedac.ciesin.columbia.edu/wildareas/downloads.jsp*), which accounts for accessibility by incorporating information on roads, major rivers, and coastlines. "Remote" lands represent the lowest 15% of human index scores, which is roughly

equivalent to the 15% least accessible land globally. Protected regions were classified as only areas of strict protection, including national parks and nature reserves, according to World Database on Protected Areas data (*www.wdpa.org*). Finally, we classified "low productivity" land using a productivity threshold of 150 gC m^{-2} yr^{-1}, the threshold at which harvest energy inputs (e.g., establishment, management, harvest, etc.) exceed potential energy outputs (Nonhebel 2002; Schmer *et al.* 2008). The resulting area considered "low productivity" was estimated to extend 20.3 Mkm^2 (Fig. 1.1), which is consistent with estimates of roughly 16 and 24 Mkm^2 reported by Haberl *et al.* (2010) and Edenhofer (2011), respectively.

Current agricultural and forestry harvest. Current agricultural and forestry harvest were assumed to occur on crop and accessible forestlands only. We estimated agricultural and forestry harvest rates as a proportion of MODIS NPP according to current harvest statistics (*http://faostat.fao.org*). Four relevant harvest pools were considered: (1) total harvest (H_{TOTAL}) or total aboveground biomass at the time of harvest; (2) recoverable harvest (H_{REC}) or the fraction of H_{TOTAL} removed from the field at the time of harvest; (3) harvest losses (H_{LOSS}) or the fraction of H_{TOTAL} remaining in the field post-harvest; and (4) harvest residues (H_{RES}) or the fraction of H_{LOSS} recoverable without impacting nutrient cycling (primary residues, e.g., felled branches), plus the fraction of H_{REC} unutilized following harvest processing (secondary residues, e.g., sawdust). Harvest pools were estimated at a spatial resolution of 10-km^2 according to Box 1.1.

Box 1.1. Calculating current agricultural and forestry harvest

Harvest (H) pools including total harvest (H_{TOTAL}), recoverable harvest (H_{REC}), harvest losses (H_{LOSS}), and harvest residues (H_{RES}) were estimated at a spatial resolution of 10-km^2 according to the below equations:

$$H_{TOTAL} = \sum_{i=1}^{n} NPP_i \times r_{abv} \times y_{total} \; ; \qquad 1.1$$

Where r_{abv} and y_{total} represent literature-derived aboveground NPP and total aboveground yield potential ratios, respectively. For agricultural harvest, r_{abv} and y_{total} were estimated as 0.83 (range: 0.80-0.85) and 1.00 (range: 0.90-1.00), respectively, which represents the global average for four dominant global crops (i.e., maize, rice, wheat, and soybean), accounting for 70% of global agricultural land (Saugier et al. 2001, Monfreda et al. 2008). Due to significant spatial variability in forestry harvest, r_{abv} and y_{total} were estimated regionally (UNSD, 2006; Supplementary Fig. 1.1) according to literature-derived aboveground ratios and average harvest volume data (Saugier et al. 2001, FAO 2010; Table S1.1). H_{TOTAL} was calculated as the sum of all agricultural or forestry pixels (n). H_{REC}, H_{LOSS}, and H_{RES} were estimated as proportional to H_{TOTAL} according to Equations 1.2-1.4:

$$H_{REC} = \sum_{i=1}^{n} (H_{TOTAL_i} \times y_{rec} \times (1 - y_{res2})) \; ; \qquad 1.2$$

$$H_{LOSS} = \sum_{i=1}^{n} (H_{TOTAL_i} \times (1 - y_{rec}) \times (1 - y_{res1})) \; ; \qquad 1.3$$

$$H_{RES} = \sum_{i=1}^{n} (H_{TOTAL_i} \times (1 - y_{rec}) \times y_{res1} + H_{TOTAL_i} \times y_{rec} \times y_{res2}) \; ; \qquad 1.4$$

Where y_{rec}, y_{res1}, and y_{res2} represent literature-derived yield potential ratios describing the average proportion of H_{TOTAL} recovered at the time of harvest, H_{LOSS} recoverable without impacting nutrient cycling (primary residuals), and H_{REC} available following harvest processing (secondary residuals), respectively. For agricultural harvest, y_{rec} and y_{res2} were estimated to be 0.50 (range: 0.40-0.60) and 0.10 (range: 0.05-0.15), respectively (Monfreda et al. 2008). For forest harvest, y_{rec} and y_{res2} were estimated to be 0.80 (range: 0.70-0.90) and 0.40 (range: 0.30-0.50), respectively (Haberl et al. 2007, Smeets et al. 2007). Finally, y_{res1} was estimated to be 0.30 (range: 0.25-0.35) for both agricultural and forestry harvest (Smeets et al. 2007, Gregg and Smith 2010). A summary of the calculated global agricultural and forestry harvest pools are presented by region in Tables S1.2 and S1.3, respectively. Also, a spatial representation of total harvest (H_{TOTAL}) is shown in Supplementary Fig. 1.2. For additional methodological detail see Smith et al. 2012.

Maximum sustainable agricultural and forestry harvest. Maximum sustainable harvest (MSH) – defined as the maximum harvest without impacting future yields and nutrient cycling - was estimated independently for potential agricultural land (i.e., current cropland, pastureland, accessible range, and remote range) and potential forestry land (i.e., accessible forests and remote forests). We did not consider the conversion of forest to agricultural land since it has been well documented that this type of landcover conversion results in a net detrimental climate change impact (Tilman *et al.* 2009). MSH pools (MSH_{TOTAL}, MSH_{REC}, MSH_{LOSS}, MSH_{RES}) were calculated according to Box 1.1, by simply replacing the current total harvest ratio (y_{rec}) with a literature-derived *MSH* ratio (y_{msh}). For agricultural systems, a maximum y_{msh} of 1.00 (range 0.90-1.00) was utilized, since generally all aboveground biomass on croplands is either harvested or decomposed annually (Table S1.1). For forest systems, a y_{msh} of 0.20 (range: 0.15-0.25) was utilized, based on current global forestry harvest trends (Table S1.1). We utilize a MSH value for forestry systems that is consistent with the highest current global forestry harvest rates, which resulted in a more than two-fold increase in global forest harvest (Table S1.3).

Box 1.2. Calculating primary bioenergy potential

Primary bioenergy potential (*PBP*) scenarios including the biospheric capacity (PBP_{CAP}), maximum land use (PBP_{MAX}), moderate land use (PBP_{MOD}), and minimum land use (PBP_{MIN}) were estimated at a spatial resolution of 10-km^2 according to the below equations:

$$PBP_{CAP} = \sum_{i=1}^{n_{cap}} (MSH_{REC_i} + MSH_{RES_i}); \quad 1.5$$

$$PBP_{MAX} = \sum_{i=1}^{n_{\max}} (MSH_{REC_i} + MSH_{RES_i}); \quad 1.6$$

$$PBP_{MOD} = \sum_{i=1}^{n_{\mathrm{mod}}} (H_{REC_i} + H_{RES_i}); \quad 1.7$$

$$PBP_{MIN} = \sum_{i=1}^{n_{\min}} (H_{RES_i}); \quad 1.8$$

Where n_{cap} represents all vegetated pixels; n_{max} represents the exclusion of "unavailable" sources; n_{mod} represents the exclusion of "unavailable" and "low availability" sources; and n_{min} represents only "immediately" available sources, respectively (Table 1.1). A summary of the calculated global agricultural and forest bioenergy potential pools are presented by region in Tables S1.4 and S1.5, respectively.

Primary bioenergy potential. We estimated PBP by landcover class utilizing four land use scenarios (Table 1.1). (1) As a starting point, we estimated the biospheric capacity for bioenergy over all vegetated land (PBP_{CAP}) (Fig. 1.2a). (2) From PBP_{CAP}, we calculated bioenergy assuming maximum available land use (PBP_{MAX}) (Fig. 1.2b), by removing all "unavailable" sources defined to include current crop and forestry harvest, protected areas, and low productivity land. (3) From PBP_{MAX}, we next estimated bioenergy considering only moderate land use (PBP_{MOD}) (Fig. 1.2c), by removing "low availability" sources defined to include pastures, remote regions, and accessible forest land. (4) Finally, we calculated global bioenergy considering only "immediately available" sources (PBP_{MIN}) (Fig. 1.2d), defined to include current crop and forest harvest residuals only. PBP pools were estimated at a spatial resolution of 10-km^2 according to Box 1.2.

Table 1.1. Land use scenarios utilized to evaluate primary bioenergy potential.

Land use scenario	Definition	Sources considered
Biospheric capacity (***PBP$_{CAP}$***)	All vegetated land	--
Maximum land use (***PBP$_{MAX}$***)	***PBP$_{CAP}$*** without *unavailable sources*[a]	Pastures, remote regions, accessible forests, accessible rangelands, crop and forestry harvest residues
Moderate land use (***PBP$_{MOD}$***)	***PBP$_{MAX}$*** without *low availability sources*[b]	accessible rangelands, crop and forestry harvest residues
Minimum land use (***PBP$_{MIN}$***)	*Immediately available sources*[c] only	crop and forestry harvest residues

[a]*Unavailable sources* defined to include current crop and forest harvest, protected land, and low productivity land. [b]*Low availability sources* defined to include current pastures, remote regions, and accessible forests. [c]*Immediately available sources* defined to include crop and forest harvest residues only.

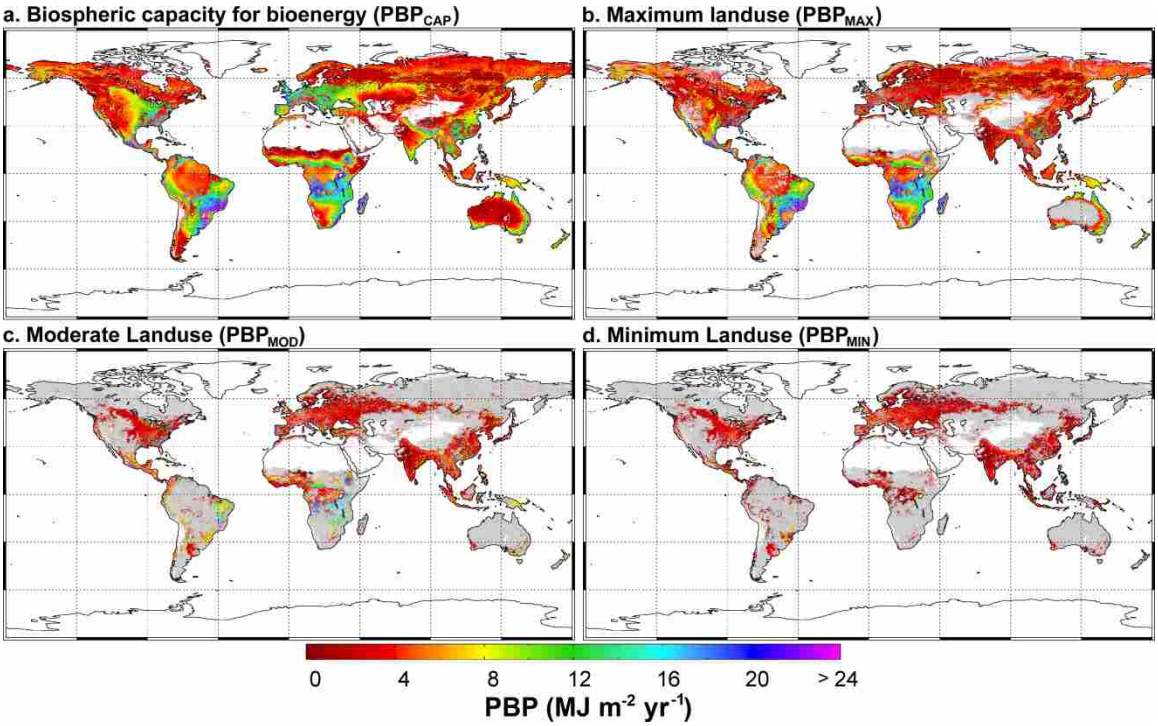

Figure 1.2. Spatially-explicit primary bioenergy potential by land use scenario. **a**, Biospheric capacity for bioenergy (PBP_{CAP}). PBP_{CAP} represents the conversion of *all terrestrial primary production to bioenergy* (Table 1.1). **b**, Maximum land use (PBP_{MAX}). We defined PBP_{MAX} to exclude "unavailable" sources, including current crop and forest harvest, protected regions, and land under a minimum productivity threshold (Table 1.1). **c**, Moderate land use (PBP_{MOD}). We defined PBP_{MOD} to exclude "unavailable sources" as well as "low availability" sources, including remote regions and pasturelands (Table 1.1). **d**, Minimum land use (PBP_{MIN}). PBP_{MIN} represents a land use scenario where only "immediately available" sources, including current harvest residuals are utilized for bioenergy production (Table 1.1). *PBP_{MIN} has the benefit of requiring no additional harvest land.*

Energy conversion. We converted biomass (gC yr^{-1}) to energy (J yr^{-1}) by applying well known energy conversion constants according to the below equation:

$$energy = biomass \times \frac{CF_{energy}}{CR_{biomass}}; \quad 1.9$$

Where *energy* (J yr^{-1}) was estimated from *biomass* (g Cyr^{-1}) assuming a 0.45 carbon-to-biomass ratio ($CR_{biomass}$; Williams & Percival 1987) and an 18 MJ kg^{-1} gross biomass energy content (CF_{energy}; Tsubo *et al.* 2001). It is important to note, we only considered primary energy, and therefore did not take into account energy losses due to energy conversion.

Results

Current global harvest. We estimated global NPP – averaged from 2000-2010 - to be 53.1 PgC yr^{-1} over 110.1 Mkm^2 (Table 1.2, Fig. 1.1), which is in range with previously reported values of 59 and 46 PgC yr^{-1}, reported by Haberl *et al.* (2007) and Grosso & Parton (2010), respectively. Croplands were estimated to account for 6.6 PgC yr^{-1} over 15.2 Mkm^2 (Table 1.2, Fig. 1.1), which is comparable to literature-derived estimates of 6.8 PgC yr^{-1} over 14.5 Mkm^2 and 6.3 PgC yr^{-1} over 15.2 Mkm^2 reported by Haberl *et al.* (2010) and Field *et al.* (2008), respectively. Current total cropland harvest (H_{TOTAL}) was estimated as 5.5 PgC yr^{-1} over 15.2 Mkm^2 (Supplementary Table 1.2, Supplementary Fig. 1.2), which again is within the range of values reported by (Haberl *et al.* (2007). Harvested forestland, defined as accessible forestland, had an associated NPP of 12.4 PgC yr^{-1} over 14.7 Mkm^2 (Table 1.2, Fig. 1.1). While forestry area varies significantly by definition, we report a total forest harvest (H_{TOTAL}) of 0.95 PgC yr^{-1} (Supplementary

Table 1.3, Supplementary Fig. 1.2), which is consistent with estimates of 1.0 and 1.1 PgC yr-1 reported by Haberl *et al.* (2010) and Vitousek *et al.* (1986), respectively.

Table 1.2. Global area, net primary productivity, and primary bioenergy potential by landcover type.

Landcover Type	Area (Mkm^2)	NPP[a] ($PgC\ yr^{-1}$)	Mean NPP ($gC\ m^{-2}\ yr^{-1}$)	PBP[a] ($EJ\ yr^{-1}$)	Mean Yield ($MJ\ m^{-2}\ yr^{-1}$)
Crop	15.2	6.6	434 (229)	143.9	9.5 (5.0)
Pasture	17.8	8.5	478 (298)	184.3	10.4 (6.3)
Accessible Range	9.6	5.6	583 (280)	121.8	12.7 (6.1)
Remote Range	12.9	4.3	333 (197)	92.3	7.1 (4.2)
Protected Range	1.6	0.7	438 (259)	14.8	9.3 (5.5)
Accessible Forest	14.7	12.4	844 (412)	67.3	4.5 (2.2)
Remote Forest	14.9	10.7	718 (398)	55.9	3.8 (2.1)
Protected Forest	3.1	2.8	903 (404)	14.4	4.7 (2.1)
Low Productivity	20.3	1.5	74 (42)	32.8	1.6 (0.9)
Total/Average	**110.1**	**53.1**	**482 (402)**	**727.5**	**6.6 (5.5)**

[a]NPP = net primary production; PBP = primary bioenergy potential. Values in parentheses represent one standard deviation of the mean.

Global primary bioenergy potential. We estimated the biospheric capacity for bioenergy (PBP_{CAP}) to be 727.5 EJ yr^{-1} over 110.1 Mkm^2 (Table 1.3, Fig. 1.3). Upon the removal of unavailable sources (i.e., current crop and forestry harvest, protected land, and low productivity areas), PBP_{MAX} was reduced to 548.4 EJ yr^{-1} over 55.2 Mkm^2, with an associated yield potential range from 3.0 to 14.8 MJ m^{-2} yr^{-1} (Table 1.3, Fig. 1.3). Regionally, Sub-Saharan Africa (26.8%), South America (24.2%), North America (11.1%), East Europe (9.5%), and Central Asia (6.5%) accounted for 78.1% of total PBP_{MAX} (Fig. 1.4). Further removal of low availability sources (i.e., accessible forest, pastures, and remote regions) resulted in a PBP_{MOD} of 180.4 EJ yr^{-1} over 9.6 Mkm^2 (Table 1.3, Fig. 1.3). However, the yield potential range increased to 6.6 to 18.8 MJ m^{-2} yr^{-1} (Table 1.3, Fig. 1.3). Regional contributions also changed with Sub-Saharan Africa (28.9%), South America (15.4%), North America (11.9%), Western Europe (11.4%), and Central Asia (7.2%) accounting for 74.8% of total PBP_{MOD} (Fig. 1.4). Finally, considering only immediately available sources (i.e., current crop and forestry residuals), PBP_{MIN} was reduced to 58.6 EJ yr^{-1} (Table 1.3, Fig. 1.3). Note, PBP_{MIN} is highly dependent on the proportion of harvested losses considered recoverable, which is still relatively unresolved in the literature (Haberl *et al.* 2010). Nonetheless, our estimate of PBP_{MIN} is within the range reported in the current literature and is therefore representative of current understanding (Table 1.3). Western Europe (17.9%), North America (16.8%), South Asia (11.8%), Sub-Saharan Africa (10.3%), and Central Asia (9.9%) were estimated to account for 66.7% of total PBP_{MIN} (Fig. 1.4).

Table 1.3. A comparison of global area, yield, and primary bioenergy potential. a. Primary bioenergy potential by land use scenario. b. Current primary bioenergy potential estimates from the literature.

a. Land use scenario		Area (Mkm^2)	Yield Range[a] ($MJ\ m^{-2}\ yr^{-1}$)	Primary Energy ($EJ\ yr^{-1}$)
Biospheric Capacity (PBP_{CAP})[b]		110.1	1.1-12.1	727.5
Maximum Land Use (PBP_{MAX})[b]		55.2	3.0-14.8	489.8
Moderate Land Use (PBP_{MOD})[b]		9.6	6.6-18.8	121.8
Minimum Land Use (PBP_{MIN})		--	--	58.6
b. Literature	**Source**	**Area (Mkm^2)**	**Yield Potential ($MJ\ m^{-2}\ yr^{-1}$)**	**Primary Energy ($EJ\ yr^{-1}$)**
Current				
Pacca et al. (2011)	Sugarcane Crop	0.7	69	46
Field et al. (2008)	Abandoned Crop	3.9	6.9	27
Campbell et al. (2008)	Abandoned Crop	3.9-4.7	8-9	32-41
Circa 2050				
Haberl et al. (2012)	Maximum Crop	3.8-9.9	11-14	40-133
Haberl et al. (2012)	Residuals Crop	--	--	24-28
Beringer et al. (2011) [I][c]	Maximum Crop	1.4-4.5	33-40	52-174
Beringer et al. (2011) [R][c]	Maximum Crop	1.4-4.5	18-26	26-116
Erb et al. (2009)	Maximum Crop	2.3-9.9	12-13	28-128
van Vuuren et al. (2009)	Maximum Crop	0.0-6.0	20-60	65-300
Smeets et al. (2007)	Maximum Crop	7.3-35.9	29-39	215-1272
Hoogwijk et al. (2005)	Maximum Crop	29-37	10-18	300-650
Literature Reviews				
Chum et al. (2011)	All Available	--	--	120-300
Dornburg et al. (2010)	All Available	--	--	120-330
Haberl et al. (2010)	All Available	--	--	160-270
Haberl et al. (2010)	All Residues	--	--	15-84

[a]Yield range represents a range of one standard deviation. [b]PBP_{CAP}, PBP_{MAX}, PBP_{MOD} reported without the inclusion of harvest residual (PBP_{MIN}). [c][I] = irrigated; [R] = rainfed.

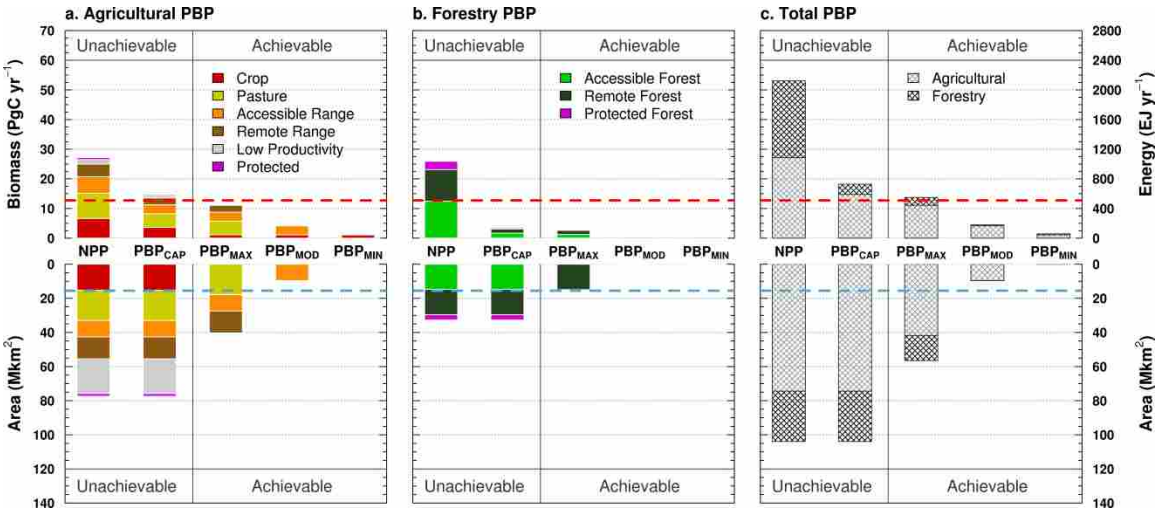

Figure 1.3. Primary bioenergy potential and corresponding land area requirements by land use scenario. PBP_{CAP}, PBP_{MAX}, PBP_{MOD}, PBP_{MIN} represent land use scenarios defined according to Table 1.1. Land use scenarios are divided into *available* and *unavailable* based on whether or not "unavailable" sources (i.e., current crop and forest harvest, protected regions, and land under a minimum productivity threshold) are considered (Table 1.1). For comparison, 2009 global primary energy consumption (509 EJ) and current cropland area (15.2 Mkm^2) are represented by red and blue dashed lines, respectively. **a**, Primary bioenergy potential on agricultural lands, defined to include crop, pasture, accessible range, remote range, and protected range. **b**, Primary bioenergy potential on forestry land, defined to include accessible forests, remote forests, and protected forests. **c**, Primary bioenergy potential on all land, divided between agricultural and forestry land.

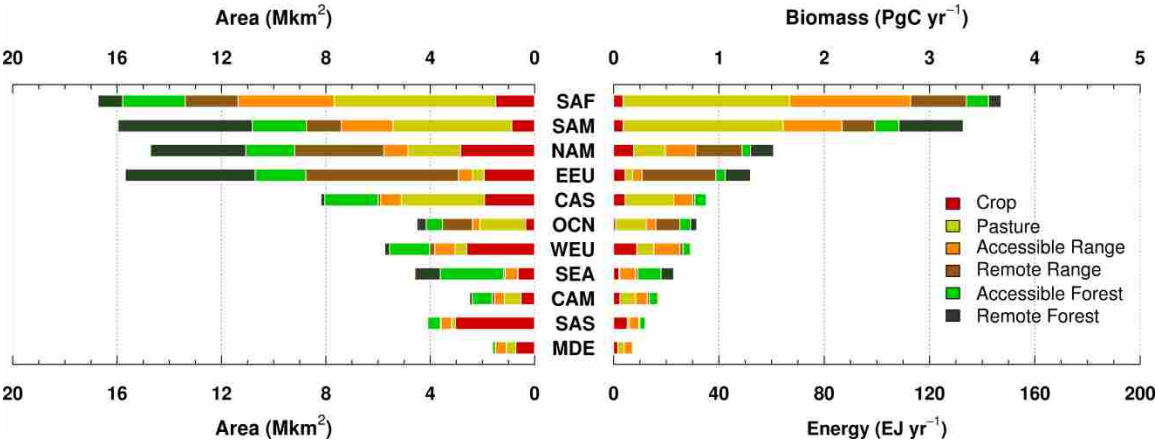

Figure 1.4. Primary bioenergy potential and corresponding land area requirements by region. Regions were aggregated according to the classification of the macro geographical regions and geographic sub-regions as defined by the United Nations Statistical Division (Fig. S1.1). The full region names are Sub-Saharan Africa (SAF), South America (SAM), North America (NAM), East Europe (EEU), Central Asia (CAS), Oceania and Australia (OCN), West Europe (WEU), Southeast Asia (SEA), Central America (CAM), South Asia (SAS), and Middle East (MDE) (Fig. S1.1). **a**, Maximum land use (PBP_{MAX}), defined to include all vegetated land excluding "unavailable" sources (Table 1.1). **b**, Maximum primary bioenergy potential (PBP_{MAX}), estimated utilizing MODIS NPP as an upper-envelope constraint.

Discussion

Global primary bioenergy potential and yield. We calculated maximum primary bioenergy potential (PBP) to range from 35% to 108% of 2009 global primary energy consumption (GPEC09; USEIA 2010) (Fig. 1.3). A main driver of PBP was average yield potential, which varied by land use scenario from 6.6 to 12.7 MJ m^{-2} yr^{-1}, *a range roughly four times lower than multiple previous published estimates* (Table 1.3). For instance, Smeets & Faaij (2007) utilized an average yield potential range from 29 to 39 MJ m^{-2} yr^{-1} to conclude that maximum global bioenergy potential could reach nearly 300% of GPEC09 by the year 2050 (Table 1.3, Fig. 1.5). Smeets & Faaij (2007) assumed steadily increasing yields as well as the availability of the most advance human management practices (e.g., irrigation and fertilization). Similarly, Beringer *et al.* (2011) estimated irrigated yield potentials for the year 2050 to range from 33-40 MJ m^{-2} yr^{-1}, although significantly less land was considered available for bioenergy production (Table 1.3, Fig. 1.5). Finally, Pacca & Moreira (2011) utilized an average yield potential value of 69 MJ m^{-2} yr^{-1} – the present day yield potential for Sugarcane grown under optimum nutrient availability, temperature, and water availability – to suggest that all the world's automobiles could be powered using only 4% of global croplands (Table 1.3, Fig. 1.5). Methodologically these studies include different assumptions and are over different time frames (Table 1.3, Fig. 1.5); however they utilize yield potentials near the upper-end of literature-derived estimates mainly due to the shared assumption of the availability of human management to mitigate biophysical constraints on crop productivity and yield.

Compared with current rates of vegetation productivity and yield potential, we show these studies utilize average yields significantly greater than both current crop yields and

natural yield potentials (Table 1.3, Fig. 1.5). Since global agricultural yields have been reported as generally less than natural productivity Haberl *et al.* (2007), *we argue that these analyses over-estimate bioenergy potential by failing to realistically limit the potential for human management to overcome natural biophysical constraints on yield potential* (Table 1.3, Fig. 1.5). Human management, especially irrigation, has been observed to increase productivity above natural rates over relatively localized areas (DeFries 2002; Haberl *et al.* 2007). Therefore, increases in yield potential above the natural potential – as reported by Beringer *et al.* (2011)– may be theoretically achievable (Table 1.3, Fig. 1.5). However, due to limited freshwater availability as well as the numerous detrimental effects of fertilization, maintaining yield potentials at levels higher than natural rates of productivity would likely be unsustainable over large spatial scales (see section *Natural productivity as a yield potential constraint*).

In contrast, our yield potential estimates are consistent with studies that utilize more restrictive assumptions regarding human management and the influence of biophysical factors on yield potential (Hoogwijk *et al.* 2005; Field *et al.* 2008; Campbell *et al.* 2008; Erb *et al.* 2009; Haberl *et al.* 2012) (Table 1.3, Fig. 1.5). Campbell *et al.* (2008) and Field *et al.* (2008) utilized satellite-derived NPP to calculate current yield potential on degraded agricultural land, and reported yield potential values at the lower end of the yield range reported here (Table 1.3, Fig. 1.5). We attribute this difference to landcover assumptions, since degraded lands are known to experience relatively low productivity. Hoogwijk *et al.* (2005) estimated crop-specific yield potentials for the year 2050 utilizing a process model driven by climate data, and documented yield potential values at the high end of our reported range (Table 1.3, Fig. 1.5). Note, even these yield potential estimates

may still be unrealistic, since our estimates represent upper-envelope natural yield potentials and likely overestimate the potential for crop-specific yields (Haberl *et al.* 2007). This is most apparent in Fig. 1.5, where trends in productivity on agricultural lands are shown to be significantly less than productivity trends for all PBP scenarios.

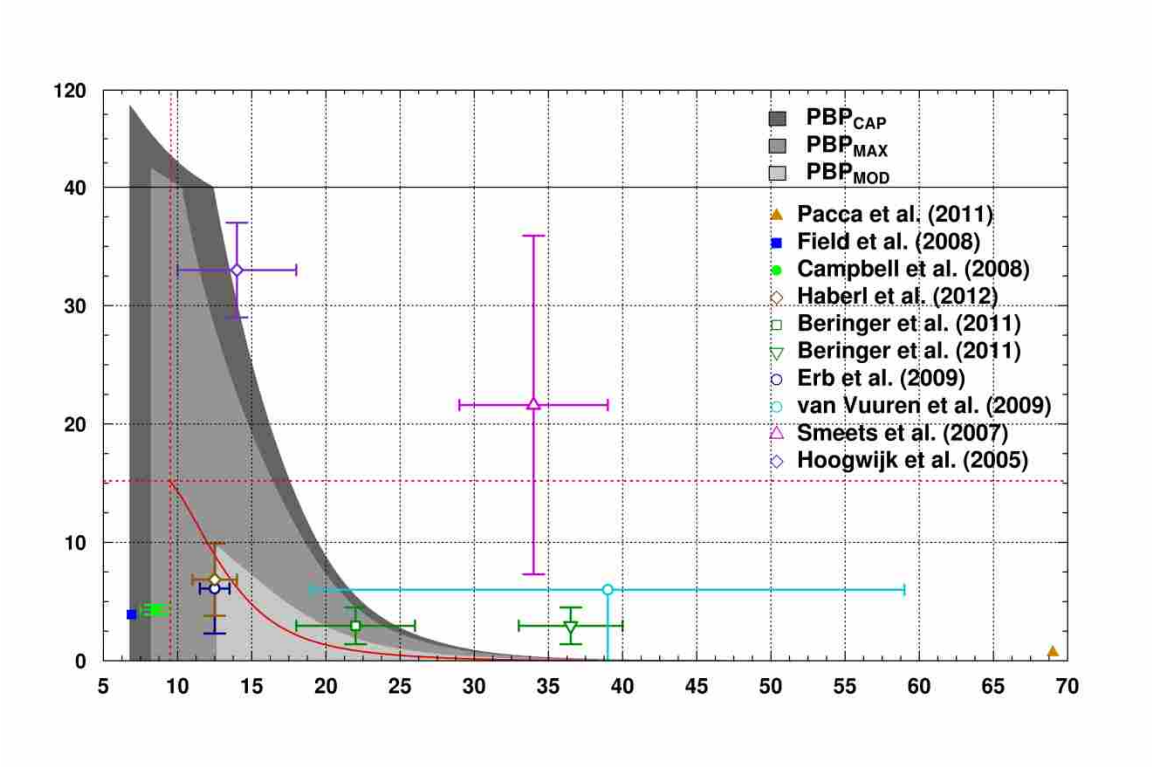

Figure 1.5. Cumulative maximum yield potential by land use scenario. PBP_{CAP}, PBP_{MAX}, PBP_{MOD} represent cumulative maximum yield potential curves for each land use scenario, which are described in Table 1.1. We calculated cumulative maximum yield potential by sorting all 10-km^2 yield potential pixel values for a given scenario from highest to lowest, and then averaging over the highest yield values for a given land area. Therefore, for any given land area from 10 km^2 to 110 million km^2 (Mkm^2), the corresponding value of the curve represents the maximum yield potential for that given area. For comparison, current cropland cumulative maximum yield potential is represented by the red solid line. Total cropland area (15.2 Mkm^2) and the corresponding maximum yield over total cropland area (9.5 MJ m^{-2} yr^{-1}) are represented by red dotted lines. Additionally, the area and corresponding yield potential estimates from recent bioenergy analyses are displayed as mean values with whiskers denoting the full range of values considered by the study. Studies focused on current conditions are represented by solid symbols, while those based on the year 2050 are represented by open symbols (see Table 1.3 for more detail). *We show that a number of recent studies utilize yield potential values higher than maximum natural yield potentials, which we attribute to over-optimistic assumptions regarding human management and/or unrealistic consideration of biophysical constraints on yield potential*.

Global bioenergy potential and land use. We estimated maximum land availability for bioenergy cultivation to range from 9% - 50% of total vegetated land area (Fig. 1.3), a range at the upper end of recent studies (Table 1.3, Fig. 1.5). Since our goal was an upper-envelope evaluation of bioenergy potential, we include landcover classes often removed by previous studies, such as remote regions and pastures. Bioenergy cultivation on these low availability landcover types has many associated trade-offs. Expansion into remote regions represents roughly 20% of global bioenergy potential (Table 1.2, Fig. 1.3); however, infrastructure establishment and land conversion in these regions would require large-scale fossil fuel energy inputs, resulting in a significant initial carbon debt of bioenergy systems (Fargione *et al.* 2008). Remote regions are distributed over 27.8 Mkm^2 (Table 1.2), which means that to reach the full energy potential of these regions, a network of access roads would be required over an area greater than the total extent of North America. Additionally, since average yield potential on remote land is relatively low (Table 1.2, Fig. 1.3), the associated time required to offset the initial fossil fuel inputs would be significant, decreasing the attractiveness of remote regions (Fargione *et al.* 2008).

More notably, pastures – defined as areas permanently managed for livestock grazing - were estimated to account for nearly half of global bioenergy potential over an area of 17.8 Mkm^2, an area larger than the total extent of South America (Table 1.2, Fig. 1.3). Potential may exist for the conversion of pastures to bioenergy production land, since only roughly 20% of annual aboveground productivity is consumed by grazers (Haberl *et al.* 2007). Yet, conversion of pasturelands has already been associated with significant detrimental impacts (McAlpine *et al.* 2009; Arima *et al.* 2011). For instance, Arima *et al.*

(2011) documented that deforestation rates in the Brazilian Amazon were indirectly associated with pastureland displacement by bioenergy plantations [i.e., indirect land use change (ILUC)]. Considering that global meat consumption trends continue to rise (McAlpine *et al.* 2009), the detrimental impacts associated with pastureland-to-bioenergy conversion are only likely to increase in the future (McAlpine *et al.* 2009; Arima *et al.* 2011).

In contrast, if we consider only current harvest residues, we estimated a bioenergy potential (PBP_{MIN}) equivalent to 12% of GPEC09 (Table 1.3, Fig. 1.3). Residuals are an attractive potential energy source since they are currently accessible and do not require additional land use, which reduces the significant detrimental impacts (e.g., carbon debt and ILUC) discussed above. Since current global bioenergy utilization accounts for approximately 10% of GPEC09 (Haberl *et al.* 2010), the utilization of current harvest residuals has the potential to more than double current global bioenergy utilization. Potentially easily developed sources of residual bioenergy include forestry slash piles, agricultural field residues, as well as forestry post-processing sawdust and debris (Haberl *et al.* 2010). However, to fully reach the above mentioned 12% GPEC09 offset, we estimate that residuals would have to be harvested over 29.9 Mkm^2, an area greater than the total extent of North America (Table 1.3).

Natural productivity as a yield potential constraint. We base our analysis on the assumption that natural rates of productivity represent an upper-envelope constraint on bioenergy potential, which raises the question: what is the potential for increasing productivity above natural rates? Enhancing productivity beyond the natural potential

would require either increased efficiency of light capture (light interception efficiency) or enhanced efficiency of the conversion of captured light into biomass (light use efficiency), neither of which are likely near-future scenarios. Under optimal growing conditions (i.e., no temperature, moisture, or nutrient constraints), Long *et al.* (2006) suggests light interception efficiency as near a theoretical maximum for major crops, leaving only light use efficiency as a mechanism to increase productivity. However, despite a long history, genetic manipulation by plant breeding has yet to significantly enhance light use efficiency per unit area (Richards 2000), which partially explains why agricultural percent yield increase rates have been declining since the green revolution (Funk & Brown 2009). Next generation bioenergy crops such as perennial rhizomatous grasses (PRGs) (e.g., *Panicum*, *Miscanthus,* etc.) are fundamentally different from food crops in that they utilize the C4 photosynthesis pathway which significantly improves light use efficiency and maximizes productivity (Heaton *et al.* 2004). Yet, PRGs achieve higher light use efficiency at the cost of energy (Heaton *et al.* 2004), which reduces their competitive advantage in sub-optimal growing conditions (e.g., nutrient-poor, dry, or cold climates). Thus, PRGs could significantly increase yields in agricultural systems where less efficient food crops are currently grown and conditions are maintained at near-optimal (Heaton *et al.* 2008). On natural landscapes however, C4 species are already distributed according to climate and nutrient availability, which limits the potential of PRGs to improve natural productivity without fertilization and/or irrigation inputs – the limited potential for which we discuss in detail next.

Under sub-optimal growing conditions, light use efficiency can be increased by reducing growth constraints (e.g., temperature, precipitation, nutrients) via human

management (i.e., irrigation and/or fertilization), which results in increased photosynthesis per unit time (Long *et al.* 2006). However, evidence suggests global rates of irrigation and fertilization are approaching peak levels in many regions, with significant associated detrimental impacts. For instance, global groundwater depletion has more than doubled from 1960 to 2000, mainly due to increased rates of irrigation (Wada *et al.* 2010). Given 40% of the global food supply comes from irrigation-dependent croplands (Gleick 2003), a more likely scenario for the future may be *decreased* global yield potentials as irrigation limits are reached and droughts become more frequent (Gleick 2003; Wada *et al.* 2010; Dai 2011). Similarly, current fertilization demand has more than doubled global reactive nitrogen availability, resulting in extensive eutrophication of freshwater and coastal zones, along with increased emission of the potent GHG nitrous oxide (N_2O), a trace gas species with a global warming potential roughly 300 times greater than an equal mass of CO_2 (Galloway *et al.* 2008). Thus, any productivity increases associated with future increases in irrigation and/or fertilization will be at the cost of freshwater pollution and possibly GHG emissions (Galloway *et al.* 2008; Wada *et al.* 2010).

Conclusions

We calculate *maximum* global bioenergy potential to range from 35% - 108% of GPEC09 (Fig. 1.3). However, a number of key assumptions and factors need to be considered to determine the difference between "maximum" and "realistic maximum" bioenergy potential. Our upper-end maximum calculation (PBP_{MAX}) required the conversion of 55.6 Mkm^2 of natural vegetation for bioenergy production, an area more

than the total extent of Asia and Europe combined. Whereas our lower-end maximum calculation (PBP_{MOD}) required the conversion of 9.6 Mkm^2 of natural vegetation, an area nearly equivalent to the total extent of Europe. Even the complete utilization of current harvest residues (PBP_{MIN}) was shown to require biomass collection over 29.9 Mkm^2, an area greater than the total extent of North America. Given the scale associated with these scenarios, we conclude that realistic maximum global bioenergy potential ranges somewhere between 12% of GPEC09 - the potential associated with current harvest residuals (PBP_{MIN}) - and 35% of GPEC09 (PBP_{MOD}) - the lower-end maximum calculation (PBP_{MOD}). By 2050, global primary energy demand is projected to more than double (Haberl et al. 2010), thus we estimate that the realistic maximum contribution of bioenergy ranges from roughly 5% to 15% of our future energy needs. We do not advocate global bioenergy production at the levels reported in this analysis; instead, we simply report an *upper-envelope constraint* for primary bioenergy potential based on existing satellite observations of global vegetation productivity.

Supplementary Information

Table S1.1. Global forestry harvest data by region.

Region	NPP[a] (Pg C yr^{-1})	Area (Mkm^2)			r_{abv}[c]	ANPP (PgC yr^{-1})	FAO[b] (Mm^3 yr^{-1})	Density[d] (t dm m^{-3})	H_{TOTAL} (PgC yr^{-1})	r_{harv}[e]
		C	B	M						
Managed										
North America	1.14	0.41	0.55	0.73	0.75	0.86	651.26	0.49	0.14	0.17
Central America	0.65	0.01	0.57	0.10	0.77	0.50	93.99	0.57	0.03	0.05
South America	2.16	0.04	1.82	0.02	0.78	1.68	346.52	0.59	0.11	0.07
Oceania	0.76	0.01	0.55	0.00	0.78	0.59	61.09	0.60	0.02	0.03
West Europe	0.92	0.56	0.13	0.69	0.74	0.69	461.60	0.46	0.11	0.16
East Europe	0.83	0.45	0.03	1.27	0.75	0.62	173.69	0.45	0.04	0.06
Middle East	0.07	0.02	0.00	0.08	0.75	0.05	65.56	0.45	0.02	0.30
Sub-Saharan Africa	2.16	0.00	2.16	0.00	0.78	1.68	568.87	0.60	0.17	0.10
Central Asia	1.24	0.02	0.25	1.57	0.75	0.93	338.88	0.47	0.09	0.10
South Asia	0.37	0.02	0.26	0.15	0.77	0.28	403.87	0.54	0.13	0.45
Southeast Asia	2.14	0.01	2.16	0.01	0.78	1.67	278.26	0.60	0.10	0.06
Average/Total	**12.43**	**1.55**	**8.47**	**4.62**	**0.76**	**9.56**	**651.26**	**0.53**	**0.95**	**0.17**
Remote										
North America	1.59	2.44	0.05	0.79	0.74	1.17	-	-	-	-
Central America	0.09	0.00	0.07	0.02	0.77	0.06	-	-	-	-
South America	4.19	0.05	4.54	0.04	0.78	3.71	-	-	-	-
Oceania	0.38	0.01	0.31	0.00	0.78	0.35	-	-	-	-
West Europe	0.07	0.15	0.00	0.01	0.73	0.06	-	-	-	-
East Europe	1.66	3.07	0.01	1.40	0.74	1.33	-	-	-	-
Middle East	0.00	0.00	0.00	0.00	0.75	0.00	-	-	-	-
Sub-Saharan Africa	1.03	0.00	0.85	0.00	0.78	0.69	-	-	-	-
Central Asia	0.06	0.02	0.00	0.11	0.75	0.03	-	-	-	-
South Asia	0.03	0.01	0.01	0.01	0.78	0.02	-	-	-	-
Southeast Asia	0.94	0.00	0.87	0.01	0.76	0.75	-	-	-	-
Average/Total	**10.04**	**5.76**	**6.71**	**2.39**	**0.76**	**8.16**	**-**	**-**	**-**	**-**

[a]NPP represents the MODIS-derived total annual NPP averaged from 2000-2010. [b]FAO represents regionally aggregated data recorded by the Food and Agriculture Organization of the United Nations and averaged over multiple years. [c]r_{abv} represents the ratio of aboveground-to-total biomass, estimated as a weighted average using literature-derived biomass ratio estimates of 0.73, 0.78, and 0.75 for coniferous (C), broadleaf (B), and mixed (M) forestlands, respectively. [d]Density represents average wood density, estimated by region as a weighted average using literature-derived wood density estimates of 0.43, 0.6, and 0.45 for coniferous (C), broadleaf (B), and mixed (M) forestlands, respectively. [e]r_{harv} represents the ratio of H_{TOTAL} to ANPP, utilized to estimate forest harvest.

Table S1.2. Current global crop harvest by region.

Region	NPP[a] ($PgC\ yr^{-1}$)	NPP_{AVG} ($gC\ m^{-2}\ yr^{-1}$)	Area (Mkm^2)	H_{TOTAL}[b] ($PgC\ yr^{-1}$)	H_{REC}[b] ($PgC\ yr^{-1}$)	H_{LOSS}[b] ($PgC\ yr^{-1}$)	H_{RES}[b] ($PgC\ yr^{-1}$)
North America	1.14	445.43	2.55	0.95	0.43	0.33	0.19
Central America	0.36	760.56	0.47	0.30	0.14	0.11	0.06
South America	0.54	680.85	0.79	0.45	0.20	0.16	0.09
Oceania	0.12	401.97	0.31	0.10	0.05	0.04	0.02
West Europe	1.32	564.99	2.34	1.10	0.50	0.39	0.22
East Europe	0.66	378.63	1.74	0.55	0.25	0.19	0.11
Middle East	0.23	357.29	0.65	0.19	0.09	0.07	0.04
Sub-Saharan Africa	0.51	379.82	1.34	0.43	0.19	0.15	0.09
Central Asia	0.67	385.07	1.73	0.56	0.25	0.19	0.11
South Asia	0.76	276.72	2.73	0.63	0.28	0.22	0.13
Southeast Asia	0.33	577.46	0.57	0.27	0.12	0.10	0.05
Average/Total	**6.63**	**435.58**	**15.22**	**5.54**	**2.49**	**1.94**	**1.11**

[a]NPP represents the MODIS-derived total annual NPP averaged from 2000-2010. [b]Harvest pools (H) estimated according to Equations 1-4.

Supplementary Table S1.3. Current global forestry harvest by region.

Region	NPP[a] (PgC yr^{-1})	NPP_{AVG} (gC m^{-2} yr^{-1})	Area (M km^2)	H_{TOTAL}[b] (PgC yr^{-1})	H_{REC}[b] (PgC yr^{-1})	H_{LOSS}[b] (PgC yr^{-1})	H_{RES}[b] (PgC yr^{-1})
North America	1.14	677.68	1.68	0.14	0.08	0.01	0.06
Central America	0.65	949.80	0.68	0.03	0.01	0.00	0.01
South America	2.16	1153.84	1.87	0.11	0.05	0.02	0.04
Oceania	0.76	1356.03	0.56	0.02	0.01	0.00	0.01
West Europe	0.92	670.03	1.38	0.11	0.05	0.02	0.04
East Europe	0.83	472.96	1.75	0.04	0.02	0.00	0.01
Middle East	0.07	709.27	0.10	0.02	0.01	0.00	0.01
Sub-Saharan Africa	2.16	998.00	2.16	0.17	0.08	0.02	0.07
Central Asia	1.24	671.96	1.84	0.09	0.04	0.02	0.03
South Asia	0.37	836.35	0.44	0.13	0.05	0.03	0.05
Southeast Asia	2.14	984.51	2.18	0.10	0.04	0.02	0.04
Average/Total	**12.43**	**848.96**	**14.65**	**0.95**	**0.45**	**0.14**	**0.36**

[a]NPP represents the MODIS-derived total annual NPP averaged from 2000-2006 [6-8]. [b]Harvest pools (H) estimated according to Equations 1-4.

Table S1.4. Bioenergy potential of agricultural lands by region.

Region	NPP[a] ($PgC\ yr^{-1}$)	NPP_{AVG} ($gC\ m^{-2}\ yr^{-1}$)	Area (Mkm^2)	PBP_{CAP}[b] ($EJ\ yr^{-1}$)	PBP_{MAX}[b] ($EJ\ yr^{-1}$)	PBP_{MOD}[b] ($EJ\ yr^{-1}$)	PBP_{MIN}[b] ($EJ\ yr^{-1}$)
Crop							
North America	1.14	445.43	2.55	24.65	7.58	7.58	7.58
Central America	0.36	760.56	0.47	7.80	2.40	2.40	2.40
South America	0.54	680.85	0.79	11.73	3.61	3.61	3.61
Oceania	0.12	401.97	0.31	2.68	0.82	0.82	0.82
West Europe	1.32	564.99	2.34	28.69	8.83	8.83	8.83
East Europe	0.66	378.63	1.74	14.28	4.39	4.39	4.39
Middle East	0.23	357.29	0.65	5.05	1.55	1.55	1.55
Sub-Saharan Africa	0.51	379.82	1.34	11.08	3.41	3.41	3.41
Central Asia	0.67	385.07	1.73	14.48	4.46	4.46	4.46
South Asia	0.76	276.72	2.73	16.40	5.05	5.05	5.05
Southeast Asia	0.33	577.46	0.57	7.10	2.19	2.19	2.19
Average/Total	**6.63**	**435.58**	**15.22**	**143.94**	**44.29**	**44.29**	**44.29**
Pasture							
North America	0.65	249.04	2.60	14.05	12.16	-	-
Central America	0.29	399.53	0.72	6.25	5.94	-	-
South America	2.85	628.45	4.54	61.92	60.82	-	-
Oceania	0.68	214.36	3.16	14.72	11.49	-	-
West Europe	0.30	744.64	0.40	6.48	6.47	-	-
East Europe	0.13	294.68	0.42	2.72	2.65	-	-
Middle East	0.13	202.68	0.62	2.72	2.27	-	-
Sub-Saharan Africa	3.07	394.69	7.78	66.70	63.32	-	-
Central Asia	1.14	191.97	5.92	24.68	18.25	-	-
South Asia	0.08	104.67	0.76	1.72	0.71	-	-
Southeast Asia	0.01	709.16	0.02	0.25	0.25	-	-
Average/Total	**9.31**	**345.68**	**26.94**	**202.21**	**184.33**	**-**	**-**
Accessible Range							
North America	0.54	601.37	0.90	11.70	11.58	11.58	-
Central America	0.20	549.59	0.37	4.41	4.36	4.36	-
South America	1.03	555.84	1.86	22.40	22.23	22.23	-
Oceania	0.17	619.76	0.27	3.68	3.63	3.63	-
West Europe	0.47	623.73	0.75	10.11	10.05	10.05	-
East Europe	0.18	315.38	0.56	3.87	3.72	3.72	-
Middle East	0.16	308.82	0.53	3.54	3.25	3.25	-
Sub-Saharan Africa	2.15	548.60	3.93	46.77	45.82	45.82	-
Central Asia	0.35	435.76	0.80	7.54	7.37	7.37	-
South Asia	0.18	297.98	0.59	3.84	3.57	3.57	-
Southeast Asia	0.29	665.32	0.43	6.20	6.18	6.18	-
Average/Total	**5.71**	**520.33**	**10.98**	**124.05**	**121.77**	**121.77**	**-**
Remote Range							
North America	0.93	217.72	4.26	20.16	17.72	-	-
Central America	0.03	283.56	0.11	0.71	0.66	-	-
South America	0.59	431.02	1.37	12.82	12.43	-	-
Oceania	0.59	191.35	3.08	12.80	9.05	-	-
West Europe	0.06	210.79	0.28	1.29	1.14	-	-
East Europe	1.44	213.91	6.71	31.16	27.90	-	-
Middle East	0.00	89.09	0.05	0.10	0.03	-	-
Sub-Saharan Africa	1.01	448.55	2.25	21.95	21.19	-	-
Central Asia	0.06	127.69	0.48	1.34	0.96	-	-
South Asia	0.02	540.75	0.03	0.33	0.32	-	-
Southeast Asia	0.04	684.25	0.06	0.87	0.87	-	-
Average/Total	**4.77**	**255.04**	**18.70**	**103.52**	**92.28**	**-**	**-**
Protected Range							
Average/Total	**0.62**	**246.03**	**2.52**	**16.00**	**-**	**-**	**-**

[a]NPP represents the MODIS-derived total annual NPP averaged from 2000-2010. [b]Primary bioenergy potential (PBP) estimated according to Equations 5-8.

Table S1.5. Bioenergy potential of forest lands by region.

Region	NPP[a] (PgC yr^{-1})	NPP_{AVG} (gC m^{-2} yr^{-1})	Area (M km^2)	PBP_{CAP}[b] (EJ yr^{-1})	PBP_{MAX}[b] (EJ yr^{-1})	PBP_{MOD}[b] (EJ yr^{-1})	PBP_{MIN}[b] (EJ yr^{-1})
Accessible Forest							
North America	1.14	677.68	1.68	6.45	3.30	2.26	2.26
Central America	0.65	949.80	0.68	3.54	3.01	0.41	0.41
South America	2.16	1153.84	1.87	11.09	9.07	1.68	1.68
Oceania	0.76	1356.03	0.56	4.35	3.99	0.26	0.26
West Europe	0.92	670.03	1.38	4.74	2.68	1.63	1.63
East Europe	0.83	472.96	1.75	4.42	3.66	0.58	0.58
Middle East	0.07	709.27	0.10	0.53	0.23	0.23	0.23
Sub-Saharan Africa	2.16	998.00	2.16	11.67	8.33	2.62	2.62
Central Asia	1.24	671.96	1.84	6.00	4.44	1.34	1.34
South Asia	0.37	836.35	0.44	4.04	1.88	1.88	1.88
Southeast Asia	2.14	984.51	2.18	10.47	8.84	1.45	1.45
Average/Total	**12.43**	**848.96**	**14.65**	**67.30**	**49.43**	**14.34**	**14.34**
Remote Forest							
North America	1.59	483.00	3.29	8.75	8.75	-	-
Central America	0.08	861.41	0.09	0.41	0.41	-	-
South America	4.76	1028.83	4.63	24.49	24.49	-	-
Oceania	0.44	1409.38	0.32	2.56	2.56	-	-
West Europe	0.08	458.29	0.17	0.39	0.39	-	-
East Europe	1.80	402.14	4.48	9.50	9.50	-	-
Middle East	0.00	605.60	0.00	0.00	0.00	-	-
Sub-Saharan Africa	0.88	1041.06	0.85	4.79	4.79	-	-
Central Asia	0.04	326.09	0.13	0.21	0.21	-	-
South Asia	0.03	791.75	0.03	0.13	0.13	-	-
Southeast Asia	0.99	1123.90	0.88	4.68	4.68	-	-
Average/Total	**10.69**	**719.35**	**14.86**	**55.90**	**55.90**	**-**	**-**
Protected Forest							
Average/Total	**2.79**	**908.79**	**3.07**	**14.40**	**-**	**-**	**-**

[a]NPP represents the MODIS-derived total annual NPP averaged from 2000-2010.
[b]Primary bioenergy potential (PBP) estimated according to Equations 5-8.

Figure S1.1. Regional map. Regions were aggregated according to the classification of the macro geographical regions and geographic sub-regions as defined by the United Nations Statistical Division.

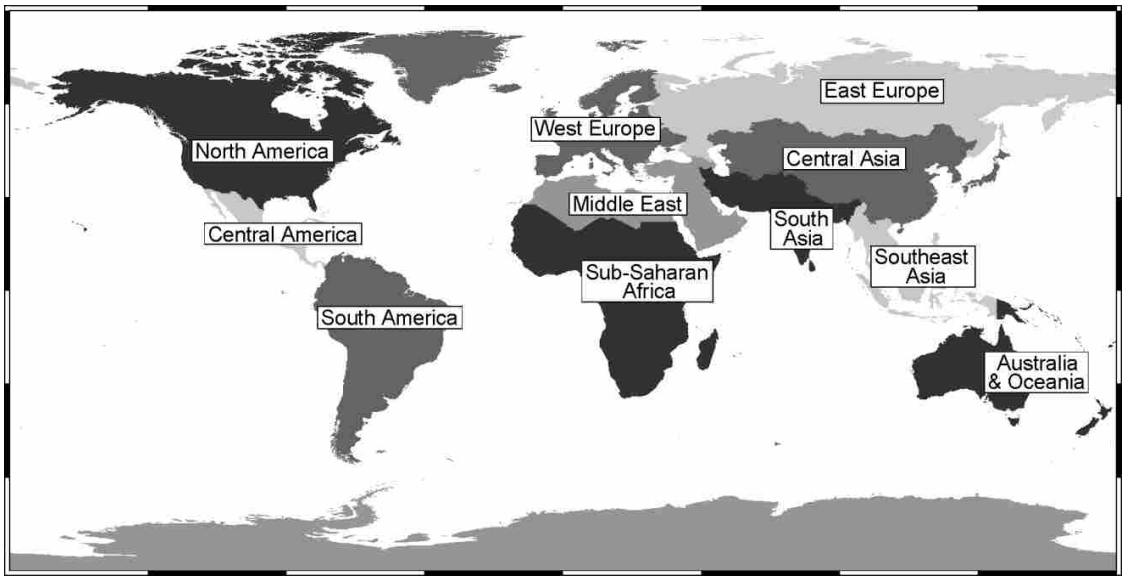

Figure S1.2. Current global harvest. **a**, Total cropland harvest (H_{TOTAL}; gC m^{-2} yr^{-1}). **b**, Total forestry harvest (H_{TOTAL}; gC m^{-2} yr^{-1}).

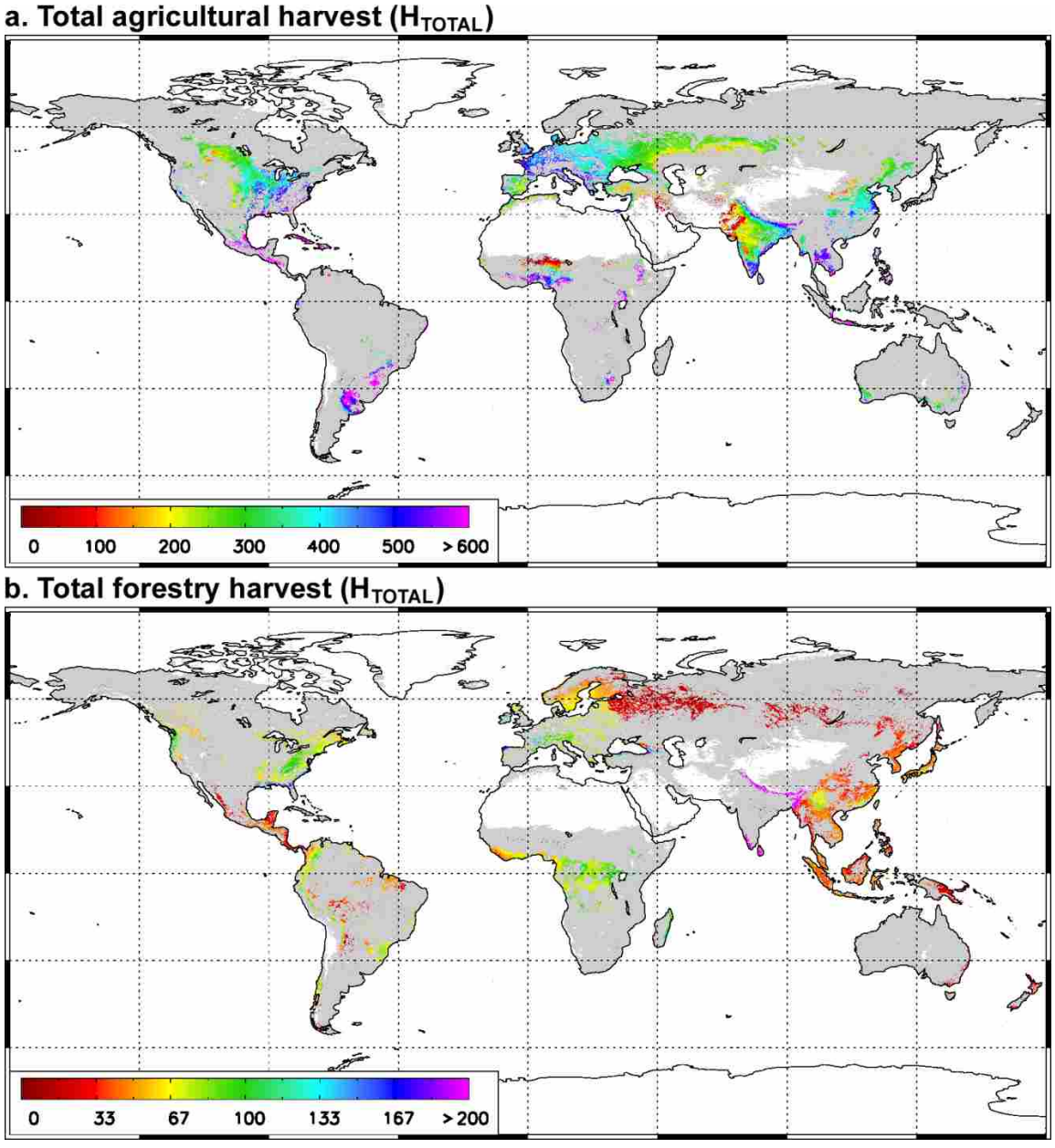

CHAPTER 2

Bioenergy potential of the United States constrained by satellite observations of existing productivity

Introduction

Concerns about energy security and rising greenhouse gas (GHG) emissions continue to stimulate an unprecedented increase in the utilization of biomass as a source of renewable energy (bioenergy) (Scarlat & Dallemand 2011). The United States (U.S.) leads this current bioenergy trend, producing 40 billion liters of ethanol (secondary bioenergy) in 2009, approximately half of the world's total ethanol supply (Scarlat & Dallemand 2011). Current renewable energy policy, namely the Energy Independence and Security Act of 2007 (EISA), has established even more ambitious secondary bioenergy targets for the U.S., stipulating a domestic ethanol production of 136 billion liters by 2022 (US Congress 2007).

Yet, these bioenergy targets are largely derived from highly uncertain estimates of future bioenergy potential, commonly based on implicit assumptions regarding relatively unresolved, complex factors such as yield potential, land availability, and energy conversion technology (Field *et al.* 2008; Campbell *et al.* 2008; Dornburg *et al.* 2010; Haberl *et al.* 2010; Johnston *et al.* 2011). In fact, evidence indicates that previous evaluations have generally over-estimated bioenergy potential, suggesting that bioenergy policy targets based on these previous evaluations could be unrealistic (Field *et al.* 2008; Campbell *et al.* 2008; Dornburg *et al.* 2010; Haberl *et al.* 2010; Johnston *et al.* 2011). For instance, a number of previous evaluations have simply applied crop-specific maximum yield values across all land considered available for bioenergy cultivation (Lubowski *et al.* 2006; UN 2009; Pan *et al.* 2011). Applying maximum yield values across spatial scales without adequate consideration of biophysical factors (e.g., temperature and precipitation), has been documented to overestimate bioenergy

potentials by more than 100% in particular cases (Johnston *et al.* 2011). Despite these findings, policy-oriented studies that utilize this methodology are still being published, and have the potential to adversely influence the success of energy policy (Lubowski *et al.* 2006; UN 2009; Pan *et al.* 2011).

Constraining estimates of primary bioenergy potential (PBP) represents a significant step forward in our ability to define realistic future energy targets. Here, we utilized 1-km^2 net primary productivity (NPP) values - estimated from satellite data [Earth Observing System (EOS), Moderate Resolution Imaging Spectroradiometer (MODIS) data] - as an upper-envelope constraint on PBP of the conterminous U.S. (Running *et al.* 2004; Zhao *et al.* 2005; Zhao & Running 2010). MODIS NPP integrates global climatic data (e.g., temperature and precipitation), as well as remotely-sensed vegetation dynamics [e.g., Fraction of Photosynthetically Active Radiation (FPAR) and Leaf Area Index (LAI) data], providing quantitative estimates of current terrestrial biomass growth capacity for every 1-km^2 of vegetated land (Running *et al.* 2004; Zhao *et al.* 2005; Zhao & Running 2010). This approach differs from multiple previous efforts (Lubowski *et al.* 2006; UN 2009; Pan *et al.* 2011) in that the utilization of satellite-derived spatial data removes the need for extrapolation of plot-level bioenergy yield potentials.

NPP is influenced by a number of factors including vegetation type, soil type, climate, and human management. However, it has been shown that over relatively large areas, average agricultural productivity is significantly lower than that of the natural vegetation it replaced (Vitousek *et al.* 1986; DeFries 2002; Haberl *et al.* 2007). Even when considering human management factors that can offset or reverse this trend (e.g., fertilization and especially irrigation), the conversion of natural vegetation to agriculture

generally elicits relative declines in productivity (Vitousek *et al.* 1986; DeFries 2002; Haberl *et al.* 2007). For example, Haberl *et al.* (2007) documented that, despite wide-spread utilization of the most advanced human management practices, agricultural productivity across the U.S. was still generally less than the natural potential. Since bioenergy cultivation is subject to similar agriculturally-based human management practices, we applied this logic and utilized MODIS NPP as an upper-envelope constraint on yield potential (Field *et al.* 2008; Campbell *et al.* 2008). We also accounted for currently unavailable resources by applying constraints that included current rates of harvest (i.e., agricultural and forestry harvest) and unavailable landcover (i.e., protected areas, pastureland, wetland, and low productivity regions). Finally, we compared our resulting PBP estimates with current U.S. secondary bioenergy targets by applying well-known secondary-to-primary bioenergy conversion factors. Ultimately, our goal was to constrain estimates of PBP for the conterminous U.S. utilizing MODIS NPP as the most geographically explicit measure of the current terrestrial growth capacity in an effort to evaluate the feasibility of current U.S. bioenergy policy.

Methods

Landcover classification. We utilized a composite 1-km^2 landcover classification scheme for the conterminous U.S. that combined National Landcover and Global Human Footprint data (*http://sedac.ciesin.columbia.edu/wildareas/downloads.jsp*) (Fig. 2.1). Relevant landcover classes were separated into "managed" or "remote" utilizing a human footprint index of 10%, meaning remote lands represent the 10% most inaccessible land while managed lands represent the 90% most accessible land in the U.S. We also defined

"unavailable land" to include protected areas, pastureland, wetland, and low productivity regions (Fig. S2.1). Protected areas were defined as land under strict protection including nature reserves and national parks, which we considered unavailable for bioenergy production based on current policy (*www.wdpa.org*). Pasturelands were defined as areas specifically managed for livestock grazing, while wetlands were defined as areas periodically saturated or covered with water, according to National Landcover Data (*http://landcover.usgs.gov/*). We classified pastures and wetlands as unavailable due to the many negative tradeoffs associated with conversion of these landcover types (Campbell *et al.* 2008; Dornburg *et al.* 2010; Haberl *et al.* 2010). Finally, low productivity regions were defined as areas with annual productivity less than 150 gC m^{-2} yr^{-1}, the threshold at which harvest energy requirements exceed potential energy output (Schmer *et al.* 2008).

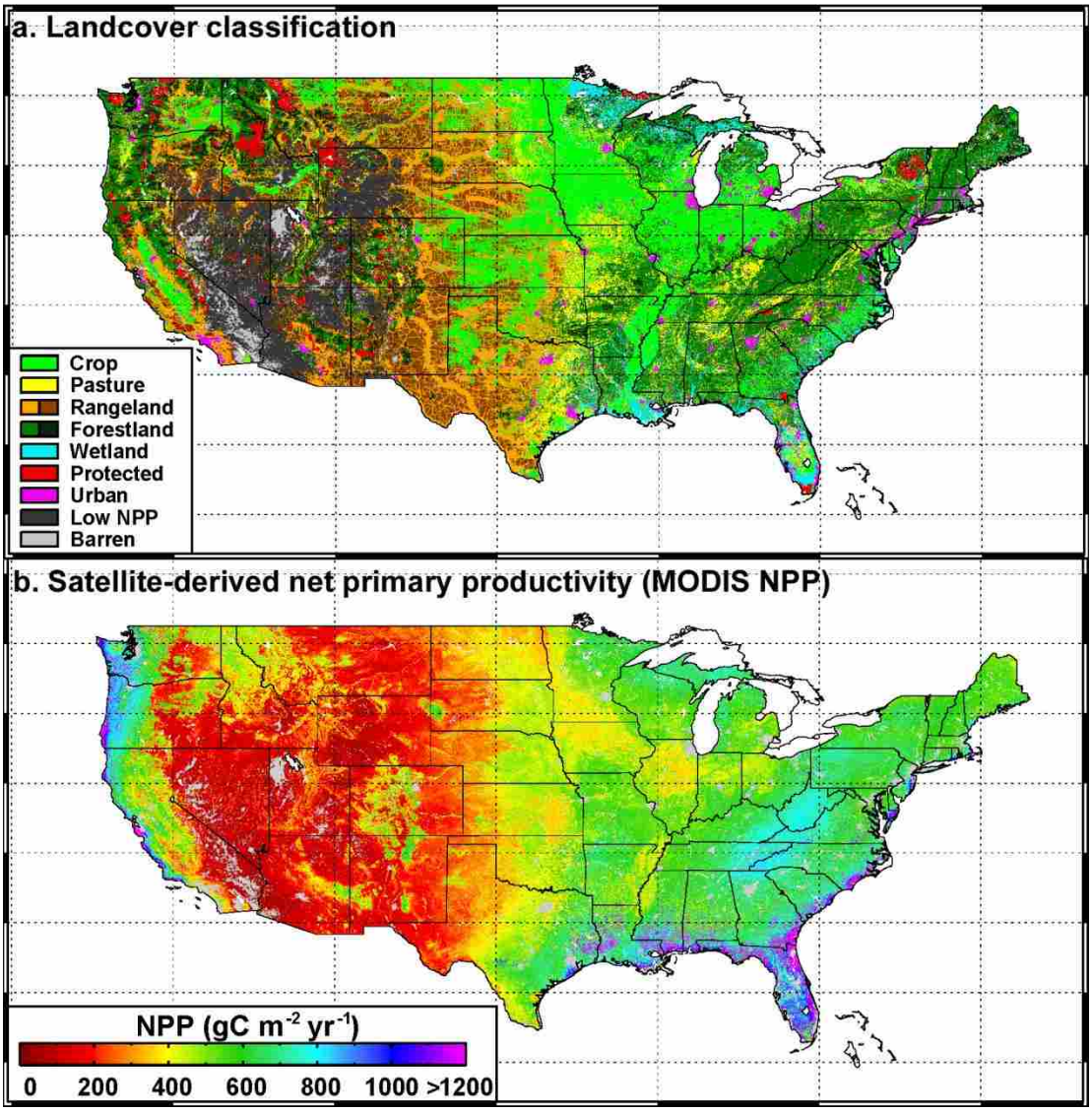

Figure 2.1. Spatially-explicit landcover classification and associated net primary productivity of the conterminous United States. **a**, Landcover classification. Classes represent the composite of National Landcover Data, Global Human Footprint, and World Database on Protected Areas datasets. For range and forest land, light colors represent managed land while dark colors represent remote land. Low productivity (Low NPP) landcover was assigned according a productivity threshold of 150 gC m^{-2} yr^{-1} utilizing MODIS NPP data. **b**, Satellite-derived net primary productivity (MODIS NPP). Estimated from the MODIS GPP/NPP algorithm from 2000-2006.

MODIS GPP/NPP algorithm. We utilized the MODIS GPP/NPP algorithm (Running *et al.* 2004; Zhao *et al.* 2005; Zhao & Running 2010) to calculate 1-km^2 MODIS NPP from 2000 through 2006 for the conterminous U.S. (Fig. 2.1). Biome-specific vegetation parameters were mapped utilizing 11 biome types that corresponded well with our NLCD-based landcover classification (Running *et al.* 2004; Zhao *et al.* 2005; Zhao & Running 2010). Remotely sensed vegetation property dynamic inputs included collection 5 (C5), 8-day composite, 1-km^2 Fraction of Photosynthetically Active Radiation (FPAR) and Leaf Area Index (LAI) data collected from the MODIS sensor (Running *et al.* 2004; Zhao *et al.* 2005; Zhao & Running 2010). Accompanying quality assessment fields were utilized to fill data gaps in the 8-day temporal MODIS FPAR/LAI caused by cloudiness (Running *et al.* 2004; Zhao *et al.* 2005; Zhao & Running 2010). Daily data obtained from the Data Assimilation Office (DAO) served as the meteorological input required to drive the algorithm(Running *et al.* 2004; Zhao *et al.* 2005; Zhao & Running 2010). A more detailed description and validation of the MODIS GPP/NPP algorithm can be found in Zhao *et al.* (2005).

Agricultural and forestry harvest. Agricultural and forestry harvest was assumed to occur only on cropland and managed forestlands, respectively (Fig. 2.1). We partitioned harvest into four relevant harvest pools: (1) total harvest (H_{TL}) or the total amount of non-living biomass following harvest; (2) recovered harvest (H_{RC}) or the fraction of H_{TL} recovered during harvest; (3) harvest losses (H_{LS}) or the fraction of H_{TL} remaining in the field following harvest; or (4) harvest residues (H_{RS}) or the fraction of H_{LS} recoverable without impacting natural nutrient cycling (primary residues, e.g., felled branches), plus

the fraction of H_{RC} that is ultimately remaining following processing (secondary residues, e.g., sawdust). Harvest pools were estimated regionally (Fig. S2.2) at a spatial resolution of 1-km^2 according to Equations 2.1-2.4:

$$H_{TL} = \sum_{i=1}^{n} NPP_i \times r_{ag} \times r_{hv}\ ; \qquad 2.1$$

Where r_{ag} and r_{hv} represent literature-derived aboveground NPP and total harvest ratios, respectively. For agricultural harvest, we utilized aboveground NPP (r_{ag}) and total harvest (r_{hv}) ratios of 0.83 (range: 0.80-0.85) and 1.00 (range: 1.00-1.00), respectively (Table S2.1). These values represent the average for the three dominant U.S. crop types (i.e. maize, soybean, and wheat), which account for roughly 70% of total agricultural area (Lobell *et al.* 2002; Monfreda *et al.* 2008). Due to substantial regional variability regarding forest C allocation and harvest rates, r_{ag} and r_{hv} were estimated regionally (Fig. S2.2) according to literature-derived aboveground NPP ratios (Roy *et al.* 2001) and average harvest volume data (Howard *et al.* 2009) (Table S2.2). H_{TL} was calculated as the sum of all vegetated pixels (n). H_{RC}, H_{LS}, and H_{RS} were estimated as proportional to H_{TL} according to Equations 2.2-2.4:

$$H_{RC} = \sum_{i=1}^{n} (H_{TL_i} \times r_{rc} \times (1 - r_{rs2}))\ ; \qquad 2.2$$

$$H_{LS} = \sum_{i=1}^{n} (H_{TL_i} \times (1 - r_{rc}) \times (1 - r_{rs1}))\ ; \qquad 2.3$$

$$H_{RS} = \sum_{i=1}^{n} (H_{TL_i} \times (1 - r_{rc}) \times r_{rs1} + H_{TL_i} \times r_{rc} \times r_{rs2})\ ; \qquad 2.4$$

Where r_{rc}, r_{rs1}, and r_{rs2} represent literature-derived ratios describing H_{TL} recovered, H_{LS} recoverable without impacting nutrient cycling (primary residuals), and H_{RS} available

following harvest processing (secondary residuals), respectively. For agricultural harvest, we utilize an agricultural harvest recovery ratio (r_{rc}) of 0.50 (range: 0.40-0.60; Smeets & Faaij 2007) and a secondary residue ratio (r_{rs2}) of 0.10 (range: 0.05-0.15; Smeets & Faaij 2007) resulting in a final ratio of yield to aboveground biomass of 0.45 (range: 0.38-0.52), which is consistent with values reported for the three dominant U.S. crop types (Table S1.1) (Lobell *et al.* 2002; Monfreda *et al.* 2008). For forest harvest, r_{rc} and r_{rs2} were estimated to be 0.85 (range: 0.75-0.95) and 0.40 (range: 0.30-0.50), respectively (Table S2.1) (Smeets *et al.* 2007; Haberl *et al.* 2007). These values represent the average for North American coniferous and deciduous species (Smeets *et al.* 2007; Haberl *et al.* 2007). Finally, we utilized an average primary field residual recovery rate (r_{rs1}) of 0.30 (range: 0.25-0.35) for both agricultural and forestry harvest (Table S1.1) (Smeets *et al.* 2007; Gregg & Smith 2010). A summary of the calculated agricultural and forestry harvest pools for the conterminous U.S. are presented by region in Table S2.3. Additionally, a spatial representation of current total harvest (H_{TL}) is shown in Fig. S2.3.

Maximum sustainable harvest. Maximum sustainable harvest (MSH_{TL}, MSH_{RC}, MSH_{LS}, MSH_{RS}) was calculated utilizing Equations 1-4, by simply replacing the current harvest ratio (r_{hv}) with a literature-derived MSH ratio (r_{msh}) (Equation 2.1). For agricultural systems, r_{msh} equaled r_{hv} which equaled 1.00 (range 1.00-1.00), under the assumption that all aboveground biomass is typically destroyed during harvest and current harvest recovery rates are already maximized in the U.S. (Table S2.1) (Smeets *et al.* 2007; Haberl *et al.* 2007). It is important to note that we do not consider the potential to increase productivity on current agricultural land up to that of the natural vegetation

replaced (Johnston *et al.* 2011; Foley *et al.* 2011). For forest systems, a r_{msh} of 0.20 (range: 0.15-0.25) was utilized based on current forestry harvest trends (Table S2.1) (Smeets *et al.* 2007; Haberl *et al.* 2007). We utilize a maximum sustainable forest harvest value consistent with the highest current global forestry harvest rates (Smeets *et al.* 2007; Haberl *et al.* 2007), which results in a near doubling of current average U.S. forest harvest (Table S2.3). Values for maximum sustainable forest harvest could increase in the future if natural forests are replaced with high yielding plantations; however, we consider this potential outside the scope of this analysis.

Primary bioenergy potential. We calculated PBP based on the assumption that biomass available for energy production could be derived from either intensifying harvest on currently harvested land (intensification) or expanding harvest to currently available non-harvested land (extensification) (Fig. 2.2). Intensification (PBP_I) was divided into two pools, PBP of current harvest residuals (PBP_{RS}) and PBP of maximum additional harvest on currently harvested land (PBP_{AD}) and calculated by summing over currently harvested land (n_{hv}). Again, for agricultural intensification we do not consider the potential to increase productivity up to that of the natural vegetation replaced (Johnston *et al.* 2011; Foley *et al.* 2011), and we therefore only estimate residual potential (PBP_{RS}). We calculate PBP_I according to Equations 2.5-2.7:

$$PBP_{RS} = \sum_{i=1}^{n_{hv}} (H_{RS_i}); \quad 2.5$$

$$PBP_{AD} = \sum_{i=1}^{n_{hv}} ((MSH_{RC_i} + MSH_{RS_i}) - (H_{RC_i} + H_{RS_i})); \quad 2.6$$

$$PBP_I = \sum_{i=1}^{n_{hv}} (GBP_{AD_i} + GBP_{RS_i}); \quad 2.7$$

Extensification (PBP_X) was estimated considering all currently non-harvested land excluding land areas defined as unavailable (n_{nhv}). We calculated PBP_X according to Equation 2.8:

$$PBP_X = \sum_{i=1}^{n_{nhv}} (MSH_{RC_i} + MSH_{RS_i}); \quad 2.8$$

We further subdivided extensification between managed land (PBP_{MX}) and remote land (PBP_{RX}) according to a human footprint index threshold equivalent to roughly the 10% most inaccessible areas in the U.S. A summary of the calculated PBP pools for the conterminous U.S. is presented by region in Tables S2.4 and S2.5, respectively. In addition, spatial representations of PBP are shown in Fig. S2.4 and S2.5, respectively.

Bioenergy conversion. We converted biomass (PgC yr^{-1}) and ethanol targets (liters yr^{-1}) to primary bioenergy potential (PBP; EJ yr^{-1}) according to Equations 2.9 and 2.10, respectively:

$$PBP = biomass \times \frac{CF_{energy}}{CR_{biomass}}; \quad 2.9$$

$$PBP = ethanol \times \frac{CF_{energy}}{CF_{ethanol}}; \quad 2.10$$

Where PBP (EJ yr^{-1}) was estimated from biomass (PgC yr^{-1}) assuming a 0.45 C to dry biomass ratio ($CR_{biomass}$) and an 18.0 MJ kg^{-1} primary energy content ratio for dry biomass (CF_{energy}) (Williams & Percival 1987; Tsubo *et al.* 2001). Additionally, PBP (EJ yr^{-1}) was estimated from ethanol (liters yr^{-1}) assuming an ethanol to dry biomass energy

conversion efficiency ($CF_{ethanol}$) of 3.79×10^{-4} and 3.03×10^{-4} liters g^{-1} for starch-derived and cellulosic-derived ethanol, respectively (Field *et al.* 2008).

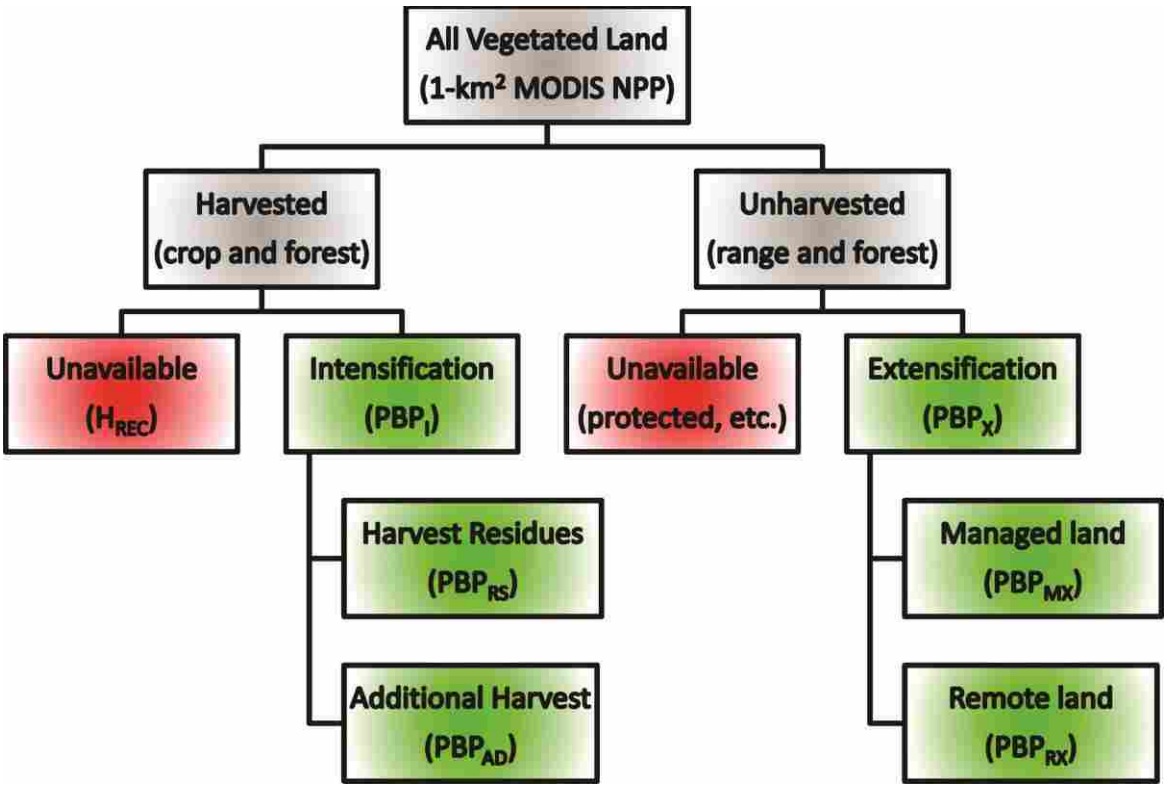

Figure 2.2. Flow diagram for the quantification of landcover and primary bioenergy potential (PBP) pools. PBP pools include extensification (PBP_X) divided between managed land (PBP_{MX}) and remote land (PBP_{RX}) extensification, and intensification (PBP_I) divided between residual (PBP_{RS}) and additional (PBP_{AD}) harvest. Unavailable resources were defined to include current agricultural and forestry harvest (H_{RC}) as well as protected areas, wetlands, pasturelands, and low productivity regions. Green indicates PBP pools while red indicates unavailable pools.

Discussion

NPP and landcover of the conterminous United States. We estimated the primary bioenergy potential (PBP) of the conterminous U.S. using satellite-derived NPP as an upper-envelope constraint, since agricultural productivity is typically less than the natural potential (Vitousek *et al.* 1986; DeFries 2002; Haberl *et al.* 2007; West *et al.* 2010). We estimated that NPP for the conterminous U.S. is 3.16 PgC yr^{-1}, which is similar to Melillo *et al.* (1995) previous values of 3.13-3.77 PgC yr^{-1} and 3.30 PgC yr^{-1} reported by and Tian *et al.* (1999), respectively (Table 2.1). In addition, our estimated total crop NPP and total forestry harvest (H_{TL}) values (0.61 and 0.12 PgC yr^{-1}, respectively), are similar to previous values of 0.62 and 0.12 PgC yr^{-1} reported by Lobell *et al.* (2002) and Turner & Koerper (1995), respectively (Table 2.1; Table S2.3).

We assumed that protected lands, pastures, wetlands, and low productivity regions were unavailable for bioenergy production. Because our definition of protected lands included national parks and nature reserves only, our estimated protected land extent (0.25 Mkm^2), is significantly less than total U.S. protected area (1.19 Mkm^2; Edenhofer 2011) (Table 2.1). In addition, the extent of pastures – defined as areas managed solely for livestock grazing – was 0.55 Mkm^2, which is significantly less than the estimated extent of total U.S. grazing lands (2.36 Mkm^2; Edenhofer 2011) (Table 2.1). Finally, we estimated that U.S. wetland and low productivity regions occupy 1.05 Mkm^2, similar to a value of 1.15 Mkm^2 reported by Edenhofer (2011) (Table 2.1). Again, we classified pastures and wetlands as unavailable due to the many negative tradeoffs (e.g. GHG emissions, deforestation) associated with displacement of these landcover types (Campbell *et al.* 2008; Dornburg *et al.* 2010; Haberl *et al.* 2010). It is important to note

that in the case of pastures especially, we significantly underestimate the full extent, since nearly all accessible U.S. rangeland is grazed to some extent (Edenhofer *et al.* 2011). By conservatively estimating unavailable land relative to the current literature, we remained consistent with our objective of providing an upper-envelope estimation of the PBP of the conterminous U.S.

Table 2.1. Total vegetated area and productivity by landcover type in the conterminous United States. Productivity was estimated from Moderate Resolution Imaging Spectroradiometer (MODIS) net primary productivity (NPP) data over the 2000-2006 period (Figure 1). Barren and urban landcover types were assumed to have no vegetation productivity and were not included in the analysis.

Landcover Type	Area (Mkm^2)	Total NPP ($PgC\ yr^{-1}$)	Mean NPP Range[a] ($gC\ m^{-2}\ yr^{-1}$)	Mean NPP Range[a,b] ($MJ\ m^{-2}\ yr^{-1}$)
Crop	1.39	0.61	308-570	12.3-22.8
Pasture	0.55	0.32	430-728	17.2-29.1
Managed Range	1.21	0.42	161-533	6.4-21.3
Remote Range	0.73	0.20	164-384	6.6-15.4
Managed Forest	1.73	1.09	410-850	16.4-34.0
Remote Forest	0.34	0.15	262-622	10.5-24.9
Wetlands	0.31	0.22	429-991	17.2-39.6
Protected	0.25	0.08	109-531	4.4-21.2
Low NPP	0.71	0.07	74-122	3.0-4.9
Total/Average	**7.22**	**3.16**	**196-680**	**7.8-27.2**

[a]Mean NPP Range represents a range of one standard deviation. [b]Mean NPP Range ($MJ\ m^{-2}\ yr^{-1}$) calculated from Mean NPP Range ($gC\ m^{-2}\ yr^{-1}$) according to Equation 2.9.

Primary bioenergy potential of the conterminous United States. Future increases in bioenergy production can be gained from either expanding harvest to currently non-harvested land (extensification) or increasing harvest on currently harvested land (intensification) (Fig. 2.2). We estimate that the maximum capacity for bioenergy production in the conterminous U.S. is 22.2 (± 4.4) EJ yr^{-1}, split between 14.6 (± 2.1) EJ yr^{-1} from extensification and 7.6 (± 2.3) EJ yr^{-1} from intensification (Table 2.2; Figures 2.3-2.4). Extensification (PBP_X) was divided between agricultural and forestry extensification, which were estimated as 13.5 (± 1.8) and 1.1 (± 0.3) EJ yr^{-1}, respectively (Table 2.2; Figures 2.3-2.4). We found that southcentral U.S. managed rangelands, southwest U.S. managed rangelands, and southwest U.S. remote rangelands have the largest associated extensification potential (Figure 2.5). Intensification (PBP_I) was divided between current harvest residues (PBP_{RS}) and additional harvest (PBP_{AD}), which we estimated to account for 5.9 (± 1.4) and 1.7 (± 0.8) EJ yr^{-1}, respectively (Table 2.2; Figures 2.3-2.4). The northcentral U.S. has the largest intensification potential, due to the region's relatively high agricultural harvest and associated agricultural residue potential (Figure 2.5). We found the northeast U.S. to be the region with the highest potential for additional forest harvest, due to relatively low current forest harvest rates (Figure 2.5).

Table 2.2. Primary bioenergy potential (PBP) of the conterminous United States.

Primary Bioenergy Potential	Area (Mkm^2)	Mean Yield Range[a] ($MJ\ m^{-2}\ yr^{-1}$)	Total PBP[b] ($EJ\ yr^{-1}$)
Agricultural Extensification (PBP_X)[b]	**1.94**	**3.4-10.6**	**13.5 (1.8)**
Managed Range (PBP_{MX})	1.21	3.5-11.9	9.2 (1.2)
Remote Range (PBP_{RX})	0.73	3.3-8.3	4.3 (0.6)
Forestry Extensification (PBP_X)[b]	**0.34**	**2.3-4.3**	**1.1 (0.3)**
Managed Forest (PBP_{MX})	--	--	--
Remote Forest (PBP_{RX})	0.34	2.3-4.3	1.1 (0.3)
Agricultural Intensification (PBP_I)[b]	**1.39**	**2.1-3.8**	**4.1 (1.0)**
Additional (PBP_{AD})	--	--	--
Residual (PBP_{RS})	1.39	2.1-3.8	4.1 (1.0)
Forestry Intensification (PBP_I)[b]	**1.73**	**1.4-2.8**	**3.5 (1.3)**
Additional (PBP_{AD})	1.73	0.7-1.6	1.7 (0.8)
Residual (PBP_{RS})	1.73	0.6-1.3	1.8 (0.4)
Total/Average	**5.40**	**2.3-5.4**	**22.2 (4.4)**

[a]Mean Yield Range represents a range of one standard deviation. [b]Primary bioenergy potential (PBP) calculated according to Equations 2.1-2.9. Values in parentheses represent parameter uncertainty as summarized in Table S2.1.

Average yield potential of the conterminous United States. We estimated an agricultural extensification potential (PBP_X) of 13.5 (± 1.8) EJ yr^{-1} for the conterminous U.S., which is significantly less than the estimate of 70.4 EJ yr^{-1} reported by the U.S. Department of Agriculture (Lubowski *et al.* 2006) and the United Nations (UN 2009) (Table 2.2; Figures 2.3-2.4). The main contributor to this discrepancy is differences in yield potential. We estimated average yield potential on managed rangelands to vary from 9.2-18.6 MJ m^{-2} yr^{-1}, while remote rangelands vary from 8.2-13.8 MJ m^{-2} yr^{-1} (Table 1). By contrast, the U.S. Department of Agriculture (2006) and the United Nations (2009) reported an average yield potential of approximately 30 MJ m^{-2} yr^{-1} over 2.35 Mkm^2 of assumed available U.S. grassland. This implies a yield potential almost three times greater than natural average U.S. rangeland productivity (Table 2.1). Even more striking, Pacca & Moreira (2011) utilized an average yield potential estimate of roughly 69 MJ m^{-2} yr^{-1} over 0.67 Mkm^2, and suggested that only 4% of global cropland area would be necessary to power the global automobile fleet. A yield potential estimate of 69 MJ m^{-2} yr^{-1} is more than double average natural productivity rates in the U.S. (Table 1).

How do we reconcile these vastly different estimates? First, it's important to note that the studies cited do not account for the geographic variability of biophysical factors, such as temperature and precipitation. Instead, maximum yield potential estimates were simply extrapolated over areas considered available, a method that has been previously shown to systemically over-estimate bioenergy potential per unit area (Johnston *et al.* 2009). Since agricultural productivity is almost always less than the natural productivity potential(Vitousek *et al.* 1986; DeFries 2002; Haberl *et al.* 2007), we argue that these yield potentials are unrealistic and thus ineffective in informing sound planning for

bioenergy development. We acknowledge that human management factors (e.g., fertilization and especially irrigation) can enhance yield potential, and assumptions regarding these factors could partially explain the large discrepancies in reported yield potential estimates (Vitousek *et al.* 1986; DeFries 2002; Haberl *et al.* 2007). However, due to concerns regarding resource availability in the U.S. (a factor discussed in detail below), sustaining yields that exceed natural rates of productivity over large areas may be unlikely (Johnston *et al.* 2011; Foley *et al.* 2011).

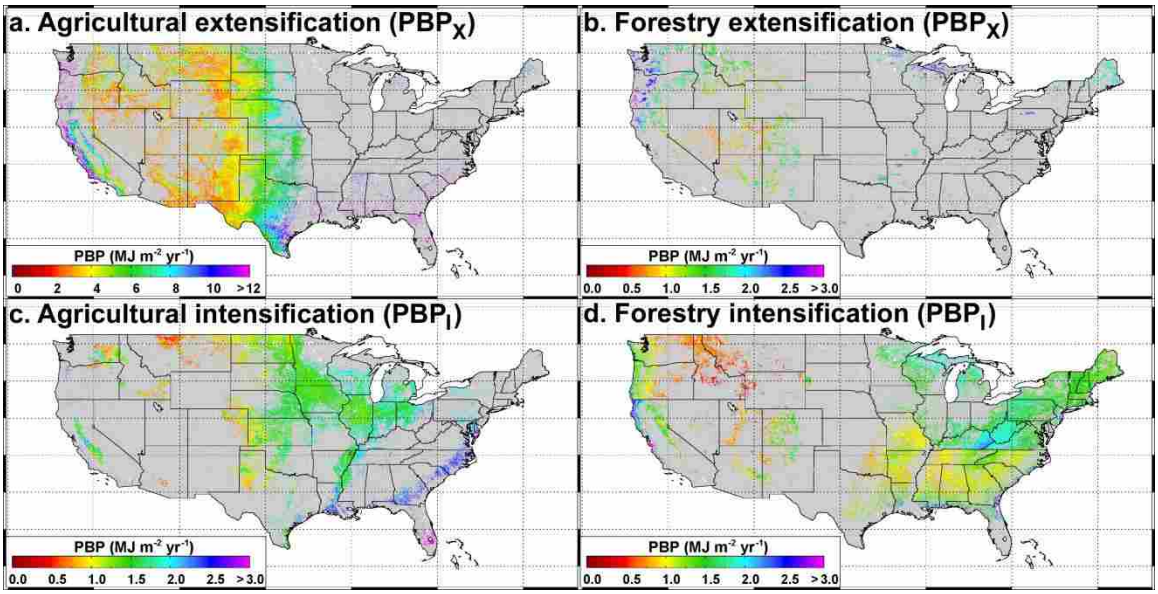

Figure 3. Spatially-explicit primary bioenergy potential (PBP) of the conterminous United States. PBP was calculated according to Equations 2.1-2.8 utilizing mean parameter values (Table S2.1). **a**, Agricultural extensification (PBP_X), including both managed (PBP_{MX}) and remote (PBP_{RX}) extensification. **b**, Forestry extensification (PBP_X) defined to include remote extensification (PBP_{RX}) only. **c**, Agricultural intensification (PBP_I) defined to include residual harvest (PBP_{RS}) only. **d**, Forestry Intensification potential (PBP_I), including both additional harvest (PBP_{AD}) and residual harvest (PBP_{RS}).

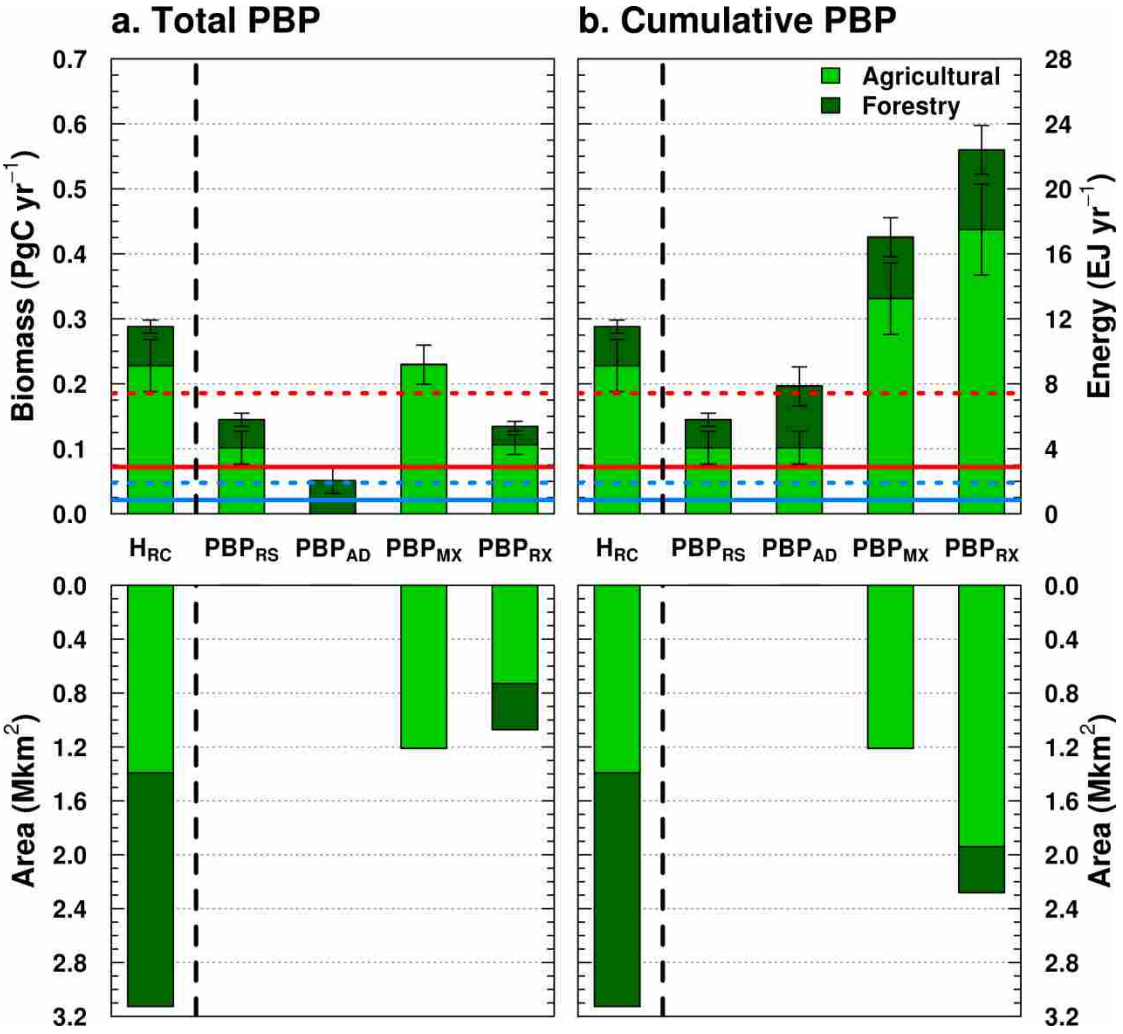

Figure 4. Primary bioenergy potential (PBP) of the conterminous United States. PBP divided into current harvest residue potential (PBP_{RS}), additional harvest potential (PBP_{AD}), extensification of managed lands (PBP_{MX}), and extensification over remote lands (PBP_{RX}). Whiskers depict parameter uncertainties as summarized in Table S2.1. For comparison, current recovered harvest (H_{RC}) is also represented. Biomass (PgC yr^{-1}) converted to energy (EJ yr^{-1}) according to Equation 2.9. The solid blue line represents U.S. net ethanol production in 2009 (40 billion liters). The dotted blue line represents U.S. primary bioenergy production in 2009 (1.91 EJ yr^{-1}; Equation 2.10). The solid red line represents the net energy required by the Energy Independence and Security Act of 2007 by 2022 (EISA; 136 billion liters; Congress 2007). The dotted red line represents the primary energy required by the EISA by 2022 (7.42 EJ yr^{-1}; Equation 2.10; Congress 2007). **a**, Total PBP. **b**, Cumulative PBP.

Table 3. Bioenergy production of the conterminous United States.

U.S. Bioenergy	Secondary Energy (S^a) (10^9 liters yr^{-1})	Secondary Energy (C^a) (10^9 liters yr^{-1})	Primary Energy[b] (S^a) (EJ yr^{-1})	Primary Energy[c] (C^a) (EJ yr^{-1})	Total Primary Energy[b] (EJ yr^{-1})
2009 Production	40	--	1.9	--	1.9
EISA Target[c]	57	79	2.7	4.7	7.4
EISA Target (S)[d]	136	--	6.5	--	6.5
EISA Target (C)[e]	--	136	--	8.1	8.1

[a]S = starch-based; C = cellulosic-based. [b]Primary energy calculated utilizing Equation 10. [c]Energy Independence and Security Act of 2007 (EISA) energy targets. [d]EISA energy targets assuming only starch-based conversion technology. [e]EISA energy targets assuming only cellulosic-based conversion technology.

Current and future United States bioenergy production. In 2009, the U.S. produced roughly 40 billion liters of starch-derived ethanol, more than half the 75 billion liter global supply, utilizing maize as the main feedstock (Scarlat & Dallemand 2011). According to Equation 2.10, we calculate an equivalent primary bioenergy requirement of 1.9 EJ yr^{-1}, which corresponds to roughly 20% of current recovered agricultural harvest (H_{RC}) (Table 2.3; Figure 2.4). Similarly, (Graham-Rowe 2011) documented that approximately 33% of U.S. maize production is currently re-allocated for bioenergy production. The U.S. is responsible for approximately 45% of global maize production and nearly 70% of global maize export, suggesting that increased maize allocation for bioenergy production could displace global export and subsequently drive increased food prices. In 2010, food prices were reported by the food and agricultural organization (FAO) as the highest they have been in their 20-year measurement record (*http://www.fao.org/worldfoodsituation/wfs-home/foodpricesindex/en/*). While the role that current U.S. bioenergy expansion has played in driving food prices is still debated (Naylor *et al.* 2007; Zhang *et al.* 2010), there is no question that at some point re-allocation of U.S. croplands will directly impact global food prices. Consequences of increased global food prices include higher rates of poverty and malnutrition as well as increased global deforestation and greenhouse gas (GHG) emissions as forests are cleared to accommodate agricultural expansion (Naylor *et al.* 2007). These detrimental impacts, associated with global food instability, highlight the importance of minimizing or even reversing current food and feed production displacement due to bioenergy expansion.

The U.S. Energy Independence and Security Act of 2007 (EISA) stipulates a total renewable energy target of 136 billion liters by 2022, with 57 billion liters of starch-

derived ethanol and 79 billion liters of cellulosic-derived ethanol (Table 2.3; Congress 2007). Again, utilizing Equation 2.10, the total equivalent primary bioenergy requirement increased to approximately 7.4 EJ yr^{-1}, nearly four times the 2009 total primary bioenergy equivalent (1.9 EJ yr^{-1}; Table 2.3). If we consider only current U.S. agricultural harvest, we estimate that roughly 80% of current recovered harvest (H_{RC}) would need to be re-allocated for the production of bioenergy to meet the target stipulated in the EISA (Figure 2.4). Conversely, if only expansion of agricultural land is considered, we estimate over 80% of managed rangeland or nearly 60% of total rangeland productivity would need to be allocated to bioenergy production to satisfy EISA targets (Figure 2.4). Again, since agricultural productivity is almost always significantly less than current natural productivity (Vitousek *et al.* 1986; DeFries 2002; Haberl *et al.* 2007), we likely underestimate the magnitude of rangeland exploitation required to meet policy targets. Not only could converting rangeland to agriculture result in significant detrimental impacts on biological diversity, but the utilization of remote regions would initially require infrastructure establishment resulting in large-scale fossil fuel energy inputs and a significant initial C debt of bioenergy systems (Fargione *et al.* 2008). Moreover, even though we excluded permanent pasturelands from our analysis, the majority of rangeland in the U.S. experiences some degree of grazing, indicating that expansion into these areas will likely displace a portion of feed production, which could ultimately drive future deforestation and consequentially, increase GHG emissions (Erb *et al.* 2009; McAlpine *et al.* 2009).

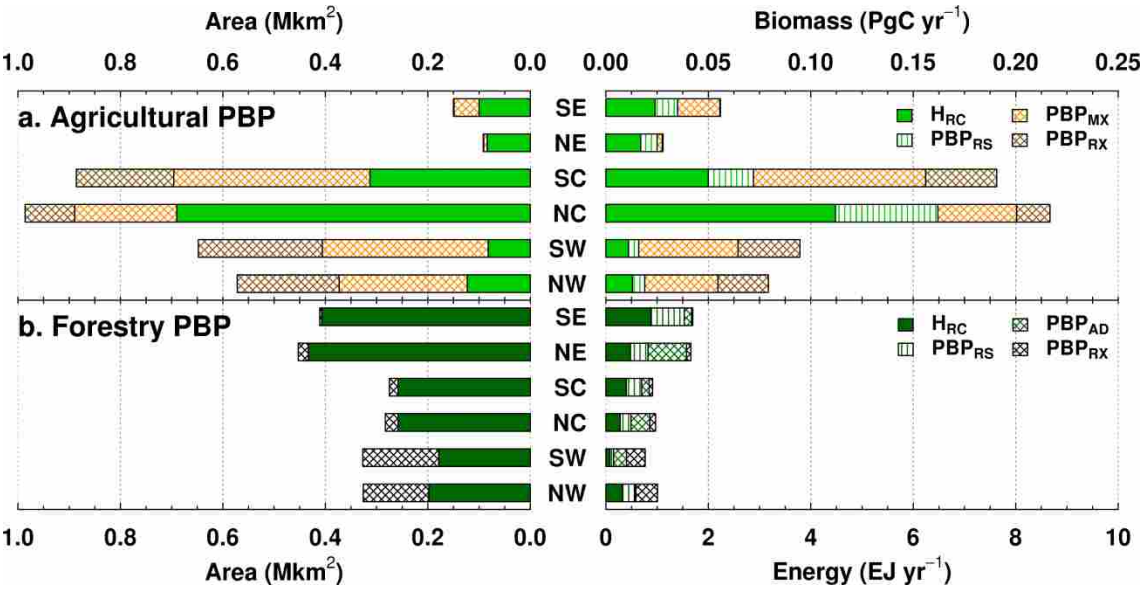

Figure 5. Primary bioenergy potential (PBP) by geographical region of the conterminous United States. PBP divided into current harvest residue potential (PBP_{RS}), additional harvest potential (PBP_{AD}), extensification of managed lands (PBP_{MX}), and extensification over remote lands (PBP_{RX}). PBP pools calculated according to Equations 2.1-2.8 utilizing mean parameter values (Table S1.1). Biomass (PgC yr^{-1}) converted to energy (EJ yr^{-1}) according to Equation 2.9. **a**, Agricultural PBP, including current recovered harvest (H_{RC}), PBP of current harvest residues (PBP_{RS}), PBP associated with extensification over currently available managed land (PBP_{MX}), and PBP associated with extensification over currently available remote land (PBP_{RX}). **b**, Forestry PBP, including current recovered harvest (H_{RC}), PBP of current harvest residues (PBP_{RS}), PBP associated with additional harvest of currently harvested land (PBP_{AD}), and PBP associated with extensification over currently available remote land (PBP_{RX}).

Alternatively, our results suggest that the cellulosic-derived energy target of 79 billion liters or 4.7 EJ could potentially be exceeded utilizing only current harvest residues, requiring no additional harvest land (Table 2.3; Figure 2.4). As expected, regions with the most forestry and agricultural land were also found to have the largest associated residue potential (Figure 2.5). However, even under this best case scenario, the EISA still requires starch-derived ethanol production to increase beyond 2009 values by roughly 30%, with an associated increase in primary energy demand from 1.9 to 2.7 EJ yr^{-1} (Table 2.3; Congress 2007). We estimate that such an increase would either require an additional re-allocation of roughly 9% of total U.S. agricultural production or the utilization of approximately 9% of accessible natural rangeland (Fig. 2.4). We acknowledge that some of this increase could potentially be satisfied via increasing productivity on current agricultural land, a factor outside the scope of this study (Johnston *et al.* 2011; Foley *et al.* 2011). However, the potential for increased agricultural productivity in the U.S. is relatively low, since the most advanced seed varieties, human management, and genetics are already widely utilized, while additional resources are limited (a factor discussed in more detail below).

Unfortunately, next generation technology is still unavailable for large-scale bioenergy production due mainly to difficulties in converting lignocellulose to a useable form (Sanderson 2011). Evaluating the EISA energy targets utilizing only starch-derived ethanol technology resulted in an equivalent primary bioenergy requirement of approximately 6.5 EJ yr^{-1}, a value significantly larger than current total U.S. maize production (Lobell *et al.* 2002). This suggests that EISA energy targets could not be satisfied under current productivity trends without total displacement of U.S. maize

production and significant rangeland expansion (Table 2.3; Figure 2.4). Already, delays in up-scaling next generation bioenergy technology have resulted in projections to expand the utilization of the starch-derived ethanol pathway, which will likely result in further displacement of food and feed production land with relatively low net bioenergy output (Van Vuuren *et al.* 2009).

Natural productivity as a constraint on yield potential. While average agricultural yields have the potential to increase (Johnston *et al.* 2011; Foley *et al.* 2011), achieving yields that exceed natural rates of productivity would likely require either enhanced photosynthetic capabilities or increased resource allocation (e.g. irrigation and fertilization), neither of which currently seems likely in future scenarios. Under optimal growing conditions, yield potential is determined genetically by the efficiency of light capture, the efficiency of the conversion of that captured light to biomass, and the proportion of that biomass partitioned into grain (Long *et al.* 2006). Long *et al.* (2006) documented that light interception and allocation to grain are near their theoretical maxima for grain crops, leaving light use efficiency as the only genetic control with significant potential to increase yield. However, despite a long history of research, genetic manipulation by plant breeding has yet to significantly increase photosynthetic rate per unit leaf area (Richards 2000).

Additionally, evidence suggests current rates of irrigation and fertilization in the U.S. are reaching peak levels, which is resulting in significant detrimental impacts. For instance, the Colorado River, a main irrigation source for the western U.S., is currently at a maximum sustainability limit, with little to none of the peak renewable flow reaching

the delta annually (Gleick & Palaniappan 2010). The Rio Grande, Santa Cruz, Gila, Verde, Salt, and other river systems flowing through urban areas of the region are under similar stress, either reaching or exceeding peak ecological limits (Gleick & Palaniappan 2010). Additionally, the Ogallala aquifer in the Great Plains has been documented as exploited, largely for irrigation, beyond its natural recharge rate, resulting in diminishing returns of an essentially nonrenewable resource (Gleick 2010). Since roughly 13% of croplands in the U.S. are irrigated (Siebert & Döll 2010), a more likely scenario for the future may be significant declines in agricultural yields as freshwater limits are exceeded (Gleick 2003; Wada *et al.* 2010).

Similarly, current nutrient fertilization rates are perturbing the natural nitrogen (N) cycle, resulting in extensive eutrophication of freshwater and coastal zones (Martin 2011). Incidental fluxes of N into the Mississippi River have contributed to freshwater pollution and an immense "Dead Zone" in the Gulf of Mexico that spans roughly 15,000 km^2 (Galloway *et al.* 2008). Equally concerning, agricultural intensification has resulted in increased emissions of the highly potent greenhouse gas nitrous oxide (N_2O), a trace gas species with a global warming potential roughly 300 times greater than an equal mass of CO_2 (Crutzen *et al.* 2008; Davis *et al.* 2012). Already, research suggests that fertilizer-derived N_2O emissions from some bioenergy cropping systems have exceeded their potential CO_2 offset, resulting in a net increase in atmospheric GHG warming potential (Crutzen *et al.* 2008; Davis *et al.* 2012). Thus, any positive impact of future increases in fertilization on productivity could be offset by amplification of freshwater degradation and acceleration of climate change (Robertson & Hamilton 2011).

Supplementary Information

Table S2.1. Parameters and associated parameter ranges utilized to calculate primary bioenergy potential (PBP) of the conterminous United States. Parameter ranges were compiled from multiple published sources.

Parameter	Low	Mean	High
Agricultural			
Aboveground ratio (r_{ag})	0.80	0.83	0.85
Total harvest ratio (r_{hv})	1.00	1.00	1.00
Recovered harvest ratio (r_{rc})	0.40	0.50	0.60
Primary residues ratio (r_{rs1})	0.25	0.30	0.35
Secondary residues ratio (r_{rs2})	0.05	0.10	0.15
Maximum harvest ratio (r_{msh})	1.00	1.00	1.00
Forestry			
Aboveground ratio (r_{ag})[a]	--	--	--
Total harvest ratio (r_{hv})[a]	--	--	--
Recovered harvest ratio (r_{rc})	0.75	0.85	0.95
Primary residues ratio (r_{rs1})	0.25	0.30	0.35
Secondary residues ratio (r_{rs2})	0.30	0.40	0.50
Maximum harvest ratio (r_{msh})	0.15	0.20	0.25

[a]Calculated according to regionally specific statistics (see SI Table 2).

Table S2.2. Conterminous United States forest harvest data by region.

Region	NPP[a] (PgC yr^{-1})	Coniferous (Mkm^2)	Deciduous (Mkm^2)	Mixed (Mkm^2)	r_{ag}[b]	ANPP[c] (PgC yr^{-1})	USDA[d] (Mm^3)	Density[e] (t dm m^{-3})	H_{RC} (PgC yr^{-1})	H_{TL} (PgC yr^{-1})	r_{hv}[f]
NW	0.113	0.189	0.002	0.006	0.731	0.082	75.968	0.435	0.013	0.015	0.182
SW	0.179	0.156	0.018	0.005	0.736	0.132	21.480	0.449	0.004	0.004	0.033
NC	0.258	0.016	0.236	0.006	0.776	0.200	48.625	0.587	0.012	0.013	0.065
SC	0.154	0.090	0.159	0.010	0.762	0.117	75.157	0.538	0.017	0.018	0.156
NE	0.280	0.042	0.345	0.045	0.772	0.216	80.587	0.575	0.019	0.021	0.097
SE	0.305	0.177	0.215	0.015	0.757	0.231	168.321	0.523	0.036	0.040	0.173
Total	1.289	0.671	0.975	0.087	0.756	0.979	470.139	0.518	0.100	0.112	0.089

[a]NPP represents the MODIS-derived total annual NPP averaged from 2000-2006. [b]r_{ag} represents the ratio of aboveground-to-total biomass, estimated as a weighted average using literature-derived biomass ratio estimates of 0.73, 0.78, and 0.75 for coniferous, deciduous, and mixed forestlands, respectively. [c]ANPP represents aboveground NPP, estimated as the product of NPP and r_{abv}. [d]USDA represents regionally aggregated USDA forest harvest volume data. [e]Density represents average wood density, estimated by region as a weighted average using literature-derived wood density estimates of 0.43, 0.6, and 0.45 for coniferous, deciduous, and mixed forestlands, respectively. [f]r_{hv} represents the ratio of H_{TL} to ANPP, utilized to estimate forest harvest as a proportion of ANPP.

Table S2.3. Conterminous United States harvest pools by region.

Region	AREA (Mkm^2)	NPP[a] ($PgC\ yr^{-1}$)	H_{TL}[b] ($PgC\ yr^{-1}$)	H_{RC}[b] ($PgC\ yr^{-1}$)	H_{LS}[b] ($PgC\ yr^{-1}$)	H_{RS}[b] ($PgC\ yr^{-1}$)
Agricultural						
NW	0.123	0.035	0.029	0.013	0.010	0.006
SW	0.082	0.029	0.025	0.011	0.009	0.005
NC	0.690	0.298	0.248	0.112	0.087	0.050
SC	0.313	0.134	0.112	0.050	0.039	0.022
NE	0.084	0.046	0.038	0.017	0.013	0.008
SE	0.100	0.065	0.054	0.024	0.019	0.011
Total	1.393	0.607	0.507	0.228	0.177	0.101
Forestry						
NW	0.198	0.113	0.016	0.008	0.002	0.006
SW	0.179	0.079	0.005	0.002	0.000	0.002
NC	0.258	0.154	0.014	0.007	0.001	0.005
SC	0.258	0.154	0.019	0.010	0.002	0.007
NE	0.433	0.280	0.022	0.011	0.002	0.009
SE	0.407	0.305	0.042	0.022	0.004	0.016
Total	1.733	1.086	0.118	0.060	0.012	0.045

[a]NPP represents the MODIS-derived total annual NPP averaged from 2000-2006. [b]Harvest (H) pools estimated according to Equations 2.1-2.4 utilizing mean parameter values (Table S2.1).

Table S2.4. Conterminous United States agricultural primary bioenergy potential (PBP) by region. PBP divided between a, intensification or PBP of currently harvested land (PBP_I) and b, extensification or the PBP of all currently available non-harvested land (PBP_X).

a. Intensification (PBP_I)

Region	AREA (Mkm^2)	NPP[a] ($PgC\ yr^{-1}$)	MSH_{RC}[b] ($PgC\ yr^{-1}$)	MSH_{RS}[b] ($PgC\ yr^{-1}$)	H_{RC}[b] ($PgC\ yr^{-1}$)	H_{RS}[b] ($PgC\ yr^{-1}$)	PBP_{RS}[c] ($EJ\ yr^{-1}$)	PBP_{AD}[c] ($EJ\ yr^{-1}$)	PBP_I[c] ($EJ\ yr^{-1}$)
NW	0.123	0.035	0.013	0.006	0.013	0.006	0.234	-	0.234
SW	0.082	0.029	0.011	0.005	0.011	0.005	0.196	-	0.196
NC	0.690	0.298	0.112	0.050	0.112	0.050	1.988	-	1.988
SC	0.313	0.134	0.050	0.022	0.050	0.022	0.896	-	0.896
NE	0.084	0.046	0.017	0.008	0.017	0.008	0.305	-	0.305
SE	0.100	0.065	0.024	0.011	0.024	0.011	0.435	-	0.435
Total	1.393	0.607	0.228	0.101	0.228	0.101	4.055	-	4.055

b. Extensification (PBP_X)

Region	AREA (Mkm^2)	NPP[a] ($PgC\ yr^{-1}$)	MSH_{RC}[b] ($PgC\ yr^{-1}$)	MSH_{RS}[b] ($PgC\ yr^{-1}$)	H_{RC}[b] ($PgC\ yr^{-1}$)	H_{RS}[b] ($PgC\ yr^{-1}$)	PBP_{MX}[c] ($EJ\ yr^{-1}$)	PBP_{RX}[c] ($EJ\ yr^{-1}$)	PBP_X[c] ($EJ\ yr^{-1}$)
NW	0.449	0.111	0.042	0.019	-	-	1.429	0.983	2.412
SW	0.567	0.145	0.054	0.024	-	-	1.938	1.206	3.144
NC	0.296	0.101	0.038	0.017	-	-	1.535	0.650	2.185
SC	0.572	0.218	0.082	0.036	-	-	3.358	1.386	4.744
NE	0.009	0.005	0.002	0.001	-	-	0.099	0.015	0.114
SE	0.050	0.038	0.014	0.006	-	-	0.824	0.011	0.835
Total	1.943	0.619	0.233	0.103	-	-	9.184	4.251	13.434

[a]NPP represents the MODIS-derived total annual NPP averaged from 2000-2006. [b]Harvest (H) and maximum sustainable harvest (MSH) pools estimated according to Equations 2.1-2.4, utilizing mean parameter values (Table S2.1). [c]PBP pools estimated according to Equations 2.5-2.9 .

Table S2.5. Conterminous United States forestry primary bioenergy potential (PBP) by region. PBP divided between a, intensification or PBP of currently harvested land (PBP_I) and b, extensification or the PBP of all currently available non-harvested land (PBP_X).

a. Intensification (PBP_I)

Region	AREA (Mkm^2)	NPP[a] ($PgC\ yr^{-1}$)	MSH_{RC}[b] ($PgC\ yr^{-1}$)	MSH_{RS}[b] ($PgC\ yr^{-1}$)	H_{RC}[b] ($PgC\ yr^{-1}$)	H_{RS}[b] ($PgC\ yr^{-1}$)	PBP_{RS}[c] ($EJ\ yr^{-1}$)	PBP_{AD}[c] ($EJ\ yr^{-1}$)	PBP_I[c] ($EJ\ yr^{-1}$)
NW	0.198	0.113	0.008	0.006	0.008	0.006	0.244	0.021	0.266
SW	0.179	0.079	0.006	0.004	0.002	0.002	0.071	0.252	0.323
NC	0.258	0.154	0.012	0.009	0.007	0.005	0.211	0.367	0.578
SC	0.258	0.154	0.012	0.009	0.010	0.007	0.299	0.146	0.445
NE	0.433	0.280	0.022	0.017	0.011	0.009	0.343	0.752	1.095
SE	0.407	0.305	0.024	0.018	0.022	0.016	0.651	0.141	0.792
Total	1.733	1.086	0.084	0.064	0.060	0.045	1.819	1.679	3.499

b. Extensification (PBP_X)

Region	AREA (Mkm^2)	NPP[a] ($PgC\ yr^{-1}$)	MSH_{RC}[b] ($PgC\ yr^{-1}$)	MSH_{RS}[b] ($PgC\ yr^{-1}$)	H_{RC}[b] ($PgC\ yr^{-1}$)	H_{RS}[b] ($PgC\ yr^{-1}$)	PBP_{MX}[c] ($EJ\ yr^{-1}$)	PBP_{RX}[c] ($EJ\ yr^{-1}$)	PBP_X[c] ($EJ\ yr^{-1}$)
NW	0.128	0.059	0.006	0.005	-	-	-	0.423	0.423
SW	0.148	0.051	0.005	0.004	-	-	-	0.364	0.364
NC	0.025	0.016	0.002	0.001	-	-	-	0.112	0.112
SC	0.017	0.009	0.001	0.001	-	-	-	0.068	0.068
NE	0.020	0.012	0.001	0.001	-	-	-	0.085	0.085
SE	0.004	0.003	0.000	0.000	-	-	-	0.024	0.024
Total	0.342	0.150	0.015	0.012	-	-	-	1.075	1.075

[a]NPP represents the MODIS-derived total annual NPP averaged from 2000-2006. [b]Harvest (H) and maximum sustainable harvest (MSH) pools estimated according to Equations 2.1-2.4, utilizing mean parameter values (Table S2.1). [c]PBP pools estimated according to Equations 2.5-2.9.

Figure S2.1. Conterminous United States unavailable landcover. **a**, Protected areas defined according to the World Database on Protected Areas as areas of strict protection including national parks and nature reserves. **b**, Pastureland defined according to National Landcover Data. **c**, Wetland defined according to National Landcover Data. **d**, Low productivity regions or areas with annual productivity less than 150 gC m^{-2} yr^{-1}, the threshold at which harvest energy requirements exceed potential energy output.

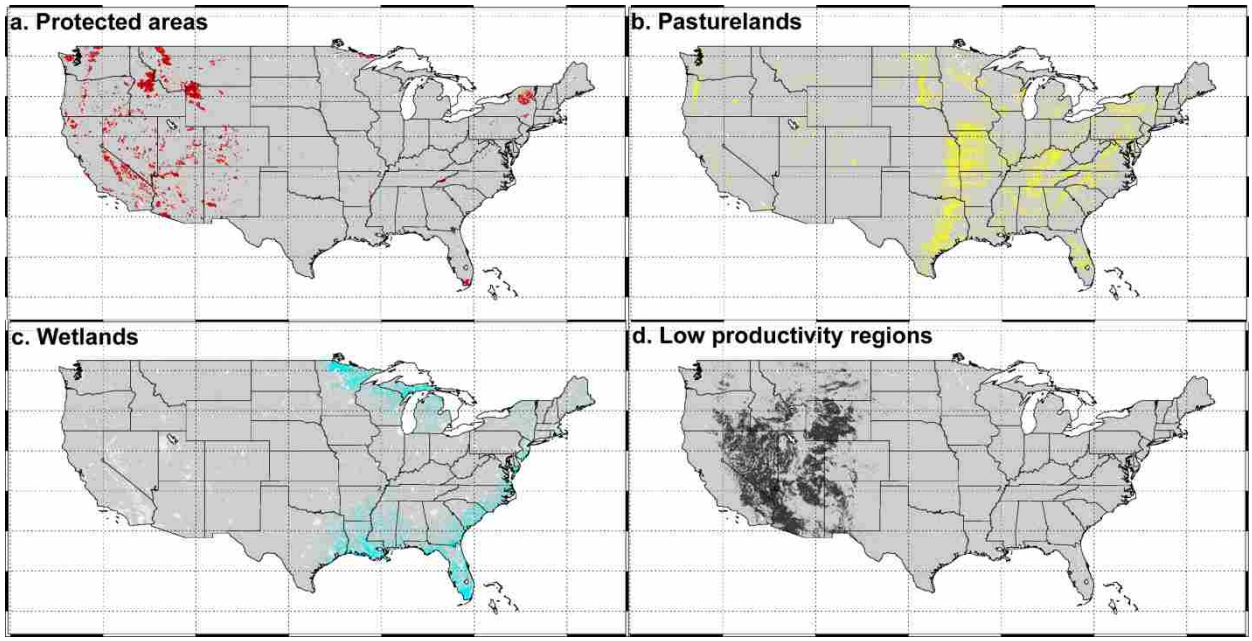

Figure S2.2. Division of the conterminous United States into 6 study regions.

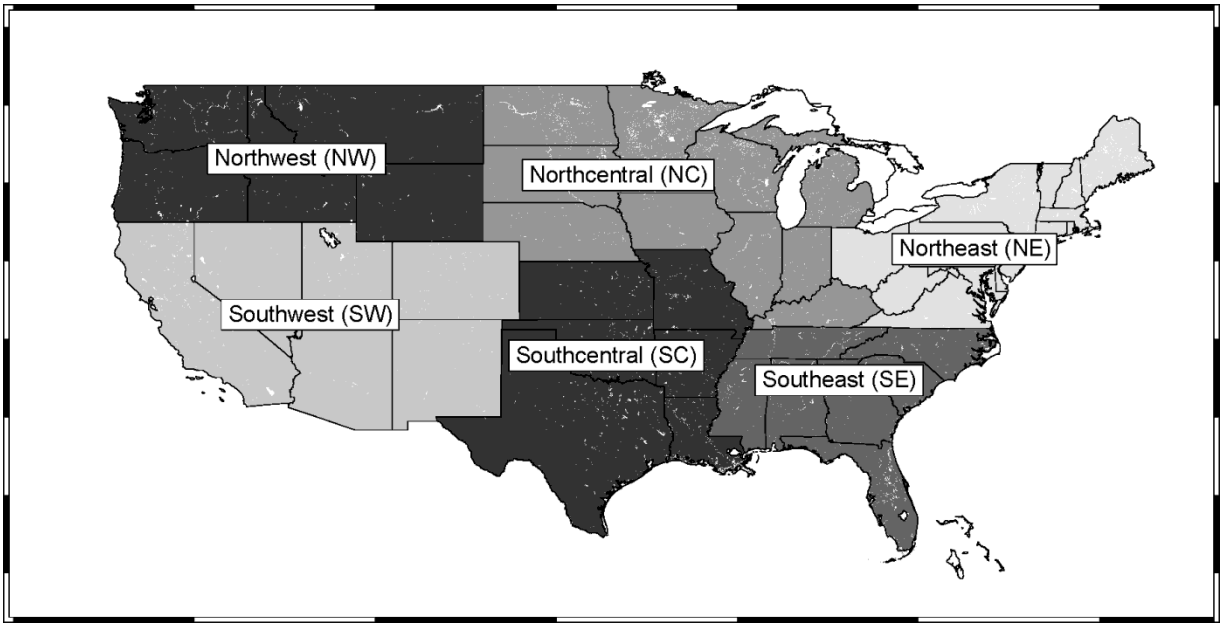

Figure S2.3. Conterminous United States current total harvest (H_{TL}). H_{TL} estimated according to Equation 1 utilizing mean parameter values (Table S2.1). **a**, Total agricultural harvest (gC m^{-2} yr^{-1}). **b**, Total forestry harvest (gC m^{-2} yr^{-1}).

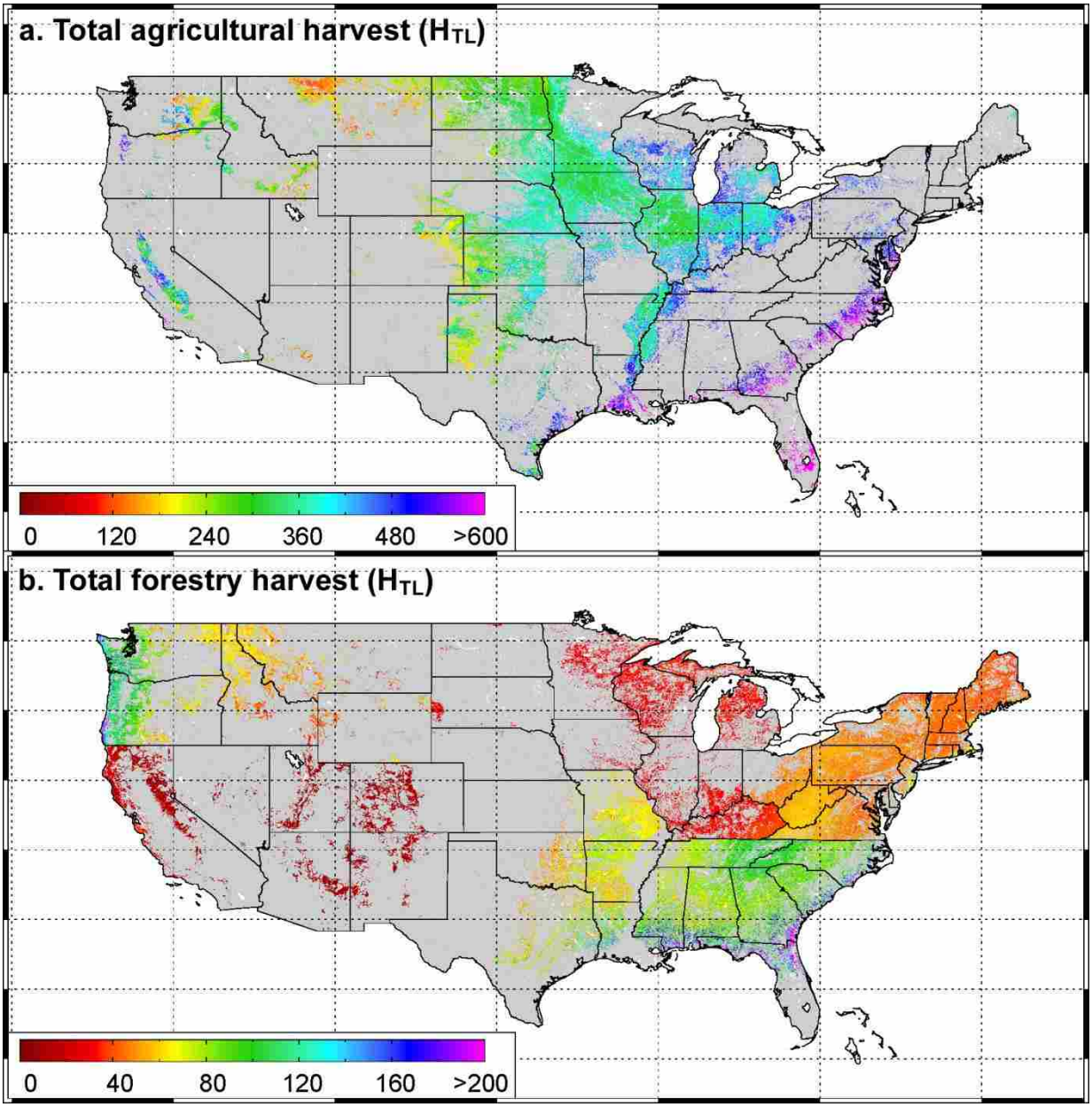

Figure S2.4. Agricultural primary bioenergy potential (PBP) of the conterminous United States. PBP calculated according to Equations 2.5-2.8 utilizing mean parameter values (Table S2.1). **a**, Current landcover. **b**, Current recovered harvest (H_{RC}; gC m^{-2} yr^{-1}). **c**, Intensification landcover, defined as currently harvested cropland only. **d**, Intensification potential (PBP_I; gC m^{-2} yr^{-1}). **e**, Extensification landcover, defined as all currently available non-harvested rangeland or marginal land. **f**, Extensification potential (PBP_X; gC m^{-2} yr^{-1}).

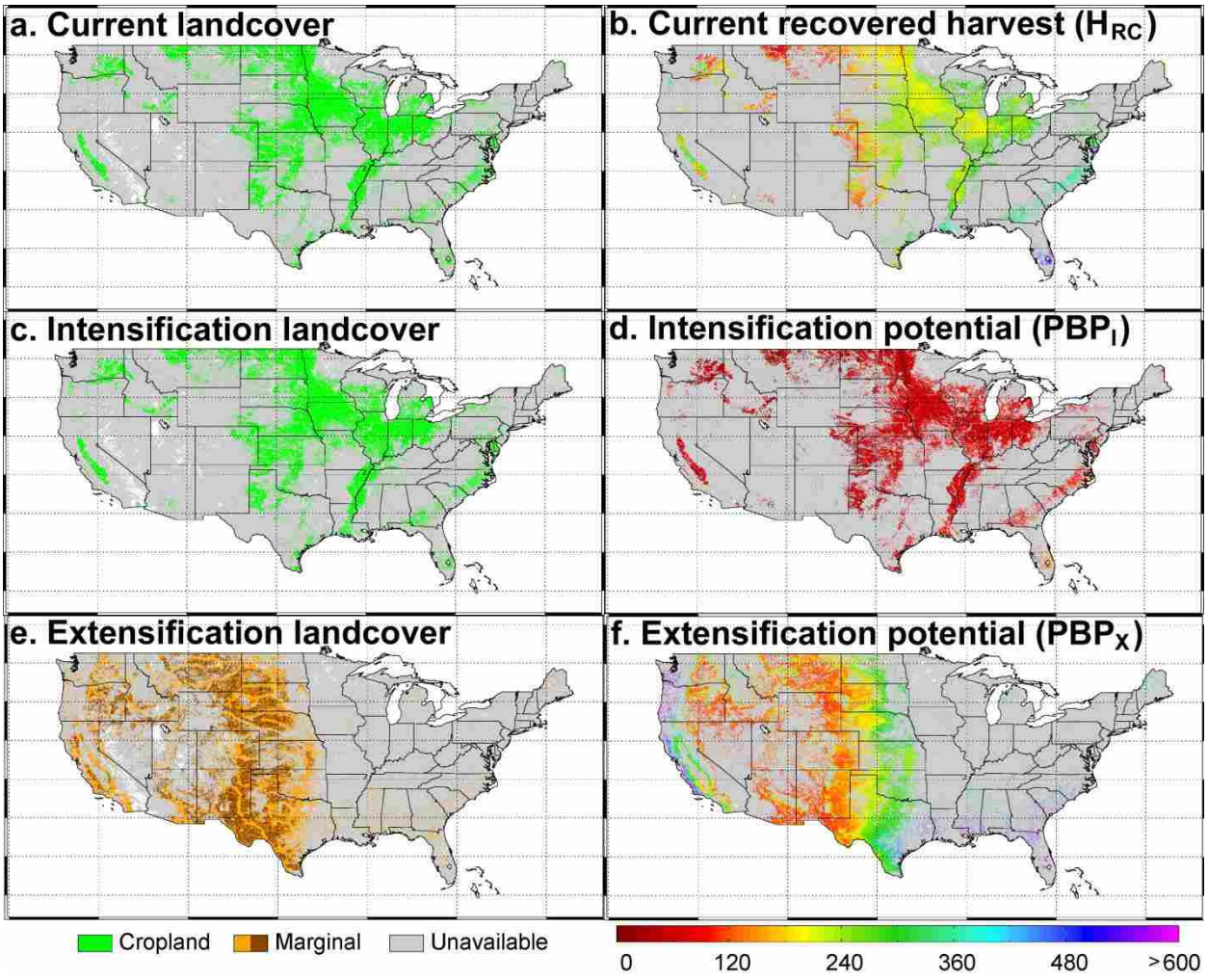

Figure S2.5. Forestry primary bioenergy potential (PBP) of the conterminous United States. PBP calculated according to Equations 2.5-2.8 utilizing mean parameter values (Table S2.1). **a**, Current landcover, defined as all managed forestland. **b**, Current recovered harvest (H_{RC}; gC m^{-2} yr^{-1}). **c**, Intensification landcover, defined as currently harvested forestland only. **d**, Intensification potential (PBP_I; gC m^{-2} yr^{-1}). **e**, Extensification landcover, defined as all currently available non-harvested forest land. **f**, Extensification potential (PBP_X; gC m^{-2} yr^{-1}).

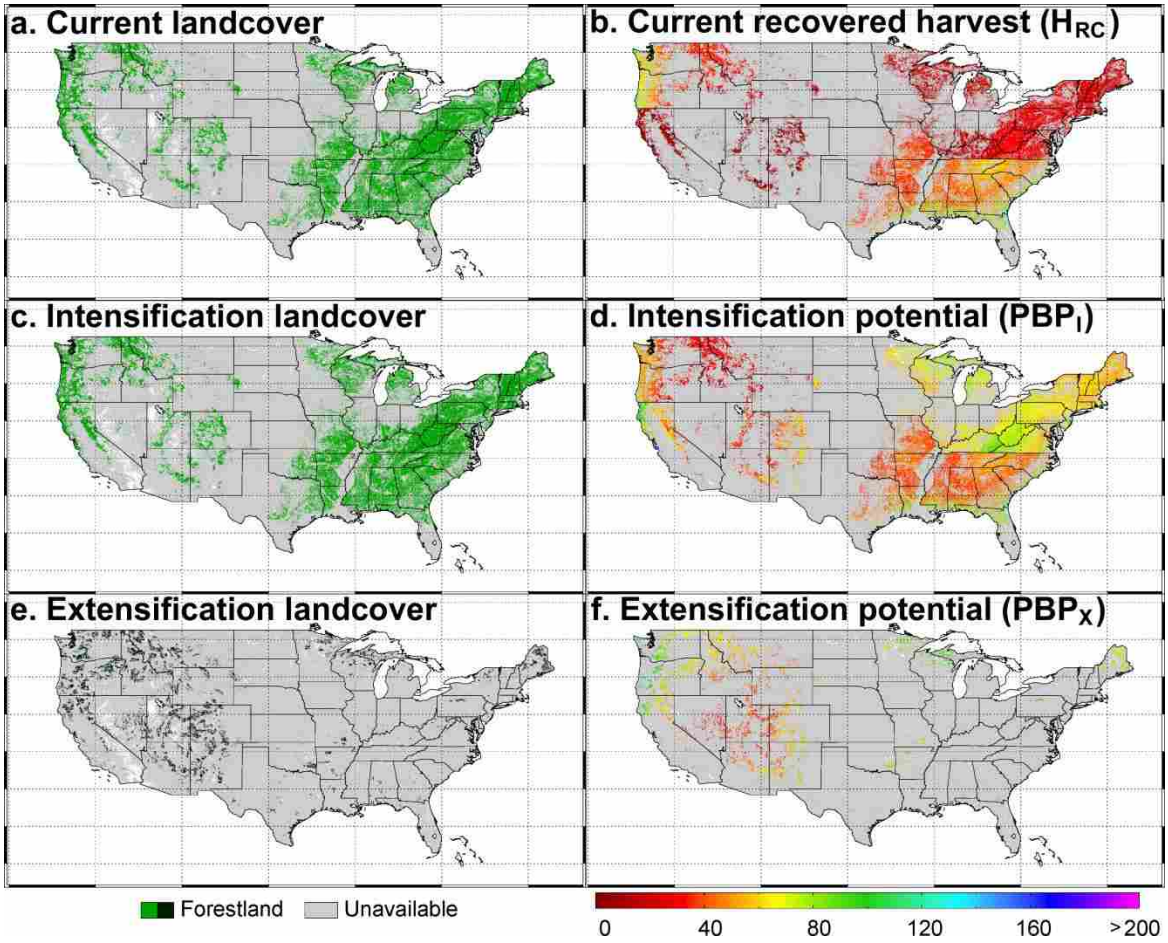

CHAPTER 3
A global scale quantification of the impact of agricultural conversion and management intensity on terrestrial vegetation productivity

Introduction

Meeting future global food and bioenergy demand while mitigating the detrimental environmental impacts associated with industrialized agricultural remains one of the greatest challenges facing humanity (Foley *et al.* 2011; Tilman *et al.* 2011; Mueller *et al.* 2012). As a result of the continued, near-exponential growth of world population and increasing global meat consumption, global food demand is expected to roughly double by 2050 (Tilman *et al.* 2011). Moreover, nearly all energy forecasts promote multi-fold increases in bioenergy production, which will further drive demand for biomass and arable land (Smith *et al.* 2012a, 2012b). Two options exist to meet this mounting demand for agricultural output: 1) agricultural intensification or increased agricultural output per unit area of existing croplands and; 2) agricultural extensification or increased agricultural output via the conversion of natural to agricultural land thereby increasing total cropland area (Tilman *et al.* 2011). The potential for these options to meet future demand is currently an area of intense scientific debate anchored by well-justified concerns that current agricultural extent and intensity may already be unsustainable (Rockström *et al.* 2009; Running 2012). For instance, evidence exists that current levels of agricultural intensification – strongly linked to management inputs (i.e., fertilization and irrigation inputs) – have largely driven humanity outside or precariously near critical safe operating thresholds in terms of climate change, nutrient cycling, and freshwater use (Rockström *et al.* 2009). Further, agricultural extent has also been proposed to be approaching critical land use (Rockström *et al.* 2009) and biomass production thresholds (Running 2012; Smith *et al.* 2012b). Ultimately, agricultural extent and intensity must increase in the future to meet well documented demand increases, yet exceeding the

critical thresholds noted above could undermine the ability of the biosphere to support adequate production over longer timescales (DeFries 2002; Haberl *et al.* 2007; Funk & Brown 2009). Thus, improving our understanding regarding current and future agricultural production relative to important ecosystem processes such as nutrient cycling, freshwater use, and terrestrial productivity is an increasingly critical area of research. The aim of this study is to 1) quantify the net impact of current agricultural landcover conversion on the capacity of the terrestrial biosphere for vegetation growth (i.e., net primary productivity or NPP), and 2) evaluate the importance of key factors including climate, landcover type, crop type, and management inputs in shaping this relationship.

Terrestrial NPP represents a major flow of the carbon cycle that is more than an order of magnitude larger than annual anthropogenic fossil fuel emissions (Ballantyne *et al.* 2012). Thus, understanding the future trajectory of NPP is of critical importance to humanity, since increases or decreases in NPP will result in relatively significant enhancement or mitigation of climate warming, respectively (Ballantyne *et al.* 2012). Over relatively local scales, the impact of agricultural landcover conversion on NPP has been observed to be strongly regulated by climate, landcover type, crop type, and management (Long *et al.* 2006). Yet, at the global scale, only a limited number of previous studies have attempted to quantify the net effect of agricultural landcover conversion on NPP and the results vary considerably (Field 2001; Bondeau *et al.* 2007; Haberl *et al.* 2007; Lawrence *et al.* 2012; DeFries *et al.* 2012). Even fewer of these studies have evaluated the relative importance of the above stated key factors in shaping the net impact of agricultural landcover conversion. Previous studies that modeled

natural NPP (i.e., pre-agriculture) based on satellite data found current agricultural conversion has had a spatially varying effect on NPP, yet the impact has been generally within the range of long-term interannual variability (Field 2001; DeFries 2002). However, these studies were based on relatively course satellite data (~100 km^2 spatial resolution), which did not fully capture cropland extent since croplands are intermixed with natural lands at much finer spatial scales. Additionally, these studies did not quantify the factors driving the spatially heterogeneous effect of agricultural conversion on NPP (e.g., climate, crop type, management, etc.). Others have compared current NPP to natural NPP using either biogeochemical process (BGC) (Lawrence *et al.* 2012) or dynamic global vegetation (DGVM) models (Bondeau *et al.* 2007; Haberl *et al.* 2007), and have generally concluded that human modifications of the landscape have significantly reduced biospheric NPP. For instance, Haberl et al. (2007) estimated that agricultural landcover conversion has reduced biospheric NPP by 6.3 Pg C (i.e., a reduction greater than 10%) annually. However, the results of these analyses are strongly influenced by their calculation of NPP, and both BGC and DGVM models have been shown to result in upper-end estimates of natural NPP (Ito 2011). Further, these models generally rely on defined crop functional types and thus do not account for variability across individual crop types or management strategies. Ultimately, the different conclusions and limitations of the above analyses indicate that the current impact of agricultural landcover conversion on biospheric NPP, and thus the potential for future agricultural intensification and extensification, is largely unresolved.

In this study, we attempt to address this gap in understanding by comparing current agricultural NPP - derived from bottom-up census data - with natural NPP - derived from

top-down satellite data - across climate zones. We estimate agricultural extent and productivity from bottom-up, census-derived agricultural yield data aggregated to a 10-km^2 spatial resolution (You *et al.* 2006; 2008); while we estimate natural NPP from top-down, satellite-derived vegetation productivity data also aggregated to a 10-km^2 spatial resolution (Running *et al.* 2004; Zhao *et al.* 2005; Zhao & Running 2010) (Text S3.1-S3.3). Our approach is novel in that we independently resolve rates of productivity for croplands and natural NPP at the sub-pixel level, since census data provides cropland percent coverage and productivity estimates, while satellite data provides productivity based on the dominant vegetation type for every 10-km^2 pixel (Text S3.4). Thus, unlike analyses that rely solely on satellite data, we include areas were croplands represent a very small percentage of the grid cell, while we independently estimate rates of productivity for natural and croplands in areas of co-dominance. To account for biases in the different methods of estimation, we validate our independent estimates of NPP using empirically-based estimates of NPP (Text S3.3). We then compare these independent estimates of agricultural and natural productivity across long-term, well-established climate zones to determine the net impact of agricultural landcover conversion on biospheric NPP (ΔNPP) (Text S3.4-S3.5). Finally, we disaggregate our results by climate zone, conversion type, crop type, and management inputs to determine the relative importance of each factor in regulating the relationship between agricultural and natural productivity (Text S3.6). Ultimately, we aim to quantify the current impact and intensity of agricultural productivity relative to the natural biospheric potential, which we hope will provide insight into how we can most effectively increase agricultural output in the

future, while simultaneously minimize the numerous detrimental tradeoffs associated with agricultural expansion and intensification.

Table 3.1. The effect of agricultural landcover conversion on net primary production (ΔNPP) for 20 staple crops. Δ NPP is divided by climate zone (tropical, temperate, cold, and arid), management intensity (irrigated, high input / rain-fed, low input / rain-fed, and subsistence), and the original landcover type (F = forest; NF = non-forest). Values in parentheses for spatial averages (g C m^{-2}) represent spatial variability of one standard deviation of the mean, while values in parentheses for annual averages (Tg C y^{-2}) represent decadal-scale (2000-2010) temporal variability of one standard deviation of the mean.

	Area (10^6 km^2)		NPP (g C m^{-2} y^{-1})		Δ NPP (g C m^{-2} y^{-1})		Δ NPP (Tg C y^{-1})		
	NF	**F**	**NF**	**F**	**NF**	**F**	**NF**	**F**	**T**
Irrigated [a]	**0.9**	**1.2**	**424 (227)**	**490 (224)**	**3 (294)**	**-426 (345)**	**3 (58)**	**-510 (111)**	**-507 (170)**
tropical	0.1	0.4	444 (211)	421 (172)	-153 (327)	-604 (359)	-15 (9)	-224 (40)	-239 (49)
temperate	0.2	0.6	511 (245)	527 (269)	-155 (378)	-454 (532)	-32 (16)	-271 (54)	-303 (69)
cold	0.1	0.1	596 (249)	598 (224)	344 (264)	130 (256)	30 (3)	17 (8)	47 (12)
arid	0.5	0.1	353 (218)	383 (153)	39 (274)	-318 (463)	20 (30)	-32 (9)	-12 (39)
High Input [a]	**1.6**	**1.5**	**318 (153)**	**380 (164)**	**-80 (242)**	**-453(310)**	**-130 (92)**	**-696 (133)**	**-826 (225)**
tropical	0.2	0.5	285 (128)	332 (135)	-312 (281)	-693 (343)	-52 (15)	-321 (51)	-373 (66)
temperate	0.4	0.6	319 (155)	391 (179)	-346 (327)	-590 (493)	-135 (29)	-337 (50)	-472 (79)
cold	0.8	0.5	355 (160)	427 (178)	103 (182)	-41 (218)	79 (31)	-19 (29)	60 (60)
arid	0.3	< 0.1	239 (148)	245 (142)	-75 (223)	-457 (460)	-22 (17)	-18 (3)	-41 (20)
Low Input [a]	**1.2**	**0.6**	**150 (99)**	**191 (156)**	**-343 (212)**	**-763 (305)**	**-426 (93)**	**-469 (61)**	**-895 (155)**
Tropical	0.4	0.3	169 (114)	208 (165)	-428 (275)	-818 (356)	-168 (35)	-238 (32)	-406 (67)
Temperate	0.3	0.2	187 (115)	198 (170)	-479 (310)	-783 (490)	-162 (26)	-183 (21)	-345 (47)
Cold	0.1	< 0.1	152 (63)	195 (129)	-100 (107)	-273 (179)	-11 (4)	-6 (1)	-17 (6)
Arid	0.4	0.1	100 (81)	89 (80)	-214 (185)	-612 (444)	-85 (28)	-42 (7)	-127 (36)
Subsistence [a]	**0.8**	**0.5**	**115 (73)**	**139 (80)**	**-389 (201)**	**-844 (274)**	**-301 (64)**	**-446 (54)**	**-747 (118)**
Tropical	0.4	0.3	129 (84)	155 (94)	-468 (264)	-871 (329)	-176 (33)	-283 (36)	-459 (69)
temperate	0.1	0.2	144 (73)	113 (59)	-521 (297)	-868 (464)	-61 (9)	-141 (15)	-203 (24)
cold	< 0.1	< 0.1	187 (72)	226 (86)	-66 (112)	-242 (151)	-1 (1)	-2 (1)	-3 (1)
arid	0.3	< 0.1	77 (58)	78 (42)	-237 (177)	-623 (439)	-63 (20)	-19 (3)	-82 (24)
Total [a]	**4.5**	**3.8**	**258 (158)**	**353 (171)**	**-189 (245)**	**-545 (314)**	**-854 (315)**	**-2121 (365)**	**-2975 (680)**
tropical	1.1	1.5	201 (120)	296 (126)	-397 (278)	-730 (340)	-411 (94)	-1066 (161)	-1477 (256)
temperate	1.0	1.6	300 (174)	383 (207)	-365 (336)	-598 (503)	-390 (82)	-932 (141)	-1322 (223)
cold	1.0	0.6	357 (182)	444 (199)	105 (201)	-24 (235)	97 (40)	-10 (40)	87 (80)
arid	1.5	0.3	208 (157)	220 (143)	-107 (229)	-481 (460)	-150 (98)	-111 (23)	-261 (121)

[a] Irrigated = High Input equipped for irrigation; High Input = high yielding cultivars, rain-fed, fertilized, plus chemical pest, disease, and weed controls; Low Input / Subsistence = traditional cultivars, rain-fed, with little to no application of fertilizers or chemicals for pest and disease control;

Results and Discussion

Our analysis indicates that the conversion of natural to agricultural land (ΔNPP) has significantly reduced terrestrial biospheric NPP beyond the range of decadal scale natural variability (Table 3.1). The annual reduction in productivity was estimated to total 3.0 ± 0.68 Pg C (i.e. a 5-7% relative reduction in global NPP) for 20 staple crops that represent nearly 90% of agricultural land globally (Table 3.1), a range roughly a third the size of annual global fossil fuel emissions (Ballantyne *et al.* 2012). When considering all 127 non-tree crops recognized by the Food and Agricultural Organization of the United Nations (FAO), this range increased to 3.7 ± 0.85 Pg C or a 6-9% relative reduction in global NPP (Table S3.2). Yet, we found that ΔNPP was highly heterogeneous and significantly impacted by climate zone, landcover conversion type, management intensity, crop type, and to a lesser extent region (Fig. 3.1). Using a Boosted Regression Tree model, the relative importance of climate, conversion type, management intensity, crop type, and region were estimated to be 60%, 19%, 14%, 7%, and 0% (Fig. 3.1; Text S3.6).

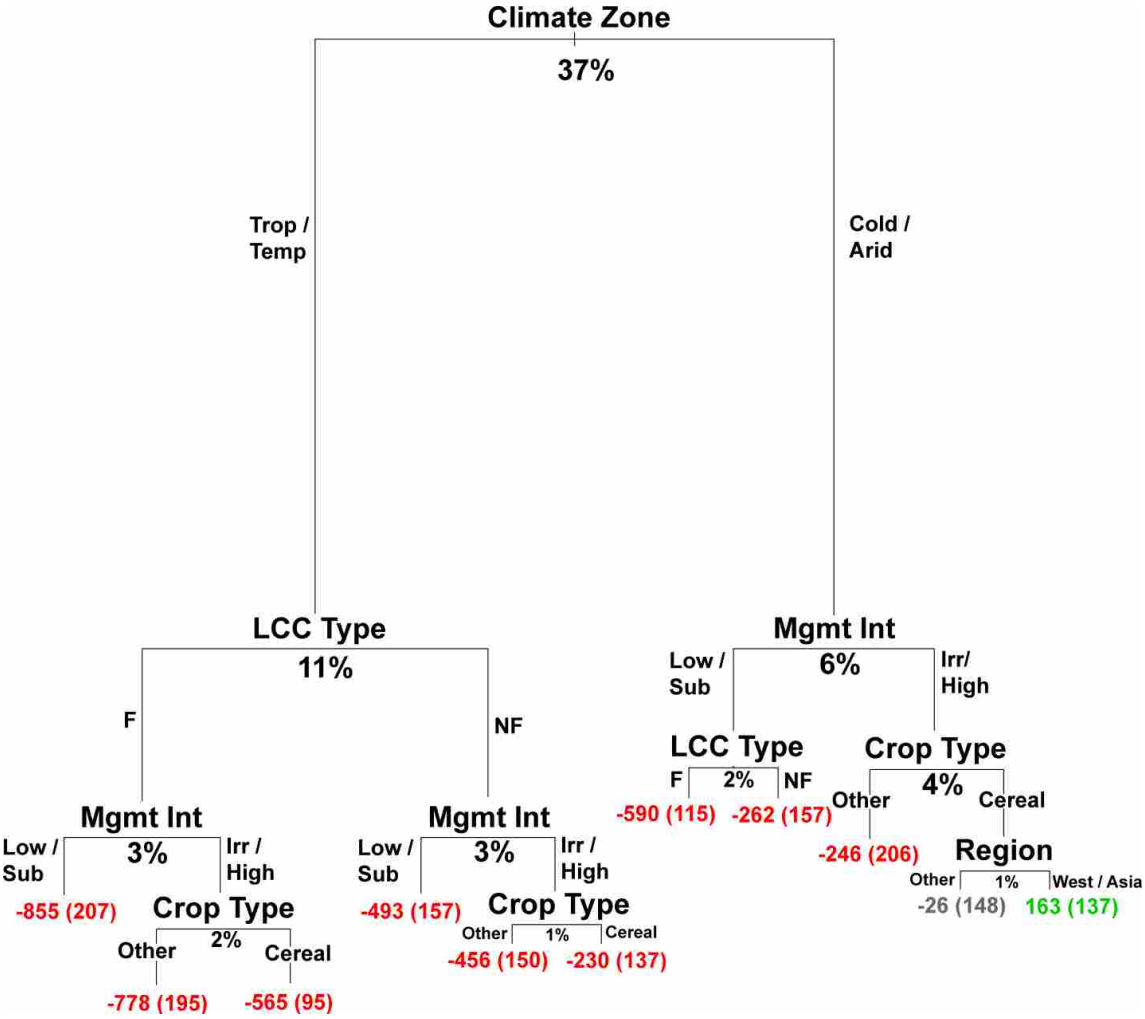

Figure 3.1. A regression tree quantification of the relative effect of key factors in determining the change in NPP due to agricultural landcover conversion (ΔNPP). The relative importance of climate, conversion type, management level, crop type, and region were estimated to be 60%, 19%, 14%, 7%, and 0%, respectively, using a boosted regression tree analysis (Text S3.6). Predictor variables are shown at the top of each branch and the mean ΔNPP is reported below the terminal node (including the decadal-scale natural variability in parentheses). Mean ΔNPP values that represent a significant decrease, a non-significant change, or a significant increase relative to the decadal-scale interannual variability are colored coded red, grey, or green, respectively. The height of each branch, as well as the percentage value below each branch, indicates the relative proportion of the total sum of squares explained by that split.

Climate zone was found to be the most important predictor variable, describing 37% of the sum of squares variance in ΔNPP (Fig. 3.1). For tropical and temperate climate zone, ΔNPP was found to be significantly negative independent of landcover conversion type, management intensity, crop type, or region; although these factors mitigated the reduction in productivity to various degrees (Fig. 3.1). For instance, we show the conversion of tropical / temperate forests results in a productivity reduction ranging from 565 –855 g C m^{-2}, while the conversion of tropical / temperate non-forest results in a reduction ranging from 230 – 493 g C m^{-2} (Fig. 3.1). This finding emphasizes the importance of preventing future agricultural conversion of natural tropical / temperate ecosystems, and, in particular, tropical / temperate forests. Multiple previous studies have supported this finding is terms of reductions in productivity (DeFries 2002), biodiversity (Foley *et al.* 2005; Thomas *et al.* 2012), and carbon stocks (West *et al.* 2010) as a result of the conversion of tropical / temperate ecosystems to agricultural land. Surprisingly, management intensity, crop type, and region had a relatively small impact in tropical / temperate zones, explaining only 9% of the sum of squares variance in ΔNPP combined (Fig. 3.1). This finding is likely related to soil quality and the high potential for soil degradation as a result of agricultural land cover conversion in tropical / temperature climate zones (Lal 2004; Townsend *et al.* 2011). Unlike natural tropical ecosystems which recycle nutrients stored in organic matter, a large portion of organic matter on agricultural lands is harvested, forcing a dependence on new nutrient inputs (e.g., fertilization) and soils capable of retaining new nutrients against leaching, a well-known limiting factor in tropical / temperate climates (Townsend & Asner 2013).

For cold and arid climate zones, ΔNPP was found to vary from positive to negative, although the net effect was still strongly negative (Fig. 3.1). Interestingly, management intensity was the most important predictor for these climate zones, describing 6% of the sum or squares variance in ΔNPP (Fig. 3.1). At the large scale, the only mean positive ΔNPP value was observed for cereal crops grown in the Industrialized West and Asia under intensive management (i.e., either irrigated or high input rain-fed management) (Fig. 3.1). In fact, cereals in general were always grouped separate from other (oil, pulse, and sugar) crop types, indicating that cereals are the most productive crop type across climate zones (Fig. 3.1). This is not surprising since cereals have been documented to be near their theoretical yield potential ceiling due to over 30 years of research and development of improved cultivars (Cassman 1999; Zhu *et al.* 2010). However, despite the high productivity of cereals crops, we show the dominant factor driving positive ΔNPP values for cold and arid climates is management intensity (Fig. 3.1). Again, it is no surprise that management intensity is most important in these climate zones, since agricultural inputs (i.e., fertilization and irrigation) can mitigate biophysical nutrient and water constraints, which are most limiting in cold and arid climates, respectively (Johnston *et al.* 2011; Foley *et al.* 2011; Mueller *et al.* 2012). We discuss this point in more detail in the next paragraph. Finally, while world regions were found to have relatively low explanatory power (Fig. 3.1), we show that much of the world (Latin America, Eastern Europe, and Africa) is under-producing relative to current levels of management intensity and, thus, future efficiency gains could significantly increase agricultural output without increase demand for nutrients, water, or land (Mueller *et al.* 2012). However, it is important to note that Latin America and Africa are largely within

tropical and temperate climate zones, within which, as noted above, management intensity was shown to have a relatively small impact on ΔNPP (Fig. 3.1).

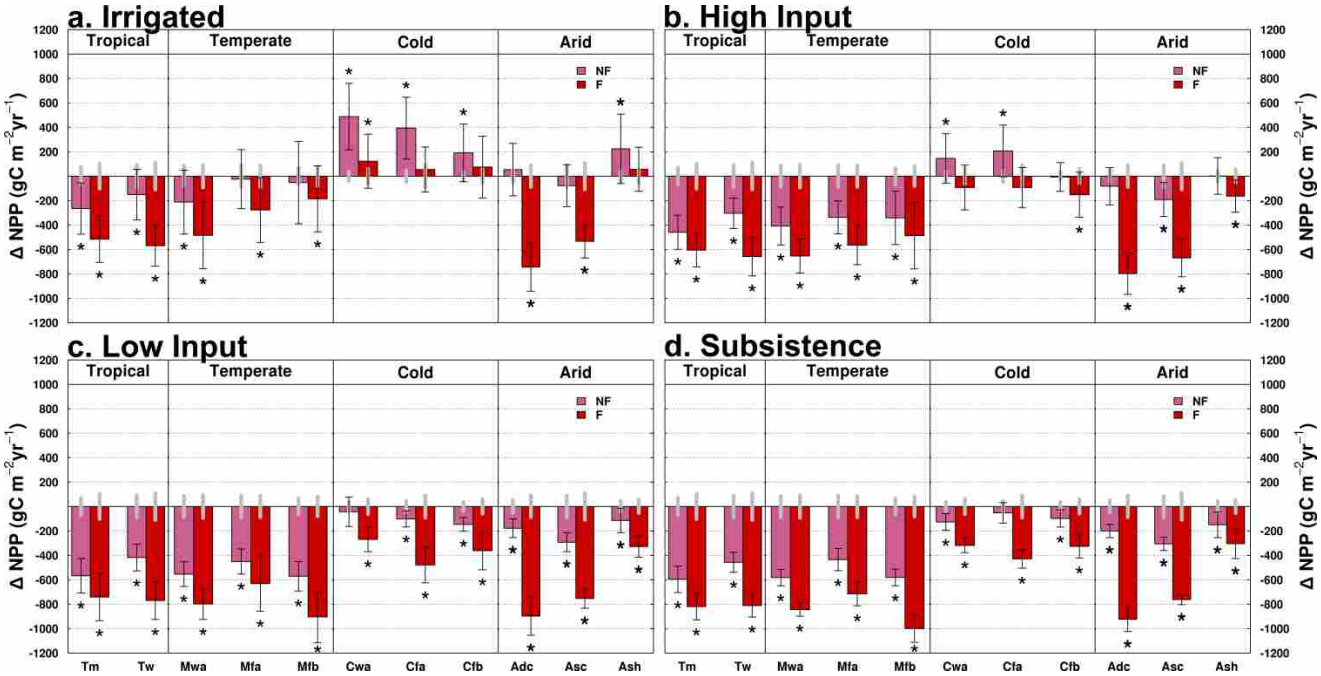

Figure 3.2. The effect of agricultural landcover conversion on net primary production across the top crop producing climate zones of the world. ΔNPP was estimated independently for **a.**, irrigated; **b.**, high input; **c.**, low input; and **d.**, subsistence management intensities. For each management intensity, we calculate ΔNPP according to the type of landcover conversion (F = forest; NF = non-forest). Error bars represent spatial variability of one standard deviation of the mean, while the grey bars represent the decadal-scale (2000-2010) temporal variability of natural NPP of one standard deviation of the mean. Asterisks represent ΔNPP values significantly outside the decadal-scale temporal variability of natural NPP for a given climate zone at a significance level of 0.001. We show that agricultural conversion of natural non-forested land results in increased productivity only under conditions of intense management (i.e., irrigation or high inputs) in climates with significant biophysical limitations (i.e., cold and arid climates); while agricultural conversion of natural forested land almost always results in a significant decrease in productivity such that management only lessens the reduction.

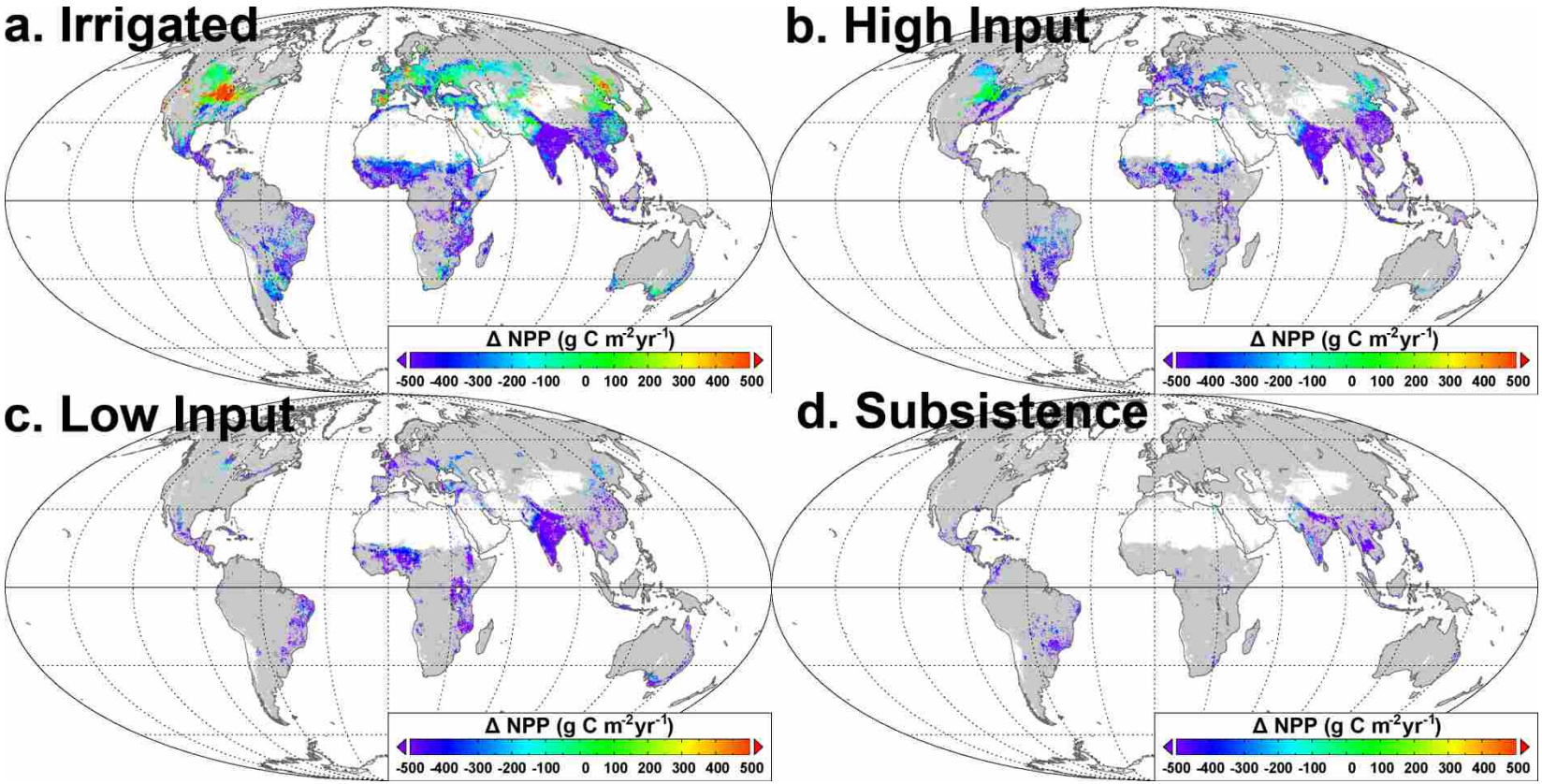

Figure 3.3. A spatially explicit estimate of the effect of agricultural landcover conversion on natural primary production for 20 staple crops. ΔNPP was estimated independently for **a.**, irrigated; **b.**, high input; **c.**, low input; and **d.**, subsistence management intensities. All remaining vegetated land is represented in grey, while barren land is represented in white. Globally, agricultural landcover conversion has reduced natural primary production by 3.0 ± 0.68 Pg C y^{-1}, with a disproportionately large percentage of this reduction attributable to the conversion of temperate and tropical ecosystems (Table 3.1).

Considering only the dominant agricultural climate zones, while controlling for the top predictor variables (conversion type and management intensity), we further elucidate the link between positive ΔNPP values and management intensity (Fig. 3.2). Again, we show that positive mean ΔNPP values depend on intensive management (i.e., irrigated or high input rain-fed) within highly biophysically constrained climate zones (i.e., cold and arid climates) (Fig. 3.2-3.3). In particular, intensive management occurs over 90% of agricultural lands within cold climates resulting in a range of annual mean ΔNPP of +103 to +344 g C m^{-2} for converted non-forest land and -41 to +130 g C m^{-2} for converted forested land (Table 3.1). Yet, these gains over natural rates of productivity have come at a cost. For example, the global unsustainable depletion of groundwater has more than doubled from 1960 to 2000, mainly due to increased rates of irrigation (Wada *et al.* 2010). Similarly, current fertilization rates are already disturbing the natural nitrogen cycle, resulting in extensive eutrophication of freshwater and coastal zones, along with increased emission of the potent GHG nitrous oxide (N_2O) (Crutzen *et al.* 2008). Thus, we argue that emphasis should be placed on increasing the resource use efficiency of agricultural lands in cold climates. Further, we argue that cold climates represent the best option for agricultural extensification since ΔNPP values are the highest of any climate zone, and future improvements in agricultural resource use efficiency could make available resources for additional croplands. Finally, climate warming will likely drive a relaxation of minimum temperature constraints resulting in an expansion of the proportion of land within a minimum growing degree day index for agricultural production (Ramankutty *et al.* 2002). Conversely, intensive management occurs over only 46% of agricultural lands within tropical climate zones resulting in a range of annual

mean ΔNPP of -153 to -312 g C m^{-2} for converted non-forest land and -604 to -693 for converted forest land. Thus, given the significantly negative change in NPP due to agricultural conversion in tropical climates even under conditions of intensive management, we argue that the best method for increasing agricultural output in tropical climate zones is via agricultural intensification, thereby conserving currently intact tropical ecosystems. Intensification could be met via improved crop cultivars, management practices, resource availability, and resource use efficiency (Foley *et al.* 2011; Ramankutty & Rhemtulla 2012).

Lastly, the results of this analysis also challenge the long-standing inherent assumption that bioenergy crops are carbon neutral. The carbon neutrality assumption stands that carbon released during biomass combustion was previously absorbed during biomass growth and thus ultimately has a net neutral impact on atmospheric CO_2 (Haberl 2013). Yet, this assumption ignores the impact of landuse change on the flow of carbon from the atmosphere to the ecosystem (Haberl 2013). For instance, we show that many of the major bioenergy crops (i.e., cereal crops, oil crops, and sugar crops) have significantly reduced biospheric vegetation productivity; thus, reducing the flow of carbon from the atmosphere to the ecosystem (Fig. 3.2-3.3; Fig. S3.4). For tropical forests in particular, the mean reduction in productivity due to agricultural landcover conversion is -871 g C m^{-2} (Table 3.1); a value significantly higher than the mean annual offset potential of bioenergy crops (Haberl 2013). Thus, future policy that ignores this important flow of carbon could undermine the fossil fuel offset potential of bioenergy, and ultimately increase annual greenhouse gas emissions (Haberl 2013).

Conclusions

We estimate that current agricultural landcover conversion has reduced biospheric primary production by 6-9% annually. This finding suggests that for agricultural output to increase while simultaneously decreasing biospheric degradation, a focus must be placed on intensification as opposed to extensification. Interestingly, 6-9% of biospheric NPP is equivalent to 80%-130% of current agricultural productivity, suggesting that if production on existing agricultural land is increased up to that of the natural potential, agricultural output could more than double. This range for "potential intensification" agrees well with recent studies that have also suggested agricultural production could be doubled via intensification (Foley *et al.* 2011). However, a majority of current agricultural land is currently in tropical and temperate climate zones, which we show to have productivity far lower than natural rates even under conditions of management. Further, we show intensification in cold and arid climates in strongly dependent on management intensity which has numerous detrimental trade-offs. Thus, an important area of future research remains exploring methods to successfully increase output on existing agricultural land while decreasing dependence on unsustainable freshwater and nutrient usage (Licker *et al.* 2010; Johnston *et al.* 2011; Foley *et al.* 2011).

Unfortunately, future projections indicate some degree of future agricultural extensification is unavoidable (Tilman *et al.* 2011), with likely disproportionately-large increases in the agricultural conversion of temperate and tropical biomes (DeFries 2002; West *et al.* 2010). Yet, recent research has found that net global CO_2 uptake – regulated by vegetation productivity – has been steadily increasing such that 55% of the total CO_2 emitted by humans to the atmosphere has moved into biospheric sinks, significantly

reducing the rate at which the Earth warms (Ballantyne *et al.* 2012). While the exact locations and mechanisms responsible for increased global CO_2 uptake remain unknown, the tropics and temperate biomes have been identified as regions with a high capacity for future productivity increases (Cleveland et al.). Our results indicate that under current agricultural practice, agricultural extensification into these highly productive biomes will significantly decrease NPP and thus CO_2 sink strength. We alternatively suggest cold climate zones as the best option for extensification, in that the impact of agriculture on NPP within this climate zone is minimized. Ultimately, agricultural output must increase in the future to keep pace with an ever growing population; results from this analysis suggest that the agricultural conversion of temperate and tropical biomes should be reserved as a last resort to avoid significant detrimental biospheric degradation, which could undermine the ability of the terrestrial biosphere in mitigate the atmospheric CO_2 growth rate.

Methods Summary

We started by merging bottom-up, census-derived agricultural NPP with top-down, satellite-derived natural NPP (Text S3.1-S3.4; Figure S3.1). Census-derived agricultural NPP was derived from two independent data sources that describe global agricultural extent and yield by crop type (You *et al.*; Monfreda *et al.* 2008). We used census-derived agricultural data from You et al. (2006) which is produced at high resolution (10-km^2) for multiple crop types (20 staple crops) and has been previously disaggregated by management level (irrigated, high input, low input, and subsistence) (Text S3.1). The irrigated class represents high input management plus croplands equipped for either full

or partial control irrigation; the high input class represents high yielding cultivars that are rain-fed and fertilized, with some level of chemical pest, disease, and weed controls; the low Input class represents traditional cultivars that are rain-fed, with little to no application of fertilizers or chemicals for pest and disease control; and the subsistence class represents traditional cultivars that are rain-fed, with little to no application of fertilizers or chemicals for pest and disease control, and are consumed locally. The definition of these input systems is included in Table 1 and follows the classification established by the FAO/IIASA Global Agro-Ecological Zones project (http://webarchive.iiasa.ac.at/Research/LUC/GAEZ/index.htm). We also incorporated census-derived agricultural data from Monfreda et al. (2008) which is produced at high resolution (10-km^2) for all 127 non-tree crop types recognized by the Food and Agricultural Organization of the United Nations (FAO). We converted agricultural yield data to NPP by applying crop specific conversion factors as described in Text S3.1, and validated that agricultural NPP produced from only 20 aggregate crop types compared well against agricultural NPP generated from all 127 crop types (Text S3.3). We used 1-km2 MODIS NPP data – calculated according to the MODIS NPP algorithm – to represent natural NPP, which we averaged over the 2000-2010 period and aggregated to a 10-km^2 spatial resolution (Running *et al.* 2004; Zhao *et al.* 2005; Zhao & Running 2010, 2011)(Text S3.2). MODIS NPP was validated against Ecosystem Model-Data Intercomparison (EMDI) NPP data, which consists of 5600 across-biome ground-based observations of NPP extrapolated globally at a 50-km^2 spatial resolution using the National Center for Ecological Analysis and Synthesis regression model (the NCEAS model) (Text S3.3). We then cross-validated our independent estimates of NPP by

compare satellite-derived and census-derived NPP estimates across regions dominated by agriculture lands (Text S3.3). We next combined census- and satellite-derived NPP estimates using a landcover classification that represented fractional cropland area merged with estimates of the dominant natural vegetation type, which we simply separated into either forest or non-forest (Monfreda *et al.* 2008; Friedl *et al.* 2010)(Text S3.4). Agricultural and natural productivity estimates were then differenced while controlling for climate zone to estimate the relative change in NPP resulting for agricultural landcover conversion (ΔNPP; Text S3.5). We then disaggregate ΔNPP by crop type, conversion type, management level, climate zone, and region and apply a boosted regression tree approach to estimate the relative importance and explanatory value of each factor in determining the relationship between agricultural output and natural biospheric productivity (Text S3.6). Finally, we constrained our results by decadal-scale interannual variability in natural NPP, estimated as the standard deviation of 10-km^2 MODIS NPP recorded from 2000 through 2010 (Text S3.6).

Supplementary Information

Text S3.1. Census-derived agricultural NPP.

Agricultural NPP was derived from 10-km^2 fractional harvest area and yield data generated for 20 staple crops globally (AGR20 NPP; You *et al.*, 2006). AGR20 NPP was produced by compiling national, state, and county level census statistics and then using a Spatial Allocation Model to attach the census data to 10-km^2 global grid, as described in You *et al.* (2006). AGR20 NPP was disaggregated by management intensity (i.e., irrigated, high input rain-fed, low input rain-fed, and subsistence) according to 1)

the ratio of crop yield under irrigated conditions to that under rain-fed conditions and 2) the ratio of yield under high-input rain-fed conditions to that under low input rain-fed conditions. These ratios were allowed to vary by both crop type and country according to spatially-explicit irrigation and fertilization application data to account for spatial heterogeneity in management efficiency. For more information regarding this dataset, please see You *et al.* (2006). We also utilized 10-km^2 fractional harvest area and yield data generated for all 127 non-tree crop types recognized by the Food and Agricultural Organization of the United Nations (FAO) (AGR127 NPP; Monfreda *et al.* 2008). These data sets are not independent since both depend on very similar national, state, and county level census statistics. Yet, utilizing both allowed us to estimate the impact of different management intensities for 20 staple crops, and the impact of agricultural landcover conversion for all 127 non-tree crops. Further, we were able to evaluate the effect of generating agricultural NPP from only 20 aggregate crop types versus generating agricultural NPP from all 127 non-tree crop types across climate zones (Text S3.3). Census-derived agricultural NPP (NPP_{Agr}) was calculated from yield and harvest area data according to Equation S3.1, as previously specified in Monfreda *et al.* (2008).

$$NPP_{Agr} = \sum_{i=1}^{n} \frac{Y_i \times DF_i \times CF}{HF_i \times ABV_i \times HA_i} \qquad \text{S3.1}$$

Where n is the total number of crop types, i is the specific crop, Y is the specific crop yield, DF is the dry fraction of the yield, CF is the carbon fraction of the yield (i.e., 0.45 g C g^{-1} dry matter), and ABV is the ratio of above ground to total production. Finally, HF refers to the harvest fraction, or the proportion of total aboveground production allocated to the harvestable part of the plant. Conversion factors used to convert crop yields to

primary productivity can be found in Table S3.1. For more detail regarding this calculation, see Monfreda *et al.* (2008).

Text S3.2. Satellite-derived and empirically-based natural NPP.

The Moderate Resolution Imaging Spectroradiometer (MODIS) GPP/NPP algorithm was used to calculate 1-km^2 MODIS NPP from 2000 through 2010 (MODIS NPP; Fig. S3.1) (Running *et al.* 2004; Zhao *et al.* 2005; Zhao & Running 2010). Biome-specific vegetation parameters were mapped according to MODIS landcover data, which represents the dominant vegetation type at a 1-km^2 spatial resolution (Friedl *et al.* 2010). The MODIS GPP/NPP algorithm was driven by daily meteorological data (i.e., temperature and vapor pressure deficit) as well as remotely sensed vegetation property dynamics (i.e., the fraction of photosynthetically active radiation and leaf area index). 1-km^2 MODIS NPP was aggregated to a spatial resolution of 10-km^2 and then averaged over the 2000-2010 time period to account for decadal-scale interannual variability (Fig. S3.1). For more detail as well as a validation of the MODIS GPP/NPP algorithm see Running *et al.* (2004), Zhao *et al.* (2005), and Zhao & Running (2010).

Ecosystem Model-Data Intercomparison (EMDI) NPP data from 2000 through 2010 were used as a second independent measure of global NPP (EMDI NPP) (Grosso & Parton 2010) to validate MODIS NPP (Text S3.3). EMDI NPP consists of roughly 5600 data points spanning a range in climate zones and vegetation types. The National Center for Ecological Analysis and Synthesis regression model (the NCEAS model), was used to extrapolate EMDI NPP observations globally at a 50-km^2 resolution. For additional model details, please refer to Grosso & Parton (2010).

Text S3.3. Validation of agricultural and natural NPP datasets.

We show that census-derived, total agricultural NPP derived from 20 aggregate crop types (AGR20 NPP; You *et al.* 2006) are highly correlated with census-derived total agricultural NPP derived from all 127 non-woody crop types (AGR127 NPP; Monfreda *et al.* 2008). Although both are based on very similar national, state, and county level census statistics, a comparison shows that generating agricultural NPP from only 20 aggregate crop types is as effective as generating agricultural NPP from all 127 non-tree crop types (Fig. S3.2a). The crop-specific conversion factors utilized in this analysis to convert SPAM and M3 crop yield data to NPP can be found in Table S3.1 and were previously published in Monfreda et al. (2008).

We show that satellite-derived Moderate Resolution Imaging Spectroradiometer (MODIS) NPP for both natural forest and natural non-forest landcover types are strongly correlated with empirically-based Ecosystem Model-Data Intercomparison (EMDI) NPP estimates (Fig. S3.2b-S3.2c). MODIS NPP estimates were generally higher that EMDI NPP estimates across climate zone, especially in the case of forests (Fig. S3.2c); however this is not surprising since EMDI NPP is limited by the number of NPP observations greater than 1000 gC m^{-2} (Grosso & Parton 2010). MODIS-based average global NPP from 2000-2010 was estimated to be 53.1 Pg C y^{-1}, while EMDI-based NPP from 2000-2010 was estimated to be 42.4 Pg C y^{-1}. Since the mean across all published estimates of global NPP for the 2000s was previously found to be 59.5 (± 8.9) Pg C y^{-1} (Ito 2011), we use MODIS NPP as a conservative representation of the natural productivity potential of the biosphere.

We cross-validate census-derived agricultural NPP (AGR20 NPP) against satellite-derived MODIS NPP for the major agricultural climate zones of the world (Figure S3.2d). We show that estimates in cold and arid climates are highly correlated with very little bias (Fig. S3.2d), while MODIS NPP estimates are significantly higher than SPAM NPP estimates in temperate and tropical climates (Fig. S3.2d). This relationship between census- and satellite-derived NPP has been previously observed and can be attributed to the growth of non-crop vegetation either during or outside the growing season for a given crop type (Lobell *et al.* 2002). Thus, while census-derived estimates of NPP are solely derived from crop yield data and only consider crop growth, satellite-derived NPP incorporates all vegetation growth including non-crop growth, which is highest in temperate and tropical climate zones (DeFries 2002; Lobell *et al.* 2002). This discrepancy highlights a major limitation in agricultural remote sensing and supports our use of census-derived data to characterize the impact of agricultural on global vegetation growth. Census-derived agricultural NPP represents our best current approximation of agricultural production at the global scale, and the range of AGR20 NPP estimates are consistent with satellite-derived MODIS NPP estimates (Fig. S3.2d). Similarly, MODIS NPP is arguably the best current approximation of natural productivity at the global scale, a fact validated by multiple independent studies (Zhao *et al.* 2005; Zhao & Running 2010).

Text S3.4. Landcover classification, climate zones, and regions.

We utilized a landcover classification that consisted of agricultural, natural, and mixed landcover types (Fig. S3.3). Our classification combines bottom-up agricultural

landcover data (Monfreda et al. 2008) as well as top-down satellite landcover data (Friedl et al. 2010). Thus, the agricultural landcover class represents agriculture-dominated areas, such that both census landcover and satellite landcover data agreed. While, the mixed landcover class represents regions identified by census landcover to contain some fraction of croplands, yet identified by satellite landcover data to be dominated by natural (i.e. non-agricultural) vegetation. Finally, the natural landcover class represents areas were census and satellite data agree that croplands are not present. The natural landcover class was further partitioned into either forest or non-forest according to the dominant landcover type. Forest landcover was defined to include evergreen needleleaf, evergreen broadleaf, deciduous needleleaf, deciduous broadleaf, and mixed forest landcover types (Friedl et al. 2010). Non-forest landcover was defined to include all remaining non-barren landcover types (Friedl et al. 2010). Finally, we further partitioned the agricultural and mixed landcover classes according to the original natural vegetation type replaced, which we aggregate into forest or non-forest as defined by Ramankutty *et al.* (2002).

Climate zones were defined using the Koppen-Geiger climate classification based on a large global dataset of long-term monthly precipitation and temperature station data, as described in Peel (2007) (Fig. S3.3b). Climate zones considered in this study consisted of 3 tropical, 9 temperate, 12 cold, and 4 arid as illustrated in Fig. S3c. For algorithm details and classification criteria please see Peel (2007). By comparing NPP values across climate zones, we remove the need to model natural, pre-agriculture NPP, and instead simply apply the empirical relationship between agricultural and natural NPP generated for each climate zone to infer productivity changes that have resulted from agricultural conversion (Table 3.1; Table S3.2).

Regions represent an aggregation of the classification of the macro geographical regions and sub-regions defined by the United Nations Statistical Division (USSD 2010). The 5 region classification was determined based on the level of industrialization, which we use as a rough measure of agricultural technological development (Fig. S3.3d).

Text S3.5. Calculation of ΔNPP.

We calculated the change in NPP due to agricultural landcover conversion (ΔNPP) as the average difference between census-derived agricultural and satellite-derived natural NPP for a given climate zone, according to the below equation:

$$\Delta NPP = \sum_{i=1}^{n} \sum_{j=1}^{m} [NPP_{Agr_j} + (\overline{NPP_{Agr_i}} - \overline{NPP_{Nat_i}})]; \quad \text{S3.2}$$

Where $\overline{NPP_{Agr}}$ and $\overline{NPP_{Nat}}$ represent the mean productivity for agricultural and natural landcover types, respectively, for a given climate zone (n), while NPP_{Agr} represents agricultural productivity calculated for every 10-km^2 of the vegetated Earth (m), estimated according to Equation S3.1. ΔNPP was calculated separately according to conversion type (forest or non-forest), management intensity (irrigated, high input rain-fed, low input rain-fed, and subsistence), crop type (cereal, oil, pulse, and sugar), and region (Industrialized West, Latin America, Eastern Europe, Asia, and Africa and the Middle East).

Text S3.6. Statistical Analysis.

We first quantified the relationship between the response variable (ΔNPP) and each of the predictor variables (climate zone, conversion type, management intensity, crop type,

and region) using a boosted regression tree (BRT) model (Elith *et al.* 2008). BRT is an ensemble method for fitting statistical models that incorporates tree-based methods (i.e., models that use recursive binary splits to relate a response variable to given predictor variables) and boosting (i.e., an adaptive method to improve the explanatory power of the predictor variables by combining many simple models). Thus, BRT models are a powerful method for establishing the relative importance of a set of given predictor variables, such as the set of predictors described for this study. We also utilized a standard classification and regression tree (CART) to recursively relate ΔNPP to then predictor variables defined above (Fig. 3.1). We initially generated an over-fit regression tree considering all possible branches and interactions between predictors, and then we determined optimal tree size using cost-complexity pruning based on 10-fold cross-validation (Elith *et al.* 2008). BRT and CART were implemented using the gbm and rpart libraries in R 2.11.1 (R development Core team), respectively. Finally, we used pair-wise t-tests to quantify significant departures from decadal-scale natural variability in productivity (Fig. 3.2-3.3, Fig. S3.5). Pair-wise t-tests were implemented using the t.test() function in R 2.11.1 (R development Core team).

Table S3.1. Crop types and conversion factors used to convert crop-specific yield data to agricultural net primary productivity data. a., Crop-specific conversion factors used to convert agricultural extent and yield to primary productivity (NPP) for 20 aggregate crop types (AGR20 NPP; You *et al.* 2006). **b.**, Crop-specific conversion factors used to convert agricultural extent and yield to primary productivity (NPP) for all 127 Food and Agricultural Organization of the United Nations (FAO) recognized non-tree crop types (AGR127 NPP; Monfreda *et al.* 2008).

a.

Crop Type	Harvest Index	Dry Fraction	Abv Fraction	Crop Type
barley	0.49	0.89	0.50	Cereal
maize	0.45	0.89	0.85	Cereal
millet	0.40	0.90	0.88	Cereal
rice	0.40	0.89	0.80	Cereal
sorghum	0.40	0.89	0.80	Cereal
wheat	0.39	0.89	0.81	Cereal
cotton	0.55	0.92	0.86	Fiber
other fibers	0.28	0.80	0.80	Fiber
banana-plantain	0.30	0.20	0.75	Other
groundnut	0.40	0.92	0.80	Oil
other oils	0.52	0.73	0.80	Oil
soybean	0.42	0.91	0.85	Oil
coffee	0.28	0.80	0.50	Other
beans	0.42	0.91	0.85	Pulse
other pulses	1.00	0.20	0.65	Pulse
cassava	0.48	0.32	0.85	Root
potato	0.50	0.28	0.80	Root
sugarbeet	0.40	0.12	0.80	Root
sweetpotato	0.50	0.25	0.80	Root
sugarcane	0.85	0.15	0.85	Sugar

b.

Crop Type	Harvest Index	Dry Fraction	Abv Fraction	Crop Type
Barley	0.49	0.89	0.50	Cereals
Buckwheat	0.40	0.88	0.80	Cereals
Canary Seed	0.40	0.88	0.80	Cereals
Cereals, other	0.40	0.88	0.80	Cereals
Fonio	0.40	0.88	0.80	Cereals
Maize	0.45	0.89	0.85	Cereals
Millet	0.40	0.90	0.88	Cereals
Mixed Grains	0.40	0.88	0.80	Cereals
Oats	0.40	0.89	0.71	Cereals
Pop Corn	0.45	0.89	0.85	Cereals
Quinoa	0.40	0.88	0.80	Cereals
Rice	0.40	0.89	0.80	Cereals
Rye	0.35	0.88	0.76	Cereals
Sorghum	0.40	0.89	0.80	Cereals
Triticale	0.46	0.90	0.80	Cereals

Wheat	0.39	0.89	0.81	Cereals
Cotton	0.55	0.92	0.86	Fiber
Coir	0.28	0.80	0.80	Fiber
Fibre Crops, other	0.28	0.80	0.80	Fiber
Flax	0.28	0.80	0.80	Fiber
Hemp	0.28	0.80	0.80	Fiber
Jute	0.28	0.80	0.80	Fiber
Jute-Like	0.28	0.80	0.80	Fiber
Abaca	0.28	0.80	0.50	Fiber
Agave Fibers, other	0.28	0.80	0.50	Fiber
Ramie	0.28	0.80	0.50	Fiber
Sisal	0.28	0.80	0.50	Fiber
Forage Products, other	1.00	0.20	0.65	Forage
Alfalfa	1.00	0.20	0.53	Forage
Beets (Fodder)	1.00	0.13	0.85	Forage
Cabbage (Fodder)	1.00	0.08	0.85	Forage
Carrots (Fodder)	1.00	0.12	0.85	Forage
Clover	1.00	0.20	0.50	Forage
Grasses, other	1.00	0.20	0.65	Forage
Green Oilseeds (Fodder)	1.00	0.35	0.80	Forage
Legumes, other	1.00	0.20	0.65	Forage
Maize (Forage and Silage)	1.00	0.35	0.85	Forage
Mixed Grasses & Legumes	1.00	0.20	0.65	Forage
Rye Grass (Forage and Silage)	1.00	0.20	0.65	Forage
Sorghum (Forage and Silage)	1.00	0.35	0.85	Forage
Swedes (Fodder)	1.00	0.13	0.85	Forage
Turnips (Fodder)	1.00	0.13	0.85	Forage
Vegetables Fresh, other	0.45	0.13	0.85	Forage
Bananas	0.30	0.20	0.75	Fruit
Berries, other	0.30	0.19	0.75	Fruit
Blueberries	0.30	0.15	0.75	Fruit
Cranberries	0.30	0.19	0.75	Fruit
Gooseberries	0.30	0.19	0.75	Fruit
Grapes	0.30	0.19	0.75	Fruit
Pineapples	0.30	0.14	0.75	Fruit
Plantains	0.30	0.20	0.75	Fruit
Raspberries	0.30	0.13	0.75	Fruit
Strawberries	0.30	0.08	0.75	Fruit
Castor Beans	0.52	0.73	0.80	Oil
Groundnuts	0.40	0.92	0.80	Oil
Hempseed	0.52	0.73	0.80	Oil
Linseed	0.52	0.73	0.80	Oil
Melonseed	0.52	0.73	0.80	Oil
Mustard Seed	0.52	0.73	0.80	Oil
Oilseeds, other	0.52	0.73	0.80	Oil
Poppy Seeds	0.52	0.73	0.80	Oil
Rapeseed	0.30	0.73	0.80	Oil
Safflower Seed	0.52	0.91	0.80	Oil
Sesame Seed	0.52	0.92	0.80	Oil
Soybeans	0.42	0.91	0.85	Oil
Sunflower Seed	0.39	0.94	0.94	Oil
Anise, Badian and Fennel	0.28	0.80	0.50	Other
Chicory Roots	0.28	0.80	0.80	Other
Ginger	0.28	0.80	0.50	Other
Peppermint	0.28	0.80	0.50	Other
Pimento	0.28	0.80	0.80	Other

Tobacco Leaves	0.28	0.80	0.80	Other
Cocoa Beans	0.28	0.80	0.50	Other
Coffee, Green	0.28	0.80	0.50	Other
Hops	0.28	0.80	0.50	Other
Mate	0.28	0.80	0.50	Other
Nutmeg, Mace and Cardamons	0.28	0.80	0.50	Other
Pepper	0.28	0.80	0.50	Other
Pyrethrum, Dried Flowers	0.28	0.80	0.50	Other
Tea	0.28	0.80	0.50	Other
Vanilla	0.28	0.80	0.50	Other
Bambara Beans	0.49	0.90	0.85	Pulse
Beans, Dry	0.55	0.90	0.74	Pulse
Broad Beans, Dry	0.49	0.90	0.85	Pulse
Chick-Peas	0.44	0.90	0.85	Pulse
Cow Peas, Dry	0.55	0.90	0.85	Pulse
Lentils	0.46	0.89	0.85	Pulse
Lupins	0.41	0.89	0.85	Pulse
Peas, Dry	0.45	0.89	0.85	Pulse
Pigeon Peas	0.23	0.90	0.85	Pulse
Pulses, other	0.49	0.90	0.85	Pulse
Vetches	0.49	0.90	0.85	Pulse
Cassava	0.48	0.32	0.85	Root
Potatoes	0.50	0.28	0.80	Root
Roots and Tubers, other	0.40	0.20	0.80	Root
Sweet Potatoes	0.50	0.25	0.80	Root
Taro	0.40	0.20	0.80	Root
Yams	0.40	0.30	0.80	Root
Yautia	0.40	0.20	0.80	Root
Sugar Beets	0.40	0.12	0.80	Sugar
Sugar Cane	0.85	0.15	0.85	Sugar
Sugar Crops, other	0.28	0.56	0.85	Sugar
Artichokes	0.45	0.13	0.85	Vegetable / Melon
Asparagus	0.45	0.08	0.85	Vegetable / Melon
Beans, Green	0.45	0.10	0.85	Vegetable / Melon
Broad Beans, Green	0.45	0.13	0.85	Vegetable / Melon
Cabbages	0.45	0.08	0.85	Vegetable / Melon
Cantaloupes	0.45	0.10	0.85	Vegetable / Melon
Carrots	0.45	0.12	0.85	Vegetable / Melon
Cauliflower	0.45	0.08	0.85	Vegetable / Melon
Chillies & Peppers, Green	0.45	0.08	0.85	Vegetable / Melon
Cucumbers	0.45	0.04	0.85	Vegetable / Melon
Eggplants	0.45	0.08	0.85	Vegetable / Melon
Garlic	0.45	0.13	0.85	Vegetable / Melon
Green Corn (Maize)	0.45	0.13	0.85	Vegetable / Melon
Lettuce	0.45	0.05	0.85	Vegetable / Melon
Mushrooms	0.45	0.13	0.85	Vegetable / Melon
Okra	0.45	0.10	0.85	Vegetable / Melon
Onions, Dry	0.45	0.13	0.85	Vegetable / Melon
Onions & Shallots, Green	0.45	0.09	0.85	Vegetable / Melon
Peas, Green	0.45	0.13	0.85	Vegetable / Melon
Pumpkins, Squash, Gourds	0.45	0.20	0.85	Vegetable / Melon
Spinach	0.45	0.08	0.85	Vegetable / Melon
String Beans	0.45	0.13	0.85	Vegetable / Melon
Tomatoes	0.45	0.06	0.85	Vegetable / Melon
Vegetables & Roots (Fodder)	1.00	0.13	0.85	Vegetable / Melon
Watermelons	0.45	0.09	0.85	Vegetable / Melon

Table S3.2. The effect of agricultural landcover conversion on net primary production (ΔNPP) for all 127 crops. Δ NPP is divided by climate zone (tropical, temperate, cold, and arid) and the original landcover type (F = forest; NF = non-forest). Values in parentheses for spatial averages (g C m^{-2}) represent spatial variability of one standard deviation of the mean, while values in parentheses for annual averages (Tg C y^{-2}) represent decadal-scale (2000-2010) temporal variability of one standard deviation of the mean.

	Area (10^6 km^2)		**NPP (g C m^{-2} y^{-1})**		**Δ NPP (g C m^{-2} y^{-1})**		**Δ NPP (Tg C y^{-1})**		
	NF	**F**	**NF**	**F**	**NF**	**F**	**NF**	**F**	**T**
Total	**6.2**	**5.5**	**250 (139)**	**337 (101)**	**-143 (225)**	**-455 (280)**	**-1041 (384)**	**-2687 (463)**	**-3728 (847)**
trop	1.1	1.5	190 (100)	265 (118)	-406 (269)	-761 (337)	-427 (91)	-989 (150)	-1416 (241)
temp	1.4	2.2	293 (139)	387 (163)	-369 (319)	-594 (487)	-469 (105)	-1250 (193)	-1719 (298)
cold	1.9	1.5	289 (153)	351 (165)	36 (176)	-116 (206)	39 (75)	-295 (91)	-257 (166)
arid	1.8	0.3	210 (148)	226 (112)	-87 (219)	-371 (403)	-184 (114)	-152 (28)	-336 (142)

Figure S3.1. Global net primary productivity (NPP). a., Global census-derived agricultural productivity, **b.**, satellite-derived natural non-forest productivity, and **c.**, satellite-derived natural forest productivity. All vegetated land is represented in grey, while barren land is represented in white.

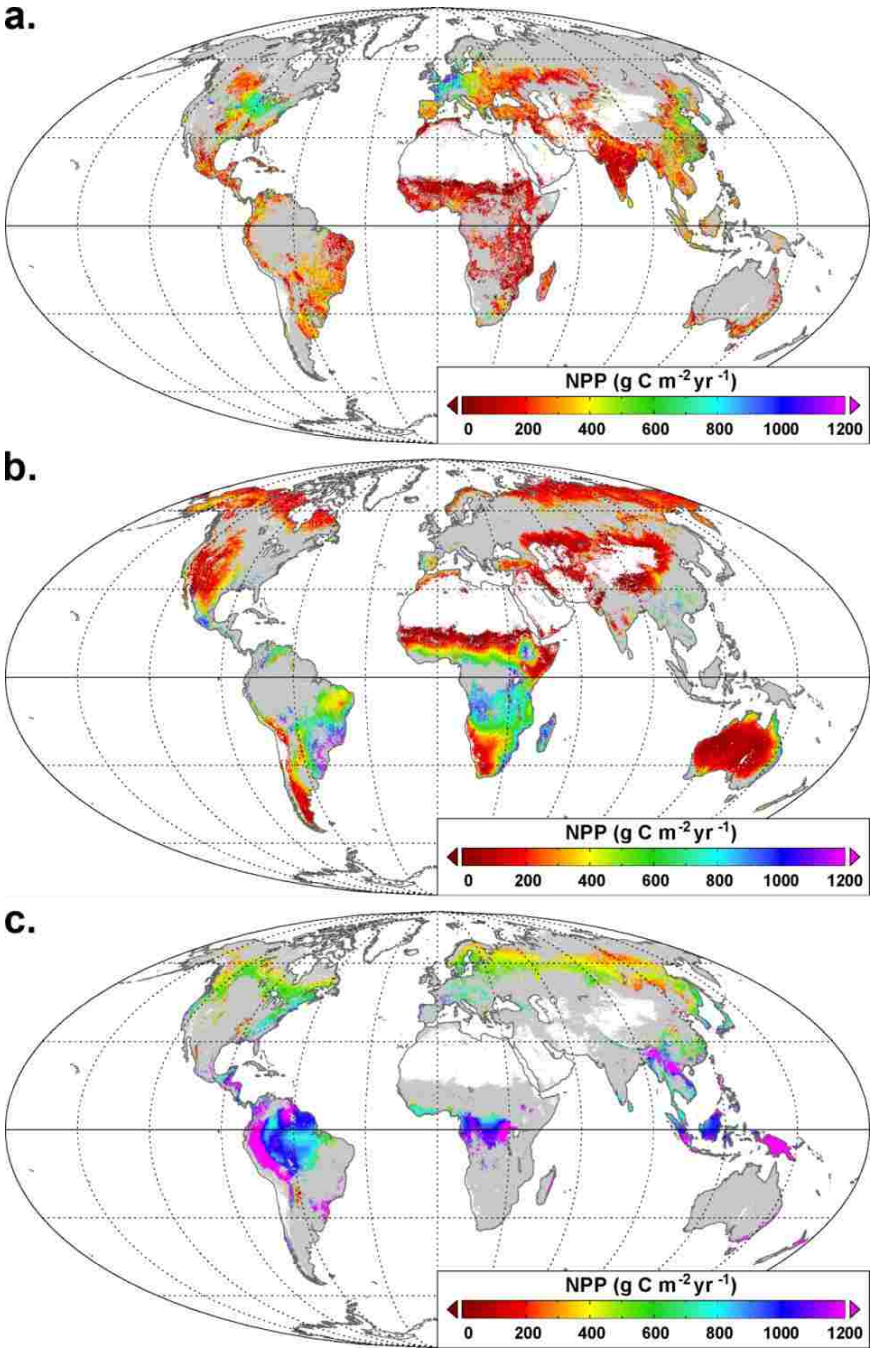

Figure S3.2. A comparison of independent estimates of agricultural and natural NPP across climate zones. **a.**, Census-derived agricultural NPP data from 20 aggregate crop types (AGR20 NPP) compared against census-derived agricultural NPP derived from all 127 FAO recognized crop types. **b.**, Satellite-derived natural non-forest NPP (MODIS NPP) compared against empirically-based natural non-forest NPP (EMDI NPP). **c.**, Satellite-derived natural forest NPP (MODIS NPP) compared against empirically-based natural forest NPP (EMDI NPP). **d.**, Census-derived agricultural NPP data from 20 aggregate crop types (AGR20 NPP) compared against satellite-derived agricultural NPP (MODIS NPP). Climate zones – defined using the Koppen-Geiger climate classification (Peel 2007) – are listed in Fig. S3b-c. Error bars represent one standard deviation of the mean.

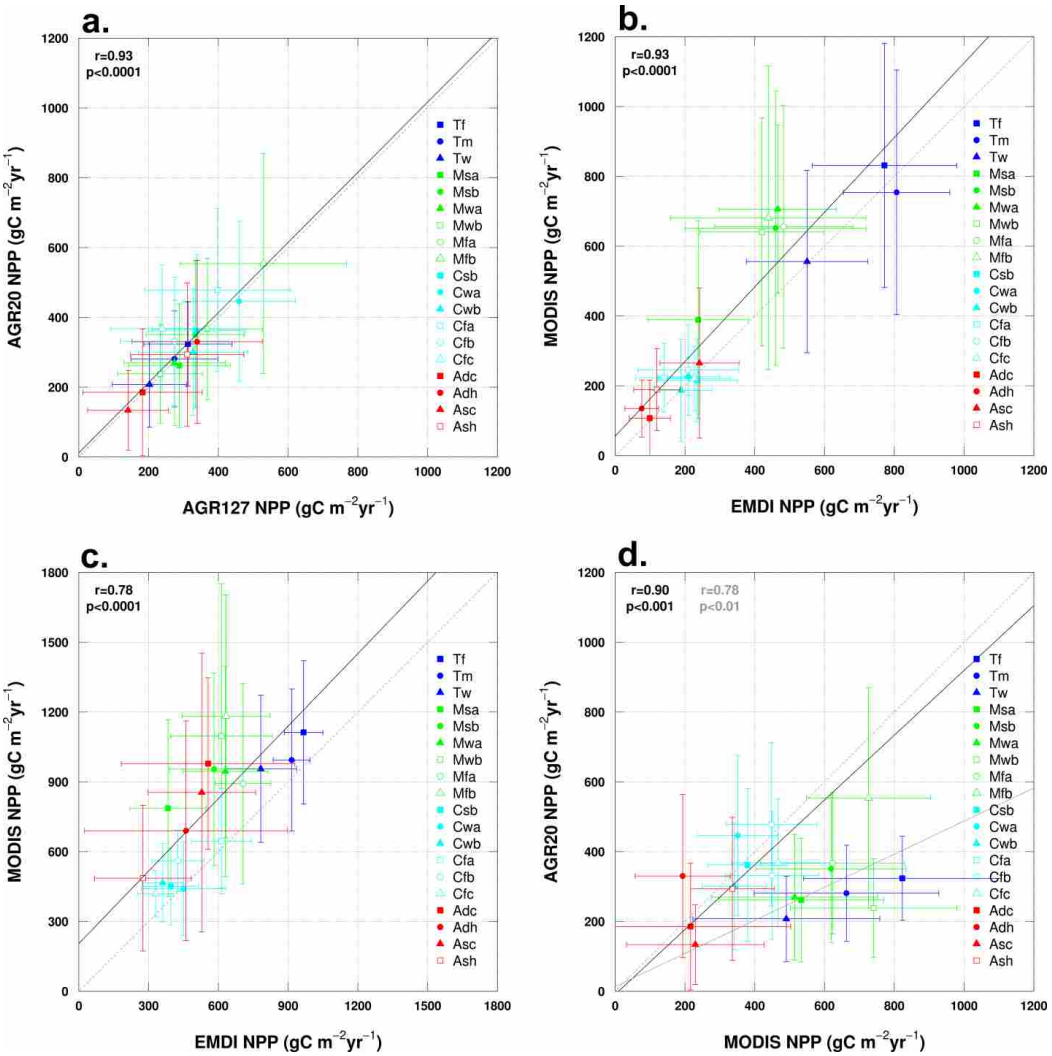

Figure S3.3. Global landcover, climate zones, and world regions. a., Global landcover classification defined to include agricultural dominated lands (Agr), natural dominated lands (Nat) and mixed agricultural and natural lands (Mix). We further divided natural lands into either forest (F) or non-forest (NF), while we divided agricultural land according to the original landcover type replaced (i.e., F or NF). **b.**, Global climate zones defined according to the Koppen-Geiger climate classification based on a large global dataset of long-term monthly precipitation and temperature station data, as described Peel (2007). **c.**, The full definition and partitioning of Koppen-Geiger climate zones, as described in Peel (2007). **d.**, World regions representing an aggregation of the macro regions defined by the United States Statistical division (USSD 2010).

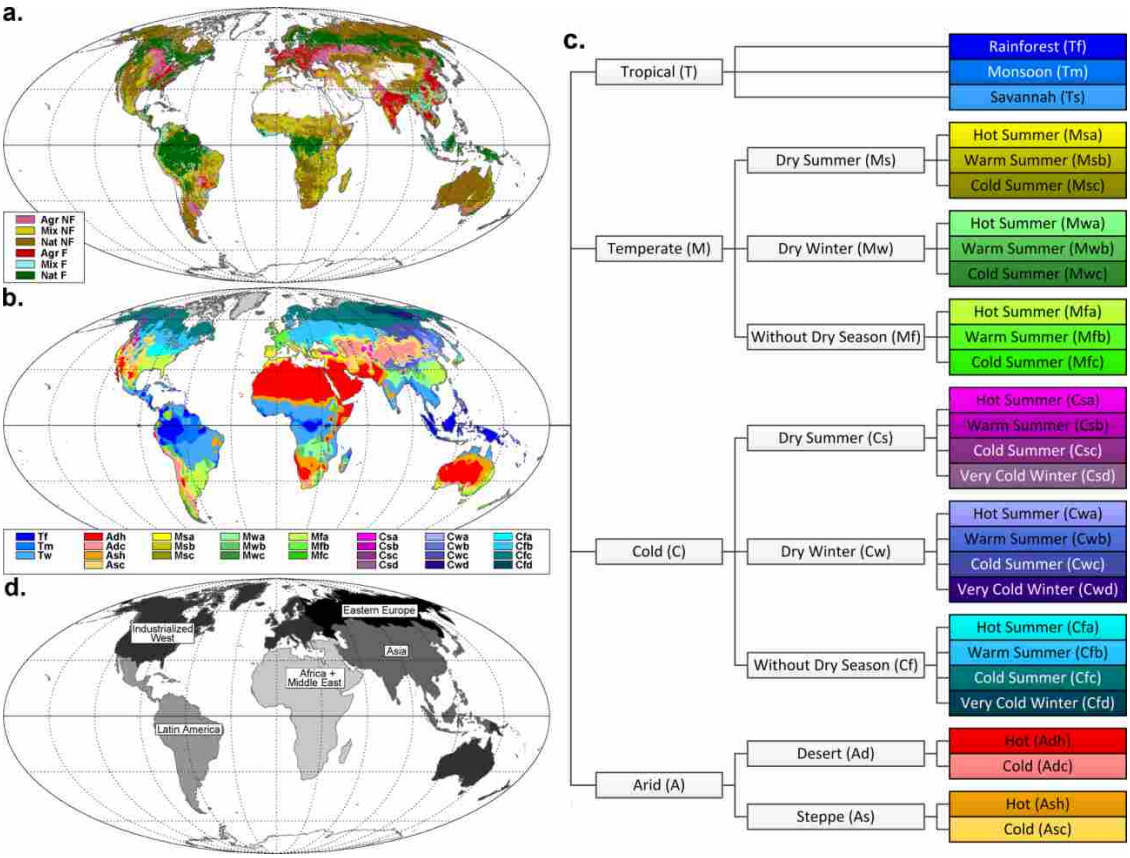

Figure S3.4. A spatially explicit estimate of the effect of agricultural landcover conversion on natural primary production (ΔNPP) by aggregate crop type. ΔNPP was estimated independently for **a.**, cereal; **b.**, oil; **c.**, pulse; and **d.**, sugar crop types. All remaining vegetated land is represented in grey, while barren land is represented in white.

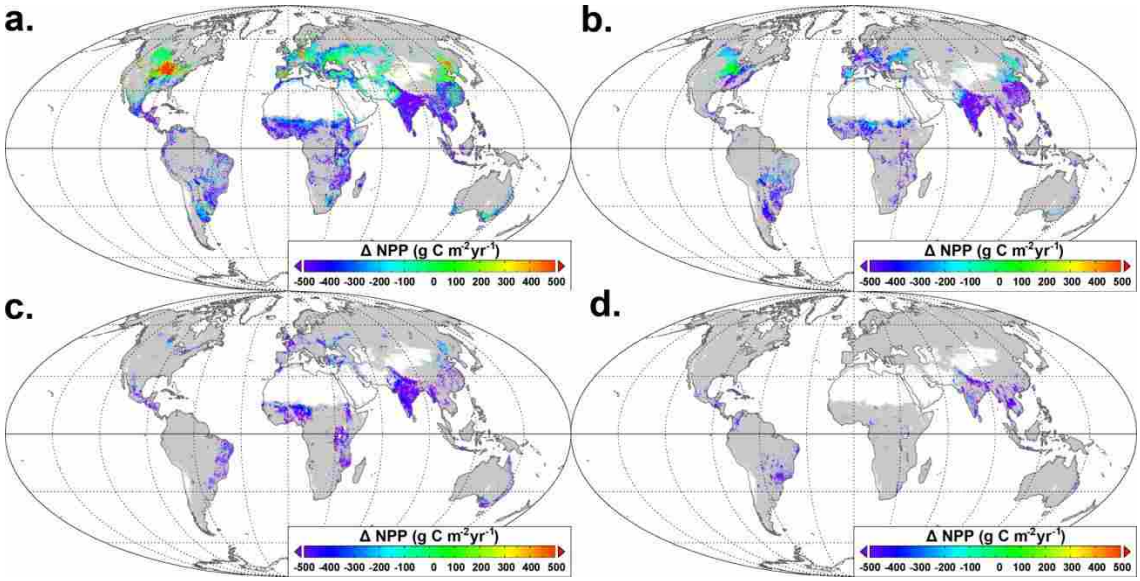

Figure S3.5. Decadal-scale interannual variability of NPP. We represent decadal-scale natural interannual as one standard deviation of the mean for 10-km^2 MODIS NPP recorded from 2000 through 2010 (Running *et al.* 2004; Zhao *et al.* 2005; Zhao & Running 2010).

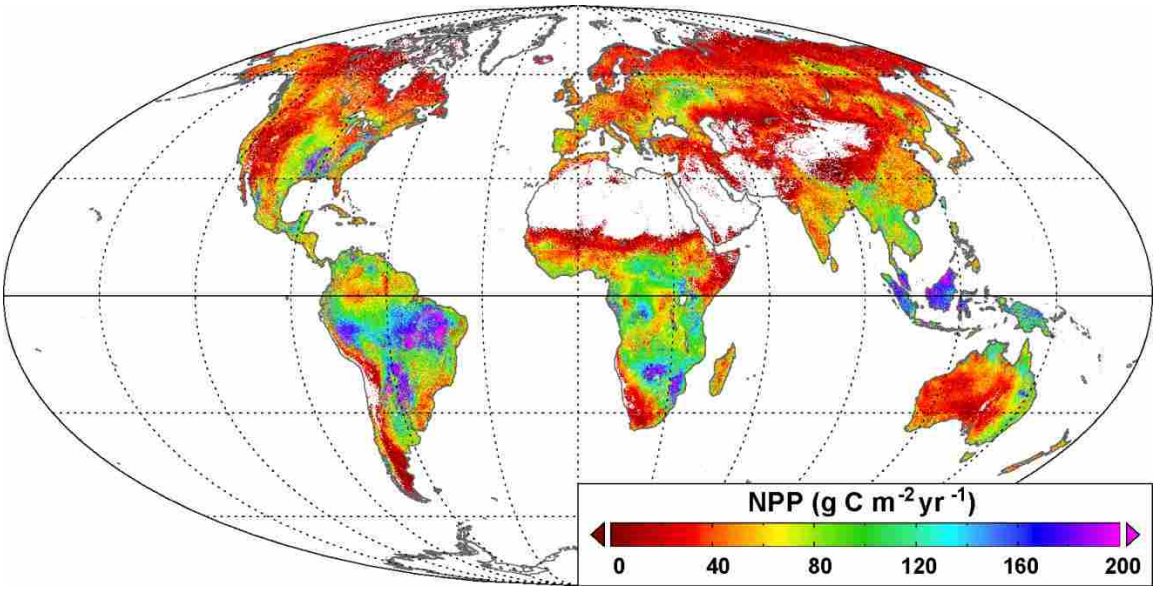

REFERENCES

Arima EY, Richards P, Walker R, Caldas MM (2011) Statistical confirmation of indirect land use change in the Brazilian Amazon. *Environmental Research Letters*, **6**, 024010.

Ballantyne AP, Alden CB, Miller JB, Tans PP, White JWC (2012) Increase in observed net carbon dioxide uptake by land and oceans during the past 50 years. *Nature*, **488**, 70–2.

Beringer T, Lucht W, Schaphoff S (2011) Bioenergy production potential of global biomass plantations under environmental and agricultural constraints. *GCB Bioenergy*, **3**, 299–312.

Bondeau A, Smith PC, Zaehle S, *et al.* (2007) Modelling the role of agriculture for the 20th century global terrestrial carbon balance. *Global Change Biology*, **13**, 679–706.

Campbell JE, Lobell DB, Genova RC, Field CB (2008) The global potential of bioenergy on abandoned agriculture lands. *Environmental Science & Technology*, **42**, 5791–4.

Cassman KG (1999) Ecological intensification of cereal production systems: yield potential, soil quality, and precision agriculture. *Proceedings of the National Academy of Sciences of the United States of America*, **96**, 5952–9.

Crutzen P, Mosier A, Smith K, Winiwarter W (2008) N2O release from agro-biofuel production negates global warming reduction by replacing fossil fuels. *Atmospheric Chemistry and Physics Discussions*, **8**, 389–395.

Dai A (2011) Characteristics and trends in various forms of the Palmer Drought Severity Index during 1900–2008. *Journal of Geophysical Research*, **116**, D12115.

Davis SC, Parton WJ, Grosso SJ Del, Keough C, Marx E, Adler PR, DeLucia EH (2012) Impact of second-generation biofuel agriculture on greenhouse-gas emissions in the corn-growing regions of the US. *Frontiers in Ecology and the Environment*, **10**, 69–74.

DeFries RS (2002) Past and future sensitivity of primary production to human modification of the landscape. *Geophysical Research Letters*, **29**, 1–4.

DeFries RS, Chapin FS, Syvitski J (2012) Planetary Opportunities: A Social Contract for Global Change Science to Contribute to a Sustainable Future. *BioScience*, **62**, 603–606.

Dornburg V, Van Vuuren D, Van de Ven G, *et al.* (2010) Bioenergy revisited: Key factors in global potentials of bioenergy. *Energy & Environmental Science*, **3**, 258.

Edenhofer O, Pichs-Madruga Y, Atschoss P, Kadner S, Eickemeier P, Zwic- kel T (Eds.) (2011) *The IPCC Special Report on Renewable Energy Sources and Climate Change Mitigation*. Cambridge, UK and New York, NY, Cambridge University Press.

EIA (2011) *International Energy Outlook 2011*. DOE/EIA-0484. Energy Information Administration, United States Department of Energy, Washington, DC, USA.

Elith J, Leathwick JR, Hastie T (2008) A working guide to boosted regression trees. *The Journal of Animal Ecology*, **77**, 802–13.

Erb K, Haberl H, Krausmann F, *et al.* (2009) *Eating the planet. Feeding and fuelling the world sustainably, fairly and humanely–a scoping study*. Vienna, Austria.

Fargione J, Hill J, Tilman D, Polasky S, Hawthorne P (2008) Land clearing and the biofuel carbon debt. *Science*, **319**, 1235–8.

Field CB (2001) Sharing the garden. *Science*, **294**, 2490–1.

Field CB, Campbell JE, Lobell DB (2008) Biomass energy: the scale of the potential resource. *Trends in Ecology & Evolution*, **23**, 65–72.

Foley JA, Defries R, Asner GP, *et al.* (2005) Global consequences of land use. *Science*, **309**, 570–4.

Foley JA, Ramankutty N, Brauman KA, *et al.* (2011) Solutions for a cultivated planet. *Nature*, **478**, 337–42.

Friedl MA, Sulla-Menashe D, Tan B, Schneider A, Ramankutty N, Sibley A, Huang X (2010) MODIS Collection 5 global land cover: Algorithm refinements and characterization of new datasets. *Remote Sensing of Environment*, **114**, 168–182.

Funk CC, Brown ME (2009) Declining global per capita agricultural production and warming oceans threaten food security. *Food Security*, **1**, 271–289.

Galloway JN, Townsend AR, Erisman JW, *et al.* (2008) Transformation of the nitrogen cycle: recent trends, questions, and potential solutions. *Science*, **320**, 889–92.

Gleick PH (2003) Water Use. *Annual Review of Environment and Resources*, **28**, 275–314.

Gleick P (2010) Roadmap for sustainable water resources in southwestern North America. *Proceedings of the National Academy of Sciences of the United States of America*, **107**, 21300–21305.

Gleick PH, Palaniappan M (2010) Peak water limits to freshwater withdrawal and use. *Proceedings of the National Academy of Sciences of the United States of America*, **107**, 11155–11162.

Graham-Rowe D (2011) Agriculture: Beyond food versus fuel. *Nature*, **474**, S6–S8.

Gregg JS, Smith SJ (2010) Global and regional potential for bioenergy from agricultural and forestry residue biomass. *Mitigation and Adaptation Strategies for Global Change*, **15**, 241–262.

Grosso S Del, Parton W (2010) Global potential net primary production predicted from vegetation class, precipitation, and temperature: reply. *Ecology*, **91**, 923–925.

Haberl H (2013) Net land-atmosphere flows of biogenic carbon related to bioenergy: towards an understanding of systemic feedbacks. *GCB Bioenergy*, **N.A.**, 10.1111/gcbb.12071.

Haberl H, Beringer T, Bhattacharya SC, Erb K-H, Hoogwijk M (2010) The global technical potential of bio-energy in 2050 considering sustainability constraints. *Current Opinion in Environmental Sustainability*, **2**, 394–403.

Haberl H, Erb KH, Krausmann F, *et al.* (2007) Quantifying and mapping the human appropriation of net primary production in earth's terrestrial ecosystems. *Proceedings of the National Academy of Sciences of the United States of America*, **104**, 12942–7.

Haberl H, Steinberger JK, Plutzar C, Erb K-H, Gaube V, Gingrich S, Krausmann F (2012) Natural and socioeconomic determinants of the embodied human appropriation of net primary production and its relation to other resource use indicators. *Ecological Indicators*, **23**, 222–231.

Heaton EA, Dohleman FG, Long SP (2008) Meeting US biofuel goals with less land: the potential of Miscanthus. *Global Change Biology*, **14**, 2000–2014.

Heaton E, Voigt T, Long S (2004) A quantitative review comparing the yields of two candidate C4 perennial biomass crops in relation to nitrogen, temperature and water. *Biomass and Bioenergy*, **27**, 21–30.

Hoogwijk M, Faaij A, Eickhout B, Devries B, Turkenburg W (2005) Potential of biomass energy out to 2100, for four IPCC SRES land-use scenarios. *Biomass and Bioenergy*, **29**, 225–257.

Howard J, Quevedo E, Kramp A (2009) *Use of indexing to update United States annual timber harvest by state*. Research Paper FPL-RP-653. Madison, WI, USA.

Ito A (2011) A historical meta-analysis of global terrestrial net primary productivity: are estimates converging? *Global Change Biology*, **17**, 3161–3175.

Johnston M, Foley JA, Holloway T, Kucharik C, Monfreda C (2009) Resetting global expectations from agricultural biofuels. *Environmental Research Letters*, **4**, 014004.

Johnston M, Licker R, Foley JA, Holloway T, Mueller ND, Barford C, Kucharik C (2011) Closing the gap: global potential for increasing biofuel production through agricultural intensification. *Environmental Research Letters*, **6**, 034028.

Lal R (2004) Soil carbon sequestration impacts on global climate change and food security. *Science*, **304**, 1623–7.

Lawrence PJ, Feddema JJ, Bonan GB, *et al.* (2012) Simulating the Biogeochemical and Biogeophysical Impacts of Transient Land Cover Change and Wood Harvest in the Community Climate System Model (CCSM4) from 1850 to 2100. *Journal of Climate*, **25**, 3071–3095.

Licker R, Johnston M, Foley JA, Barford C, Kucharik CJ, Monfreda C, Ramankutty N (2010) Mind the gap: how do climate and agricultural management explain the "yield gap" of croplands around the world? *Global Ecology and Biogeography*, **19**, 769–782.

Lobell DB, Hicke JA, Asner GP, Field CB, Tucker CJ, Los SO (2002) Satellite estimates of productivity and light use efficiency in United States agriculture, 1982-98. *Global Change Biology*, **8**, 722–735.

Long SP, Zhu X-G, Naidu SL, Ort DR (2006) Can improvement in photosynthesis increase crop yields? *Plant, Cell and Environment*, **29**, 315–330.

Lubowski R, Vesterby M, Bucholtz S (2006) *Major uses of land in the United States, 2002*.

Martin J (2011) Perspective: Don't foul the water. *Nature*, **474**, S17.

McAlpine CA, Etter A, Fearnside PM, Seabrook L, Laurance WF (2009) Increasing world consumption of beef as a driver of regional and global change: A call for policy action based on evidence from Queensland (Australia), Colombia and Brazil. *Global Environmental Change*, **19**, 21–33.

Melillo J, Borchers J, Chaney J (1995) Comparing biogeography and geochemistry models in a continental-scale study of terrestrial ecosystem responses to climate change and CO2 doubling. *Global Biogeochemical Cycles*,.

Monfreda C, Ramankutty N, Foley JA (2008) Farming the planet: 2. Geographic distribution of crop areas, yields, physiological types, and net primary production in the year 2000. *Global Biogeochemical Cycles*, **22**, 1–19.

Mueller ND, Gerber JS, Johnston M, Ray DK, Ramankutty N, Foley JA (2012) Closing yield gaps through nutrient and water management. *Nature*, **490**, 254–7.

Naylor RL, Liska AJ, Burke MB, Falcon WP, Gaske ll JC, Rozelle SD, Cassman KG (2007) The Ripple Effect: Biofuels, Food Security, and the Environment. *Environment: Science and Policy for Sustainable Development*, **49**, 30–43.

Nonhebel S (2002) Energy yields in intensive and extensive biomass production systems. *Biomass and Bioenergy*, **22**, 159–167.

Pacca S, Moreira JR (2011) A biorefinery for mobility? *Environmental Science & Technology*, **45**, 9498–9505.

Pan Y, Birdsey RA, Fang J, *et al.* (2011) A large and persistent carbon sink in the world's forests. *Science*, **333**, 988–93.

Peel M (2007) Updated world map of the Köppen-Geiger climate classification. *Hydrology and Earth System Sciences*, **11**, 1633–1644.

Ramankutty N, Evan AT, Monfreda C, Foley JA (2008) Farming the planet: 1. Geographic distribution of global agricultural lands in the year 2000. *Global Biogeochemical Cycles*, **22**, 10.1029/2007GB002952.

Ramankutty N, Foley JA, Norman J, McSweeney K (2002) The global distribution of cultivable lands: current patterns and sensitivity to possible climate change. *Global Ecology and Biogeography*, **11**, 377–392.

Ramankutty N, Rhemtulla J (2012) Can intensive farming save nature? *Frontiers in Ecology and the Environment*, **10**, 455–455.

Richards RA (2000) Selectable traits to increase crop photosynthesis and yield of grain crops. *Journal of experimental botany*, **51 Spec No**, 447–58.

Robertson G, Hamilton S (2011) The biogeochemistry of bioenergy landscapes: carbon, nitrogen, and water considerations. *Ecological Applications*, **4**, 1055–1067.

Rockström J, Steffen W, Noone K, *et al.* (2009) A safe operating space for humanity. *Nature*, **461**, 472–475.

Roy J, Saugier B, Mooney HA (Eds.) (2001) *Terrestrial global productivity*. Academic Press, London, UK.

Running SW (2012) A measurable planetary boundary for the biosphere. *Science*, **337**, 1458–9.

Running SW, Nemani RR, Heinsch FA, Zhao M, Reeves M, Hashimoto H (2004) A Continuous Satellite-Derived Measure of Global Terrestrial Primary Production. *BioScience*, **54**, 547–560.

Sanderson K (2011) Lignocellulose: A chewy problem. *Nature*, **474**, S12–S14.

Scarlat N, Dallemand J-F (2011) Recent developments of biofuels/bioenergy sustainability certification: A global overview. *Energy Policy*, **39**, 1630–1646.

Schmer MR, Vogel KP, Mitchell RB, Perrin RK (2008) Net energy of cellulosic ethanol from switchgrass. *Proceedings of the National Academy of Sciences of the United States of America*, **105**, 464–9.

Schubert S, Rood RB, Pfaendtner J (1993) An assimilated dataset for earth science applications. *Bulletin of the American Meteorological Society*, **74**, 2331–2342.

Siebert S, Döll P (2010) Quantifying blue and green virtual water contents in global crop production as well as potential production losses without irrigation. *Journal of Hydrology*, **384**, 198–217.

Smeets EMW, Faaij APC, Lewandowski IM, Turkenburg WC (2007) A bottom-up assessment and review of global bio-energy potentials to 2050. *Progress in Energy and Combustion Science*, **33**, 56–106.

Smith WK, Cleveland CC, Reed SC, Miller NL, Running SW (2012a) Bioenergy potential of the United States constrained by satellite observations of existing productivity. *Environmental Science & Technology*, **46**, 3536–44.

Smith WK, Zhao M, Running SW (2012b) Global Bioenergy Capacity as Constrained by Observed Biospheric Productivity Rates. *BioScience*, **62**, 911–922.

Thomas CD, Anderson BJ, Moilanen A, *et al.* (2012) Reconciling biodiversity and carbon conservation (J Chave, Ed.). *Ecology Letters*, **16**, 39–47.

Tian H, Melillo JM, Kicklighter DW, McGuire AD, Helfrich J (1999) The sensitivity of terrestrial carbon storage to historical climate variability and atmospheric CO2 in the United States. *Tellus B*, **51**, 414–452.

Tilman D, Balzer C, Hill J, Befort BL (2011) Global food demand and the sustainable intensification of agriculture. *Proceedings of the National Academy of Sciences of the United States of America*, **108**, 20260–4.

Tilman D, Socolow R, Foley J, Hill J, Larson E (2009) Beneficial biofuels—the food, energy, and environment trilemma. *Science*, **325**, 270–271.

Townsend AR, Asner GP (2013) Multiple dimensions of resource limitation in tropical forests. *Proceedings of the National Academy of Sciences of the United States of America*, **110**, 4864–4865.

Townsend AR, Cleveland CC, Houlton BZ, Alden CB, White JW (2011) Multi-element regulation of the tropical forest carbon cycle. *Frontiers in Ecology and the Environment*, **9**, 9–17.

Tsubo M, Walker S, Mukhala E (2001) Comparisons of radiation use efficiency of mono-/inter-cropping systems with different row orientations. *Field Crops Research*, **71**, 17–29.

Turner D, Koerper G (1995) A carbon budget for forests of the conterminous United States. *Ecological Applications*, **5**, 421–436.

UN (2009) *The Biofuels Market : Current Situation and Alternative Scenarios*. UNCTAD/DITC/BCC/2009/1. United Nations, Geneva, Germany and New York, NY, USA.

US Congress (2007) *Energy independence and security act of 2007*. Public Law, United States Congress. Washington DC, USA.

USSD (2010) *Composition of macro geographical (continental) regions, geographic sub-regions, and selected economic and other groupings*. United States Statistical Division, New York, USA.

Vitousek P, Ehrlich P, Ehrlich A, Matson P (1986) Human appropriation of the products of photosynthesis. *BioScience*, **36**, 368–373.

Van Vuuren DP, Van Vliet J, Stehfest E (2009) Future bio-energy potential under various natural constraints. *Energy Policy*, **37**, 4220–4230.

Wada Y, Van Beek LPH, Van Kempen CM, Reckman JWTM, Vasak S, Bierkens MFP (2010) Global depletion of groundwater resources. *Geophysical Research Letters*, **37**, 1–5.

West PC, Gibbs HK, Monfreda C, Wagner J, Barford CC, Carpenter SR, Foley JA (2010) Trading carbon for food: global comparison of carbon stocks vs. crop yields on agricultural land. *Proceedings of the National Academy of Sciences of the United States of America*, **107**, 19645–8.

Williams K, Percival F (1987) Estimation of tissue construction cost from heat of combustion and organic nitrogen content. *Plant, Cell & Environment*, **10**, 725–734.

You L, Guo Z, Koo J, *et al.* Spatial Produciton Allocation Model (SPAM) 2000 Version 3 Release 1.

You L, Wood S, Wood-sichra U, Court DT (2006) Generating Global Crop Distribution Maps : From Census to Grid. In: *Selected paper, IAAE (International Association of Agricultural Economists) Annual Conference* pp1–16. Gold Coast, Australia.

Zhang Z, Lohr L, Escalante C, Wetzstein M (2010) Food versus fuel: What do prices tell us? *Energy Policy*, **38**, 445–451.

Zhao M, Heinsch FA, Nemani RR, Running SW (2005) Improvements of the MODIS terrestrial gross and net primary production global data set. *Remote Sensing of Environment*, **95**, 164–176.

Zhao M, Running SW (2010) Drought-induced reduction in global terrestrial net primary production from 2000 through 2009. *Science*, **1667**, 2–5.

Zhao M, Running SW (2011) Response to Comments on "Drought-Induced Reduction in Global Terrestrial Net Primary Production from 2000 Through 2009". *Science*, **333**.

Zhu X-G, Long SP, Ort DR (2010) Improving photosynthetic efficiency for greater yield. *Annual review of plant biology*, **61**, 235–61.